Type III Secretion Chaperones in *Chlamydia trachomatis*:

Identification of a New Effector Protein and Insights into Hierarchical Protein Secretion During Early Infection

by

Yi-Shan Chen

Department of Biochemistry
Duke University

Date:_____

Approved:

_____
Raphael Valdivia, Co-chair

_____
Margarethe Kuehn, Co-chair

_____
Jörn Coers

_____
Pei Zhou

_____
Harold Erickson

Dissertation submitted in partial fulfillment of
the requirements for the degree of Doctor
of Philosophy in the Department of
Biochemistry in the Graduate School
of Duke University

2014

ABSTRACT

Type III Secretion Chaperones in *Chlamydia trachomatis*: Identification of a New Effector Protein and Insights into Hierarchical Protein Secretion During Early Infection

by

Yi-Shan Chen

Department of Biochemistry
Duke University

Date:_____

Approved:

_____
Raphael Valdivia, Co-chair

_____
Margarethe Kuehn, Co-chair

_____
Jörn Coers

_____
Pei Zhou

_____
Harold Erickson

An abstract of a dissertation submitted in partial fulfillment of the requirements for the degree of Doctor of Philosophy in the Department of Biochemistry in the Graduate School of Duke University

2014

Abstract

Chlamydia trachomatis, the causative agent of trachoma and sexually transmitted infections, employs a type III secretion (T3S) system to deliver effector proteins into host epithelial cells to establish a replicative vacuole. Although the temporal manner in which effectors are secreted is important for the proper manipulation of host cell functions, the mechanism remains a mystery. In this study, we provide several lines of evidence that T3S chaperones may impart coherence to effector secretion. In addition, we identified a new early T3S effector in *Chlamydia*. Aside from the phosphoprotein TARP, a *Chlamydia* effector that promotes actin re-arrangements, very few factors mediating bacterial entry and early inclusion establishment have been characterized. By defining proteins that associate with the three most abundant T3S chaperones, Slc1, Scc2 and Mcsc in invasive *C. trachomatis* elementary bodies (EB) by immunoprecipitation coupled with mass spectrometry, we identified Ct875, a new Slc1 client protein and T3S effector, which we renamed TepP (Translocated early phosphoprotein). We provide evidence that T3S effectors form stable complexes with Scl1 *in vitro* and that Slc1 enhances their T3S-dependent secretion in a heterologous *Yersinia* T3S system. We demonstrate that TepP is translocated early during bacterial entry into epithelial cells and is phosphorylated at tyrosine residues by host kinases. However, TepP phosphorylation occurs later than TARP, which together with the finding that Slc1 preferentially engages TARP in EBs leads us to postulate that these effectors are translocated into the host cell at different stages during *C. trachomatis* invasion. TepP co-immunoprecipitated with the scaffolding proteins CrkI-II during infection and Crk was recruited to nascent inclusions. Importantly, *C. trachomatis*

mutants lacking TepP failed to recruit CrkI-II to inclusions, providing genetic confirmation of a direct role for this effector in the recruitment of a host factor. Finally, endocervical epithelial cells infected with a *tepP* mutant showed altered expression of a subset of genes associated with innate immune responses and lack of *C. trachomatis*-induced morphological changes. We propose a model wherein TepP acts downstream of TARP to recruit scaffolding proteins at entry sites to initiate and amplify signaling cascades important for the regulation of innate immune responses to *Chlamydia*.

Dedication

Dedicated to Mom, Dad, my sister and brother for all your love and support.

Contents

List of Tables

List of Figures

List of Abbreviations

a.a.:	amino acid
Cap1:	class I accessible protein-1
SC:	synthetic complete
Cds:	contact-dependent secretion
Cop:	*Chlamydia* outer protein
Ct:	*Chlamydia trachomatis*
DNA:	deoxyribonucleic acid
EB:	elementary body
GFP:	green fluorescent protein
GST:	glutathione-S-transferase
His:	Histidine
kDa:	kiloDalton
Inc:	inclusion membrane protein
IPTG:	isopropyl-1-thio-β-d-galactopyranoside
Mcsc:	multiple cargo secretion chaperone
MOI:	multiplicity of infection
MOMP:	major outer membrane protein
mRNA:	messenger ribonucleic acid
ORF:	open reading frame
PBS:	phosphate buffer saline
PCR:	polymerase chain reaction
PMSF:	phenylmethylsulphonyl fluoride
RB:	reticulate body
Scc2:	specific chlamydia chaperones 2
Slc1:	sycE-like chaperone 1
SNARE:	soluble NSF attachment protein receptor
STI:	sexually transmitted infection

T3S:	type III secretion
TARP:	translocated actin recruiting protein
TepP:	translocated early phosphoprotein
TPR:	tetratricopeptide repeats
Vec.:	Vector
WT:	Wild Type
Y2H:	yeast two hybrid

Acknowledgements

I thank my advisor, Dr. Raphael Valdivia, for his support throughout my graduate training. I thank him for helping to develop my scientific thinking with countless hours of troubleshooting and brainstorming. Moreover, I appreciate the encouragement and patience he gave to me throughout every stage of my training.

I thank Dr. Meta J. Kuehn, Dr. Pei Zhou, Dr. Jörn Coers and Dr. Harold Erickson for their scientific expertise and guidance. Their constructive criticism of my dissertation work helped me to progress productively to completion of my Ph.D.

Chapter 2 is a collaboration project with Dr. Pei Zhou and Dr. Chul-Jin Lee in the Biochemistry department. I thank their contribution in crystallography and biochemical assay and useful suggestions. I would like to acknowledge the contributions of Kristian L. Richards and Dr. Gregory V. Plano at U of Miami to the *Yersinia* T3S assay in Chapter 3. I thank Duke Proteomics facility for their expertise in mass spectrometry; it is crucial for the work in Chapter 3, which in turn, opens the door for Chapter 4. I would also like to thank Duke IGSP facility and Microarray facility for their help. I thank all the authors and collaborators for their contributions and useful discussions.

I thank all my fellow labmates in the Valdivia lab. I especially want to thank Dr. Alex Hector Saka, whose work was the starting point for my project written in Chapter 3 and 4 and for his countless help. I thank Dr. Robert Bastidas, who found a *Chlamydia* mutant that is critical for my project and helped with the whole genome sequencing and Victoria Carpenter, who helped with the microarray experiments. Without their help I would not be able to complete this project; for that, I am extremely grateful. I also thank all the other Valdivia lab members who helped me throughout the years: Dr. Yadunanda Kumar Nandu, who mentored me during my rotation and taught me a lot of basic techniques, Dr. Kris Spaeth, with whom I worked on a project together, Dr. Jordan Cocchiaro, for her always warm and friendly help, Dr. Ine Jorgensen, Dr. Bidong Nguyen, who developed many useful tools and is the founder of our mutant library, Marcela Kokes, who is always excited about science and a good listener, Dr. Joe Dan Dunn, who has been my office mate for 6 years and gave me a lot of feedback on my project, Dr. Jeff Barker, who has

the cutest smile in the lab and has good knowledge about microbiology. I would also like to thank Emily Snavely, Sena Bae, Ryan Baxter and Dr. Barbara Sixt.

I thank the department of Biochemistry for giving me this chance to pursue my PhD at Duke. I thank all the great Biochemistry faculty, staff, and students who have made Duke an extraordinary place to study. In particular, I would like to thank my classmates whose friendship and help accompanied me through my first two years in Duke. I wish they all move on towards their dreams.

Thanks to all my friends in Duke Taiwanese Student Association who accompany me studying in the US: Chi-Fang, who is an awesome cook and baker, Ming-Shan, Chia-Yu, Nai-Jia, my 4 year-long roommate, and Linda and Vivide for their friendship, understanding, and unyielding support. I am glad we became such great friends and, even with our dispersal from Durham, I'm sure we will remain close. Thanks also to Tsai-Yi, my classmate from college, who is studying in UMass now, for her friendship and scientific critique. I would like to especially thank Ouyang and Chance, who have been tremendous supports for my PhD. I will not make it without their patience and listening and I am very happy and proud of their achievement now. Thanks to Brian for his support and accompany in the last year of my PhD, which is very busy and stressful. Thanks for his patience, understanding and encouragement.

To my family – mom, dad, my sister and my brother – I owe the greatest thanks. Thanks to my parents for willing to let me explore a new world and study miles away from Taiwan after losing a child. Thanks to my brother for taking care of mom and dad and keep them company. Thank you for your love and compassion.

1. Introduction

1.1 *Chlamydia trachomatis*

The gram-negative bacteria of family *Chlamydiaceae* are obligate intracellular bacteria that infect a broad spectrum of hosts ranging from humans and animals to free-living amoeba (Peters, Wilson, Myers, Timms, & Bavoil, 2007). Within the family, *Chlamydia pneumonia (*or *Chlamydophila pneumonia)* and *Chlamydia trachomatis* are the two main species that infect humans. *Chlamydia pneumonia* causes acute respiratory disease and has been linked seroepidemiologically to atherosclerosis and increased risk for myocardial infarction and coronary heart disease (Campbell & Kuo, 2004). *Chlamydia trachomatis* is the causative agent of trachoma, the leading cause of infectious blindness worldwide, and the major cause of bacterial sexually transmitted infections (STI) in the developed world (Low et al., 2012). Over 15 variants of *C. trachomatis* have been serologically defined to date and are associated with distinct human diseases (Schachter, 1999). Serovars A-C infect ocular tissues and cause conjunctivitis and blindness. Serovars D-K infect mucosal epithelial cells of the genital tract and can be transmitted sexually. The sequelae of this infection include pelvic inflammatory disease (PID), which can result in infertility in women, chronic pelvic pain, salpingitis, urethritis and ectopic pregnancy (Schachter, 1999). Serovars L1-L3 are associated with lymphogranuloma venereum, a systemic infection, which is also transmitted by sexual contact. Approximately 2.9 million cases of visual impairment and ~1.17 million cases of blindness are attributed to ocular infections by *C. trachomatis* (Pascolini & Mariotti, 2012). Around 101 million cases of chlamydial infections are detected annually in the world, imposing a significant burden on the public health system (World Health Organization, 2011). Moreover, *Chlamydia* infection has been linked to an

increased risk of developing cervical carcinoma and transmission of HIV (Malhotra, Sood, Mukherjee, Muralidhar, & Bala, 2013). Although *Chlamydia* can be quickly detected by nucleic acid amplification tests and effectively treated with antibiotics such as azithromycin, doxycycline and tetracycline (Workowski, 2013), the rate of infection is increasing in the US (Centers for Disease Control and Prevention, 2013). There has not been a stable clinical isolate reported so far that is resistant to antibiotics (O'Neill et al., 2013), nevertheless, given the high frequency of re-infection and the massive usage of antibiotics, the emergence of this problem will be just a matter of time. Moreover, the immune response after *Chlamydia* exposure only provides partial protection against re-infection (Hu, Holland, & Burton, 2013). Therefore, it is necessary to develop new strategies to prevent the disease, such as a vaccine, which has been impeded by the poor understanding of the disease mechanism. This research will reveal some insights in *Chlamydia* pathogenesis.

1.2 The *C. trachomatis* developmental cycle

All *Chlamydiaceae* species have a biphasic life cycle that alternates between two unique developmental forms, the environmentally stable, infectious elementary body (EB)(size around 0.25-0.3 μm), and the metabolically active, replicative, but non-infectious, reticulate body (RB)(size around 0.5 to 1 μm)(Fig. 1) (Moulder, 1991). Infection starts with the attachment of EBs to host cell membranes. After inducing its own internalization, *C. trachomatis* rapidly modifies its endocytic vacuole, the so-called “inclusion”, to avoid fusion with endosomes and lysosomes (Heinzen, Scidmore, Rockey, & Hackstadt, 1996) and migrates to a perinuclear region of the cell (Clausen, Christiansen, Holst, & Birkelund, 1997; Grieshaber, Grieshaber, & Hackstadt, 2003) where it undergoes a developmental transition to the RB form and proliferates. Bacterial

replication occurs within the inclusion, and, mid-to-late in the infectious cycle, bacterial replication becomes asynchronous with RBs transitioning back to the EB form (for reviews, see (Abdelrahman & Belland, 2005; Moulder, 1991)). In late stages of infection, the inclusion occupies the bulk of the host cell cytoplasmic space and EBs are released to infect adjacent cells by cell lysis or extrusion of the whole inclusion (Hybiske & Stephens, 2007).

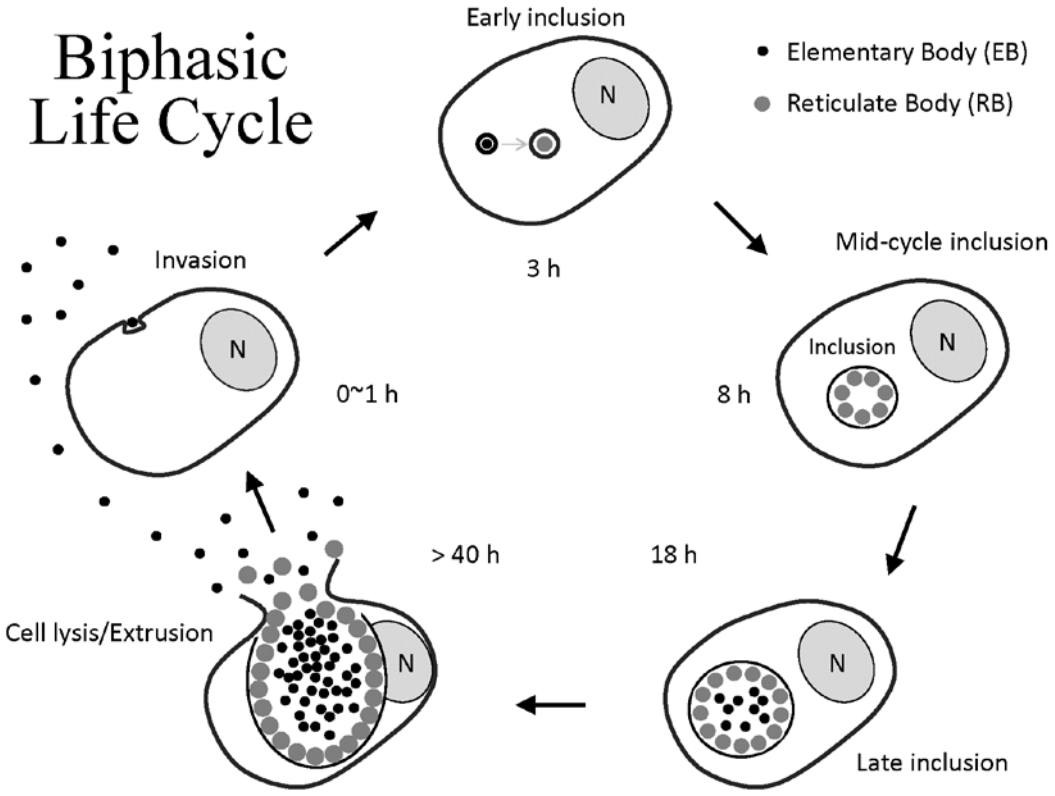

Figure 1: The developmental cycle of *C. trachomatis* serovar L2.

1.3 Modulation of host cellular functions by *C. trachomatis* effector proteins

Though staying within the inclusion throughout the developmental cycle, *Chlamydia* is capable of re-programming diverse host cellular processes for its benefit to establish a replicative niche. In the beginning of infection, *Chlamydia* induces host cellular cytoskeleton rearrangement to enhance its uptake. After entry, multiple host signaling pathways are hijacked to prevent apoptosis and evade innate immunity (Betts, Wolf, & Fields, 2009). *Chlamydia* also actively modifies the inclusion membrane and intercepts a subset of host vesicles containing sphingomyelin and cholesterol from the Golgi-apparatus to acquire nutrients and to escape from the endocytic pathway (Carabeo, Mead, & Hackstadt, 2003; Fields & Hackstadt, 2002; Hackstadt, Rockey, Heinzen, & Scidmore, 1996). These abilities are conferred by a collection of bacterial proteins, also known as effectors, that are delivered into the host cell at different stages of infection. Some of these proteins specifically localize to the inclusion membrane. These inclusion membrane proteins, designated Incs, share a common structural feature of a predictable bi-lobed hydrophobic domain that spans around 40-60 a.a. (Bannantine, Griffiths, Viratyosin, Brown, & Rockey, 2000). However, other than Incs, most chlamydial effectors cannot be predicted from primary amino acid sequences and require experimental identification. The genetic intractability of *Chlamydia* has limited our information to these effectors. Most approaches to identify effectors have been indirect and relied on heterologous expression systems (Valdivia, 2008). To date, only a handful of non-Inc effectors have been identified and, for most of them, their functions are unclear.

1.4 The *C. trachomatis* type III secretion system

Many of these effectors, including Incs, are transported to the host cell cytoplasm by a protein translocation system, called the type III secretion (T3S) system. Pathogenic Gram-negative bacteria, such as *Yersinia*, *Salmonella, Escherichia coli, Pseudomonas syringae, Xanthomonas campestris* and *Shigella*, commonly employ this system to manipulate target host cells (Mueller, Plano, & Fields, 2013). The system forms an injection-needle-like structure and spans three biological membranes: the inner and outer membranes of bacteria and host plasma membranes (during invasion), or inclusion membranes (post invasion). The targeted polypeptides are transported simultaneously across these membranes from bacterial cytosol to host cell cytoplasm. The whole apparatus is composed of around 25 proteins and can be subdivided into three components: a needle, a basal body and a C-ring compartment (Fig. 2) (Cornelis, 2006). The C-ring part of the apparatus associates with an ATPase (CdsN in *Chlamydia*) that presumably energizes the export process. In addition to the core components, a group of accessory proteins, termed T3S chaperones, are required for the assembly and operation of the system.

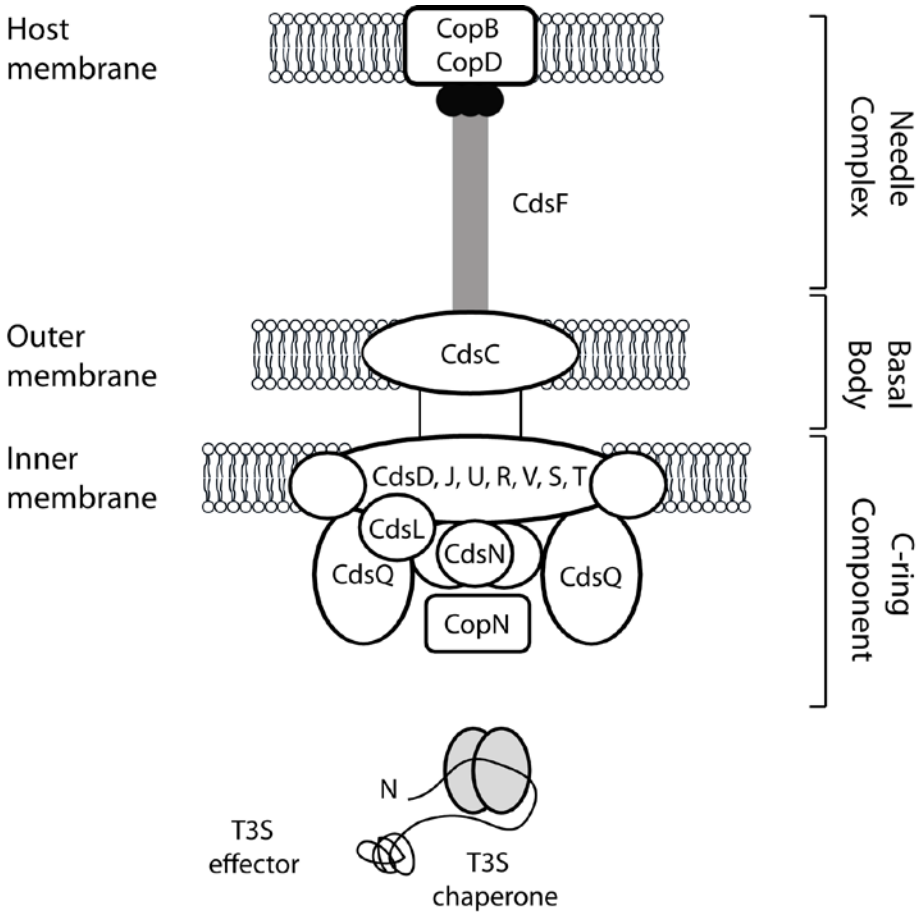

Figure 2: *Chlamydia* T3S system. The model is based on the *Yersinia* T3S system.

Although a putative chlamydial T3S apparatus was observed as early as 1979 by electron microscopy (Gregory, Gardner, Byrne, & Moulder, 1979), its existence in *Chlamydia* was not confirmed until genome sequencing efforts identified homologs of genes encoding T3S components (Peters et al., 2007; Stephens et al., 1998). Unlike the T3S genes in other pathogenic Gram-negative bacteria, which are normally clustered in chromosomal Pathogenicity Islands and on plasmids, the chlamydial T3S genes are scattered into at least three distinct genomic clusters (Peters et al., 2007). Also, the GC content of these regions are similar to the

rest of the genome, providing the lack of evidence for horizontal gene transfer (Peters et al., 2007). This implies that chlamydial T3S might directly evolve from an ancestral T3S and is probably the closest to the primordial T3S apparatus (Kim, 2001). Nevertheless, a recent review suggests that all T3S systems, including chlamydial T3S, are derived from flagella (Abby & Rocha, 2012; Mueller et al., 2013). No matter the origin, phylogenetic analysis often sorts chlamydial T3S as a distinct family in comparison to other systems, implying its uniqueness (Buttner, 2012; Cornelis, 2006).

Unfortunately, our understanding of how the chlamydial T3S system functions has been hampered by the lack of genetic tools and a complex biphasic developmental cycle. The functionality of the chlamydial T3S was not inferred until CopN, the putative T3S plug that limits premature secretion before activation, was shown to be secreted in a heterologous *Yersinia* T3S system (Fields & Hackstadt, 2000). Although indirect, this was the strongest evidence at that time supporting the hypothesis that *Chlamydia* uses T3S and brought attention to the possibility that T3S effectors helped reprogram the host cell. Although several basal components of the chlamydial T3S apparatus could be identified based on homology to those in other systems, some have diverged and the dispersion of chlamydial T3S genes in genome renders prediction difficult. Some missing components have been identified based on protein-protein interactions or by sophisticated additional bioinformatics analysis, followed by biochemical validation. For example, the chlamydial T3S translocators, CopB and CopD, were identified based on their interactions with specific chlamydial chaperones, Scc2 and Scc3 (Fields, Fischer, Mead, & Hackstadt, 2005; Spaeth, Chen, & Valdivia, 2009). Similarly, CdsF, was suspected to be a needle component due to its small size and the gene location relative to other T3S components, and

validated biochemically (Betts, Twiggs, Sal, Wyrick, & Fields, 2008). The identity of the needle tip protein remains controversial. Using computational structure prediction and biophysical analysis, Ct584 is suggested to be the T3S needle tip protein (Markham, Jaafar, Kemege, Middaugh, & Hefty, 2009). However, a structural study in Ct584 ortholog in *C. pneumoniae*, Cpn0803, as well as Ct584 in *C. trachomatis*, revealed no similarity to needle tip protein, although Cpn0803 shows interaction with multiple T3S components, including CdsN (ATPase), CdsQ (C-ring component) and CdsF and some host lipids, implying association with T3S system and host membrane (Barta et al., 2013; Stone et al., 2012). Recently, one group suggested that Ct584 functions as a T3S chaperone (Pais, Milho, Almeida, & Mota, 2013), leaving the role of Ct584 an open question.

Although the overall structure, as well as the secretion mechanism, is likely conserved, the chlamydial T3S system contains some unique features that differentiate it from other T3S systems (Betts-Hampikian & Fields, 2010). For example, *C. pneumoniae* CdsD, a YscD homolog of the inner membrane ring protein, is phosphorylated and represents the first example of T3S apparatus component that undergo phosphorylation (Johnson & Mahony, 2007), yet the function of this phosphorylation is still unclear. In addition, fractionation study indicates that CdsD may not be an integral membrane protein but a peripheral membrane protein with a high hydrophilicity (Johnson, Stone, & Mahony, 2008), rendering it difficult to define the role of CdsD. In addition, CdsC, homolog of outer membrane protein secretin, contains a unique hydrophilic domain at the N-terminus and lacks regions required for oligomerization and membrane association that are present in other homologs (Betts-Hampikian & Fields, 2010). Interestingly, unlike other known T3S system, *Chlamydia* contains two sets of translocator proteins,

CopB/CopD and CopB2/CopD2. Biochemical and localization analysis implies that these two sets of translocator proteins may function differently during *Chlamydia* infection (Chellas-Gery, Wolf, Tisoncik, Hackstadt, & Fields, 2011).

The importance of the T3S system in *Chlamydia* pathogenesis was inferred by small molecule inhibitors that were first identified in a screen for inhibitors of the *Yersinia* T3S system. These inhibitors either partially inhibited or had no effect on *Chlamydia* entry. But all of them impacted bacterial replication and RB to EB transition and reduced the yield of infectious progeny (Muschiol et al., 2006; Muschiol, Normark, Henriques-Normark, & Subtil, 2009; Wolf et al., 2006). The mechanism of inhibition, nevertheless, is still questionable. The translocation of many known T3S effectors, such as IncG, IncA, Tarp, and CADD, were affected (Muschiol et al., 2006; Wolf et al., 2006). However, these compounds have a minimal effect on bacterial entry, which is assumed to rely heavily on T3S effector translocation. Also, adding iron reversed the defect induced by some inhibitors and some gene transcriptions were affected by adding these inhibitors (Slepenkin et al., 2007; Wolf et al., 2006). More importantly, mutation in hemG, a protoporphyrinogen oxidase that catalyzes a central step in heme biosynthesis, confers resistant to these compounds (Engstrom et al., 2013). Together, these imply that the observed defects might be contributed from multiple factors, not only inhibition of T3S system.

Proteins destined for T3S contain a secretion signal located within the N terminal ~20-30 amino acids (Galan & Wolf-Watz, 2006). Although two algorithms are now available to predict T3S substrates (Arnold et al., 2009; Lower & Schneider, 2009), most potential T3S effector proteins in *Chlamydia* were identified through expression and secretion in heterologous

bacterial systems (Ho & Starnbach, 2005; Subtil et al., 2005). These findings predict that about 5~8% of the chlamydial genome encodes potential substrates of T3S (Valdivia, 2008). Since *Chlamydia* reprograms host cellular functions sequentially at different stages of development to create a suitable replicative niche, these effectors may be secreted in a defined sequence to achieve different tasks. This kind of hierarchical secretion has been observed in other T3S systems. For example, in *Salmonella typhimurium*, effectors SipA, SopE and SptP all are pre-formed in the bacterial cytosol but SipA and SopE are injected earlier than SptP (Winnen et al., 2008). Since SipA and SopE, and SptP have opposing effects on remodeling actin cytoskeleton (Zhou & Galan, 2001), this ordered secretion ensures effectors exert their functions at the right time. The mechanism through which this is achieved, however, is still unclear. The T3S apparatus-associated ATPase protein may play a role in cargo recognition by studies in *Yersinia* and *Salmonella* (Akeda & Galan, 2005; Sorg, Blaylock, & Schneewind, 2006). Nevertheless, it is unknown if this functionality is conserved in *Chlamydia*. In addition, accessory proteins such as the chaperones of cognate effectors might confer another layer of substrate specificity that helps determine the order of secretion (Birtalan, Phillips, & Ghosh, 2002; Boyd, Lambermont, & Cornelis, 2000). More studies are required to support these hypotheses.

2. Mcsc, a multiple cargo secretion chaperone, binds to its cargos with different affinities

2.1 Introduction

2.1.1 Class I T3S Chaperones

Effectors destined for T3S possess a secretion signal within the N terminal 20-30 amino acids (a.a.) that is often sufficient for secretion (Galan & Wolf-Watz, 2006). However, many effectors require ancillary chaperone proteins for efficient translocation into target cells. These class I chaperones are customized for their cognate effectors; the secreted effector generally wraps around the chaperone dimer using the secondary structural elements of the first 50-100 a.a. while the C-terminal regions remain folded (Lilic, Vujanac, & Stebbins, 2006; Parsot, Hamiaux, & Page, 2003). Depending on the number of effectors with which they can associate, class I chaperones are further divided into class IA and IB (Thomas, Ma, Prasad, & Rafuse, 2012). Class IA chaperones are specific for single effectors and the genes encoding the chaperone-effector pair are often adjacent. Class IB chaperones associate with more than one effector and the genes encoding these chaperones are often unlinked from that of its cognate cargos. Many common features are shared by class I chaperones, including small size (15~20 kDa), acidic isoelectric points (pI), a stable homodimeric conformation, and an ATP-independent chaperone function (Thomas et al., 2012). Structurally, class I chaperones contain a basic core consisting of three α-helices and five β-sheets (Izore, Job, & Dessen, 2011); however, the degree of conservation at the amino acid level is limited, making the identification of new T3S chaperones difficult.

2.1.2 Inclusion membrane proteins

After entering into the host cell, *Chlamydia* replicates inside a membrane-bound vacuole termed an inclusion. The inclusion membranes are derived from host cell membranes and then actively and continuously modified by *Chlamydia* as infection proceeds. The inclusion fuses with Golgi-derived vesicles containing sphingomyelin and cholesterol (Carabeo et al., 2003; Hackstadt et al., 1996), and a group of effectors are secreted by the T3S system and incorporated into the inclusion membrane via a still unclear mechanism. These inclusion membrane proteins, designated Incs, share a common structural feature: a bi-lobed hydrophobic domain that can be easily observed in a hydropathy plot and typically spans around 40-60 a.a. (Bannantine et al., 2000). This domain is usually at the N-terminus but can also be present at the C-terminus, and some Incs have multiple bi-lobed hydrophobic domains (Toh, Miura, Shirai, & Hattori, 2003). Around 50 Incs were predicted to be encoded in *C. trachomatis in silico* and around 40 of them were verified experimentally (Li et al., 2008). Since these Inc proteins are localized at the host-pathogen interface, they are likely central regulators of host functions and play vital roles in *Chlamydia* pathogenesis. However, due to the genetic intractability of *Chlamydia*, only a few of these Incs have known functions. For example, IncA is involved in homotypic fusion of inclusions and mediates the recruitment of SNARE proteins to inclusion membranes (Delevoye et al., 2008). In the same study, the authors also found that Ct813 is another Inc that interacts with SNARE proteins, Vamp7 and Vamp8. In addition, IncG, Ct228, Ct229 and IncD interact with 14-3-3β, MYPT1 (a subunit of myosin phosphatase), Rab4, and the lipid transporter CERT, respectively (Derre, Swiss, & Agaisse, 2011; Lutter, Barger, Nair, & Hackstadt, 2013; Rzomp, Moorhead, & Scidmore, 2006; Scidmore & Hackstadt, 2001). More studies are ongoing to uncover the function of these membrane proteins.

2.1.3 Multiple Cargo Secretion Chaperone (Mcsc)

Mcsc (Ct260), which does not share any obvious sequence homology with known T3S chaperones, was first revealed as a potential T3S chaperone experimentally in a yeast two-hybrid screen. The authors unbiasedly screened the interactions between 208 *Chlamydia*-specific conserved hypothetical open reading frames (ORFs) and found that Mcsc interacted with itself, a T3S component protein, and multiple Incs, including Cap1 (Ct529), Ct225 and Ct618 (Spaeth et al., 2009). Mcsc has several features that fit characteristic of T3S chaperone: it has a small molecular weight (18.8 kDa), an acidic pI (4.6), and it forms a dimer. Its interactions with Cap1 and Ct618 help stabilize their expression in *E. coli*; thus Mcsc was classified as a *bona fide* Class IB T3S chaperone (Spaeth et al., 2009). Cap1, or class I accessible protein-1, was originally identified because it can be recognized by $CD8^+$ cells, and it was shown to localize to the inclusion membrane (Fling et al., 2001). Similarly, Ct618 and Ct225 were shown to localize to the inclusion membrane, as revealed by immunofluorescence staining (Li et al., 2008; Sisko, Spaeth, Kumar, & Valdivia, 2006). The actual functions of these Incs remain unknown. Interestingly, expressing the cytosolic domains of Cap1 and Ct618 in yeast caused rapid growth arrest, implying that these two proteins may interfere with important cellular functions (Sisko et al., 2006).

2.1.4 Hierarchical protein secretion in T3S system

Hierarchical secretion has long been observed in T3S systems but how it is regulated is still a puzzle. Pathogens that employ T3S system usually contains a set of substrates ready to be secreted upon activation. For example, *Yersinia* has at least five Yops (*Yersinia* outer protein) that are secreted by the T3S system (Trosky, Liverman, & Orth, 2008) and in enteropathogenic

Escherichia coli (EPEC), at least 27 T3S effectors were found (Wong et al., 2011). In the case of *Salmonella typhimurium*, it is observed that SipA, SopE and SptP are all pre-formed effectors in bacterial cytosol but SipA and SopE are injected earlier than SptP (Winnen et al., 2008). Since several effector proteins are present at any one time, the T3S apparatus may have a mechanism to recognize and transport target proteins in the right time and right order. The mechanism through which this is achieved is still under debate. T3S substrates contain a secretion signal at the N-terminus; nevertheless, it is still undetermined how the signals are recognized by the system. On the side of the T3S apparatus, it is indicated that the T3S-apparatus-associated ATPase may play a role in cargo recognition. A study in *Yersinia* shows that YscN, the T3S-apparatus-associated ATPase, binds to the T3S secretion signal of YopR (Sorg, Blaylock et al. 2006). In addition, the *Salmonella* ATPase InvC has been shown to interact with SicP-SptP, a chaperone-effector complex, and induce dissociation of chaperone from effector and unfolding of the secreted effector protein in an ATP-dependent manner (Akeda and Galan 2005). These results suggest that ATPase may recognize the secretion signal and energize the transport process. Additional T3S components may contribute to recognizing secreted cargos and bringing them in proximity to the ATPase for secretion. The C-ring component of T3S apparatus may perform this duty. This is supported by the study showing that spa33, the *Shigella* C-ring component protein, interacts with multiple effectors (Morita-Ishihara et al., 2006). Also, in the plant pathogen *Xanthomonas campestris pv. vesicatoria*, the C-ring component HrcQ binds to HrcN (ATPase) and several secreted T3S substrates (Lorenz, Hausner, & Buttner, 2012). In *Chlamydia*, the *C. pneumonia* C-ring component CdsQ interacts with CdsN (ATPase) and the *C. trachomatis* ortholog interacts with Mcsc alone and Mcsc in complex with effectors Cap1 or Ct618 (Spaeth et al., 2009; Stone, Johnson, Bulir, Gilchrist, & Mahony, 2008). However, whether

this constitutes a general recognition mechanism for secreted effectors by T3S machines is not clear.

From the side of the secreted cargo, accessory proteins such as the chaperones of cognate effectors might confer another layer of substrate specificity to help determine the order of secretion (Cornelis, 2006). In agreement with this, YopE, a *Yersinia* T3S effector lacking a SycE chaperone binding site, is secreted in the absence of other T3S effectors. However, YopE secretion is severely impaired when other effectors are allowed to compete with it, indicating that additional secretion signals are either unmasked or conferred by the T3S chaperone (Boyd et al., 2000). Even for effectors sharing the same chaperone, there seems to be a defined order of secretion. For instance, CesT from EPEC binds to at least 10 T3S effectors, but one of the cargos, Tir, is secreted first, and Tir secretion is important for secretion of the remaining effectors (Thomas, Deng, Baker, Puente, & Finlay, 2007). How a chaperone can be involved in this regulation remains to be elucidated.

In this study, we focus on the interactions between Mcsc and its cargos, Cap1, Ct225 and Ct618. We mapped the chaperone binding regions in these effectors to around fifty a.a. and observed a distinct binding affinity of these peptides to Mcsc. The order of binding affinity was inversely correlated to the transcriptional timing of genes encoding these proteins, which suggests that secretion hierarchy may be partially imparted by chaperone-binding affinity. In addition, we employed newly developed DNA transformation techniques in *Chlamydia* (Wang et al., 2011) to demonstrate that Mcsc binding is important for the stability and secretion for Cap1 *in vivo*.

2.2 Materials and Methods

2.2.1 Bacterial strains, cell lines, and reagents

HeLa cell and Vero cells were maintained in Dulbecco's minimal essential medium (DMEM) (Sigma-Aldrich, St. Louis, Missouri, USA) supplemented with 10% fetal bovine serum (Mediatech, Manassas, Virginia, USA) at 37°C, 5% CO_2. Infections were synchronized by adding EBs to HeLa monolayers with specified multiplicity of infection (MOI) prior to centrifugation at 3000 rpm for 30 min at 10°C. All affinity-tagged recombinant proteins were expressed in *E. coli* BL21 DE3 and induced with 0.5 mM IPTG for 3 hr at 37°C.

2.2.2 Generation of antibodies

GST-Mcsc and GST-Ct618 (a.a.1-96) were expressed in *E. coli* and purified with glutathione-coated Sepharose 4-Fast Flow beads (GE Healthcare). Recombinant proteins was eluted with 20 mM reduced glutathione in PBS (pH 7.4) and used to immunize female White New Zealand rabbits (5~6 lbs) (Robinson Services, Inc.). Antisera were depleted of anti-GST antibodies first and affinity purified over a GST-Mcsc or GST-Ct618-crosslinked column. Bound antibodies were eluted with 0.2 M Glycine (pH 2.5) and neutralized with 1 M K_2HPO_4. The resulting antibodies were then dialyzed in PBS twice and once in PBS containing 1% BSA, 5% glycerol and 10 mM NaN_3 and stored in -80 °C.

2.2.3 Immunoblot analysis

For immunoblot analysis, protein samples were separated by SDS-PAGE, transferred to 0.45 µm nitrocellulose membranes (Bio-Rad, Berkeley, CA, USA) and blocked in 3% non-fat powder milk in TBST (50 mM Tris-Base, 150 mM NaCl, 0.2% Tween-20 pH 7.4) for 20 min at RT. Membranes were incubated with primary antibody diluted in 3% milk-TBST overnight, followed

by three times of wash with TBST and incubation with secondary antibody conjugated to horseradish peroxidase for 30 min. The signals were detected by chemiluminescence (PerkinElmer, Waltham, MA, USA) and autoradiography film (Genesee, San Diego, CA, USA). For quantitative immunoblot, membranes were incubated with dye-conjugated secondary antibodies, IRDye 800CW Goat anti-rabbit antibodies and IRDye 680LT Goat anti-mouse antibodies (LI-COR, Lincoln, Nebraska, USA). Images were acquired and signals were quantified using an Odyssey Fc Imager (LI-COR, Lincoln, Nebraska, USA). Primary antibodies include anti-Tarp (1:1000) (generated in our laboratory), MOMP (1:2000) (gift from Dr. K. Fields), Cap1 (1:1000) (gift from Dr. A. Subtil, Pasteur Institute), actin (1:1000) (Sigma-Aldrich), GSK-3β (1:1000) (Cell Signaling #9325) and phospho-GSK-3β (Ser9) (1:500) (Cell Signaling #9336) (Cell Signaling Technology, MA, USA).

2.2.4 Yeast Two Hybrid (Y2H)

Different truncation forms of Cap1 (Ct529) and Ct618 were PCR amplified from a previously established chlamydial open reading frame (ORF) library (Spaeth et al., 2009) with long tail primers containing homologous regions of yeast vector. Cloning was achieved by transforming both PCR products and digested Y2H vectors, pGAD424 or pGBT9, and ssDNA into yeast by the lithium acetate method (Brown, 1998). Successful homologous recombinations were selected by growing yeast on synthetic complete (SC) medium plates lacking either leucine (Leu) or tryptophan (Trp) for pGAD424 or pGBT9, respectively. Individual yeast colonies were then selected, inoculated into liquid culture, and grown overnight. Plasmids were extracted by phenol-chloroform and re-transformed into *E. coli*. Constructs were then purified from *E. coli* and verified by sequencing. Mcsc was cloned into pGAD424 vector, which contains the GAL4

activation domain; tested proteins were cloned into pGBT9, which contains the GAL4 DNA binding domain. To perform Y2H, reciprocal constructs were transformed into Y2H reporter strains, PJ69-4a (MATα) or AH109 (MATa), separately, and selected on appropriate SC plates. Different mating types of yeasts were mated in YPD rich media for two days, followed by selection in SC medium lacking both Leu and Trp. The resulting diploids were then plated on SC media plates lacking either Leu/Trp, histidine (His) or adenine (Ade). Growth on –His and –Ade indicated positive interaction.

2.2.5 *Chlamydia* transformation

Seed preparation. Confluent Vero cells in a T75 flask were infected with *Chlamydia trachomatis* serovar L2/434/Bu with an MOI of 10 for 40-44 hr. To collect bacteria, cells were first washed twice with 1x PBS and then scrapped in 1 mL deionized water, followed by passing through a 27G1/2 needle more than 5 times to help lysis. Lysate was centrifuged at 500xg for 5 min at 4°C to get rid of cell debris. Appropriate amount of 5X SPG was added to supernatant to reach concentration of 1X. Seeds were titered, aliquoted, and stored at -80°C.

Transformation. The transformation was performed as previously described (Wang et al., 2011) with some modifications. Briefly, a volume of *Chlamydia* seed containing around 10^8 IFUs was incubated with 6 µg plasmid or without plasmid (mock-transformed control) in 200 µl transformation buffer (10 mM Tris pH 7.4 in 50 mM $CaCl_2$) for 30 min at room temperature. Vero cells were trypsinized and pelleted down at 500xg for 5 min. The supernatant was discarded and the cells were re-suspended in 5 mL transformation buffer and pelleted down again. The supernatant was discarded and the cells were re-suspended in 500 µL transformation

buffer and counted in the hemocytometer with dilution of 1/50 to 1/100. Around $4x10^6$ cells were transferred to a new microtube and the volume was adjusted to 200 µL with transformation buffer. Two hundred µl transformed seeds were mixed with 200 µL $CaCl_2$-treated cells and incubated for 20 min at room temperature and the mixture was shaken every 5 min to prevent sedimentation of cells. In the meantime, 6-well plates with 3 mL fresh media in each well were prepared and 100 µL mixture was added into each well and the plates were spun at 3000 rpm for 30 min to increase the efficiency of infection. After centrifugation, the plate was shifted to 37°C incubator and incubated for around 40 hr. This is P_0. New confluent 6-well plates with Vero cells were prepared the second day. On day 3, bacteria were collected as described in seed preparation and ~1/8 to 1/4 volume of collected bacteria was added to a new 6-well plate with confluent cells in media supplemented with 500 ng/mL cycloheximide and 1U of penicillin G and the plates were spun at 3000 rpm for 30 min. The rest of the P_0 was stored in -80°C. After centrifugation, the plates were shifted to 37°C incubator and incubated for more than 40 hr. This is P_1. At this stage, a lot of persistent inclusions would be observed. New confluent 6-well plates with Vero cells were prepared on Day 4. Bacteria were collected as described above on day 5 and all collected bacteria were added to a new plate with confluent Vero cells. This is P_2. Bacteria were continuously passed to new cells every three to four days in the presence of 1U penicillin G until normal inclusion was observed. In mocked transformed *Chlamydia*, there should be no normal inclusion under penicillin G selection. Penicillin G concentration was increased to 10 U when expending and enriching transformed *Chlamydia*.

2.2.6 *in vivo* secretion assay

Genes encoding the cytoplasmic region of Cap1 (1-225 a.a.) and Ct618 (1-189 a.a.) were PCR amplified and cloned into a *C. trachomatis-E. coli* shuttle plasmid with a IncD promoter and a C-terminal Glycogen Synthase Kinase (GSK) tag (modified from p2TK2-SW2 (Agaisse & Derre, 2013) by Dr. Jeff Barker and Dr. Joe Dan Dunn). Cap1 H188A and H188D and Ct618 H156A and H156D were obtained using site-directed mutagenesis with QuickChange Kit (Agilent Technologies, Santa Clara, CA) as instructed by the manufacturer. Constructs were transformed into *C. trachomatis* serovar L2/434/Bu as mentioned above. Selected transformants were enriched, expanded and titered. For secretion assays, confluent HeLa cells in a 24-well plate were infected with *Chlamydia* transformed with different constructs at an MOI of 200 and collected at indicated time points. Samples were subjected to immunoblot analysis and probed with anti-GSK and anti-phospho-GSK antibodies. Images were acquired using LI-COR Odyssey Imaging system and signals were quantified using the LI-COR Odyssey software. Efficiency of secretion was determined by dividing phospho-GSK signal by GSK signal.

2.3 Results

2.3.1 Cap1 protein is expressed earlier than Ct618 during *Chlamydia* infection

Since multiple inclusion membrane proteins interact with the same chaperone, we first wanted to determine the timing of their expression in *Chlamydia*. Although Mcsc is one of the most abundant T3S chaperones in EBs, neither Cap1 nor Ct618 were detected in an EB proteome study (Saka et al., 2011). Consistent with this observation, the mRNAs for Cap1, Ct225 and Ct618 were detected 1, 3, 8 hour post infection (hpi), respectively, in a comprehensive transcriptional analysis of *Chlamydia* infection (Belland et al., 2003), which suggests that these proteins are

expressed post bacterial entry. However, the presence of mRNA does not necessary mean that the protein is expressed. To address this question, we infected HeLa cells with *Chlamydia* serovar L2 at an MOI of 50 and collected the whole cell lysates at 2, 4, 6, 8 and 12 hpi and analyzed the sample by immunoblot with anti-Cap1 and Ct618 antibodies. Because the antibodies we raised against Ct225 did not recognize any specific band during infection, we did not include Ct225 in this study. We detected Cap1 protein as early as 1 hpi; whereas Ct618 protein was not detected until 12 hpi (Figure 3). Overall, the immunoblot results are in good agreement with the transcription data.

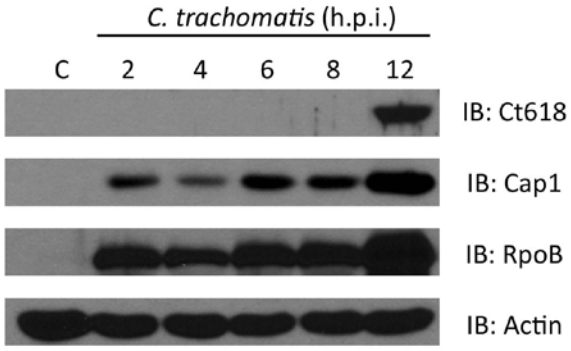

Figure 3: Cap1 is expressed earlier than Ct618 during *Chlamydia* infection. Confluent HeLa cells were infected with *C. trachomatis* L2 at an MOI of 50. Samples were collected at indicated time points and analyzed by immunoblot with antibodies against Ct618, Cap1, RopB (loading control for bacteria) and Actin (loading control for HeLa cells). Cap1 was detected as early as at 2 hpi; whereas Ct618 was detected at 12 hpi. C - HeLa cells only.

2.3.2 Mapping interaction regions between Mcsc and its cargos by Y2H

Since Mcsc binds to multiple cargos, we wanted to determine how each Inc protein interacts with Mcsc. To elucidate their binding interfaces, we collaborated with Dr. Pei Zhou (Department of Biochemistry, Duke University Medical Center) to determine the structure of

Mcsc with and without its cargos. However, expressing the cytoplasmic domains of both Cap1 and Ct618 in *E. coli* is toxic and produces a very low protein yield (data not shown). Therefore, we decided to first map the Mcsc-binding regions in Cap1 and Ct618. In our previous work, the binding domains for Cap1 and Ct618 were mapped to 100 to 298 a.a. and 100 to 214 a.a., respectively (Spaeth et al., 2009). To narrow down the minimal region, different truncated forms of Cap1 and Ct618 were cloned into the Y2H vector pGBT9 (vector containing GAL4 DNA-Binding Domain) and transformed into a Y2H reporter strain. The vector pGAD424 (vector containing GAL4 Activation Domain) that contains wild type Mcsc was transformed into another Y2H reporter strain of the opposite mating type. After mating, the resulting diploids were selected in medium lacking leucine (L) and tryptophan (T) and positive interactions were assessed by growth on plates lacking histidine (H) or adenine (A). The results show that the Mcsc-binding domain for Cap1 is within 176 to 224 a.a., and for Ct618, it is between 140 to 193 a.a. (Fig. 4A). To our surprise, this binding region is quite different from the usual chaperone-binding region, which is within the first ~50-100 a.a. of effector protein (Lilic et al., 2006). This implies that the interaction might not follow the canonical rules of effector-chaperone interactions. Additionally, these two regions have two similar properties. First, both are located adjacent to the bi-lobed hydrophobic domain, a common motif found in all Incs (Fig. 4B). Second, these regions are predicted to form two alpha helices by Network Protein Sequence Analysis (http://npsa-pbil.ibcp.fr/). Whether these patterns are coincidence or are conserved among all Mcsc effectors substrates remains to be determined. Because the original Y2H construct for Ct225 had already narrowed down the binding region to 69 to 122 a.a. after removal of the bi-lobed hydrophobic domain, we did not include Ct225 in this Y2H study. Nevertheless, the binding region for Ct225 is also adjacent to the bi-lobed hydrophobic domain, suggesting that binding to Mcsc might help

mask the bi-lobed hydrophobic domains of these Incs, which are often toxic to bacteria. These Mcsc binding domains were further fused to either GB3 protein tag (Ct618 and Ct225) or GB1 protein tag (Cap1), depending on their pI, to increase their stability and solubility (gift from Dr. P. Zhou). These fusion proteins expressed well in *E. coli*, and all fused peptides form complexes with Mcsc in gel filtration (data not shown).

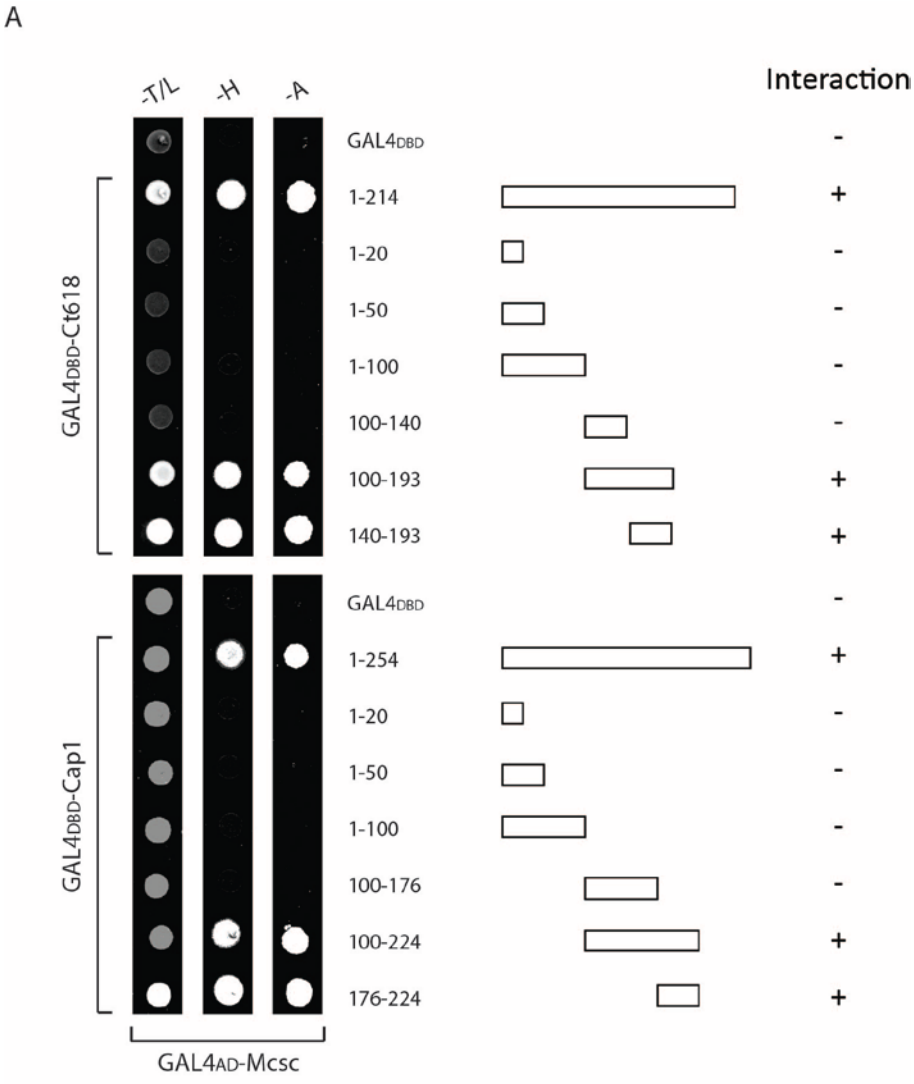

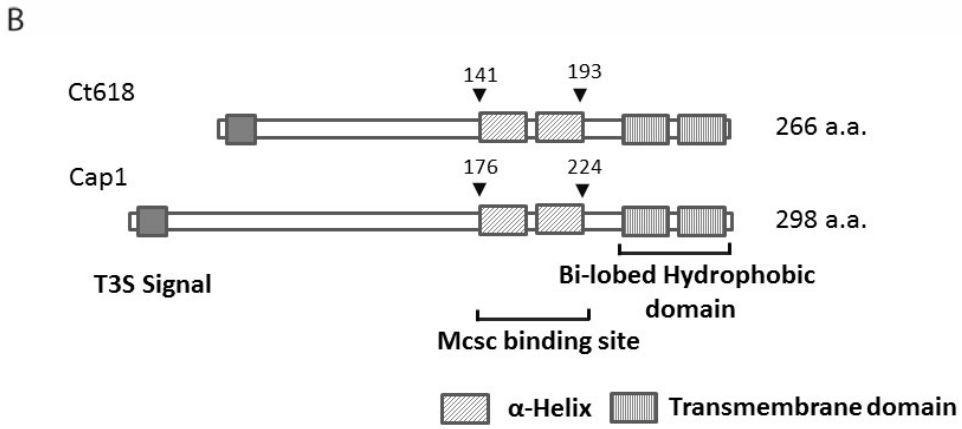

Figure 4: The central regions of Ct618 and Cap1 mediate binding to Mcsc. The Mcsc binding domains of Ct618 and Cap1 were mapped by Y2H. Different truncated forms of Cap1 and Ct618 were cloned into pGBT9 (GAL4/DNA binding domain) and transformed into Y2H reporter strain to test their interactions with Mcsc, which was fused to GAL4/activation domain. A) Positive interactions were assessed by activation of GAL4-dependent *HIS3* and *ADE2* reporter genes and growth of yeast in media lacking histidine (-H) or adenine (-A). Growth on media lacking both tryptophan (-T) and leucine (-L) are shown as controls for maintenance of the Y2H vectors. B) Cartoon schema of Mcsc binding regions in Ct618 and Cap1. Both regions are adjacent to the large hydrophobic region mediating insertion into the inclusion membrane and are mainly α-helices.

2.3.3 Chaperone binding is important for the stability of recombinant Cap1 *in vivo*

The T3S chaperones usually help stabilize or enhance the secretion of their cargo. Our previous study demonstrated that mutating the predicted effector binding sites in Mcsc reduced the protein expression levels of both Cap1 and Ct618 in an *E.coli* expression system using a bi-cistronic vector (Spaeth et al., 2009). However, whether this is the case in *Chlamydia* is unclear. New advances in genetic manipulation (Wang et al., 2011) allowed us to ectopically express proteins in *Chlamydia*. To examine the importance of Mcsc binding in the stability of its cargos in the natural environment, we ectopically expressed these proteins in *Chlamydia* and traced the expression level of these proteins after disrupting chaperone interaction. Nevertheless, this

approach would require us knowing the residues in effectors that bind to Mcsc. As mentioned above, we have mapped the Mcsc binding regions for all three Incs, Cap1, Ct225 and Ct618. By collaborating with Dr. Pei Zhou and Dr. Chul-Jin Lee in the Biochemistry department, we now have a solved structure of Mcsc both in apo form and in complex with the cargo peptides, Ct618 and Cap1, by X-ray crystallography. The attempt to solve the structure of the Mcsc/Ct225 peptide complex, however, is still in progress.

The structure of the Mcsc apo form, like other T3S chaperone, is composed of three α-helices and five β-sheets. By mutagenesis analysis, Dr. Chul-Jin Lee determined that the histidine residue at amino acid 156 in Ct618 is important for binding as it made key contacts with Mcsc and because mutating this residue to alanine (A) reduced the binding affinity by more than 200-fold and mutating to aspartic acid (D) completely abolished the interaction (Table 1) (Dr. Chul-Jin Lee, unpublished data). Similarly, mutating the respective histidine in Cap1 at a.a. 188 disrupted the binding between Cap1 peptide and Mcsc. The interacting residue in Ct225, however, is still undetermined because there is no histidine in the corresponding position. We applied this information to our system to test whether disrupting chaperone binding affects effector stability. We first cloned the cytoplasmic region of Cap1 and Ct618 in a *C. trachomatis-E. coli* shuttle plasmid under the control of the IncD promoter with a Glycogen Synthase Kinase (GSK) tag fused to the C-terminus of these proteins. Finally, we introduced H188A and H188D mutations to the Cap1-GSK construct and H156A and H156D mutations to the Ct618-GSK construct. These six constructs were than transformed into *C. trachomatis* serovar L2/434/Bu individually and selected under penicillin G for several passages. To assess the steady-state levels of these recombinant proteins, HeLa cells were infected with *Chlamydia* expressing these

various constructs at an MOI of 200 and cell lysates were collected at indicated time points. Collected samples were subjected to quantitative immunoblot analysis with antibodies against GSK to determine the total levels of recombinant protein expressed and MOMP, which served as a control for bacteria loads. The signals were quantified using a LI-COR Odyssey imaging system and software. GSK signals were first normalized to the MOMP signal and compared to wild type recombinant protein, which was set to be 100%. The protein expression level of WT Ct618 is much lower than Cap1 and was barely detected at later time points (> 24 h). Hence, Ct618 was not studied further. The results showed that all mutations decreased the stability of recombinant Cap1. This level of decrease was inversely correlated with the binding affinity to Mcsc and time post infection, indicating that Mcsc binding is important for the stability of recombinant Cap1 in *Chlamydia* (Fig. 5).

Table 1: Binding affinity between Mcsc and its cargos by isothermal titration calorimetry (ITC) (Dr. Chul-Jin Lee, unpublished data).

	Mcsc	
Ligand	Mutation	K_d (nM)
Ct618 CBR[a]	None	52
	H156A	9700
	H156D	*
Cap1 CBR[a]	None	2010
	H188A	64520
	H188D	*
Ct225 CBR[a]	None	135
	-	-
	-	-

*no appropriate binding isotherm obtained for data fitting.

[a]CBR- chaperone binding region.

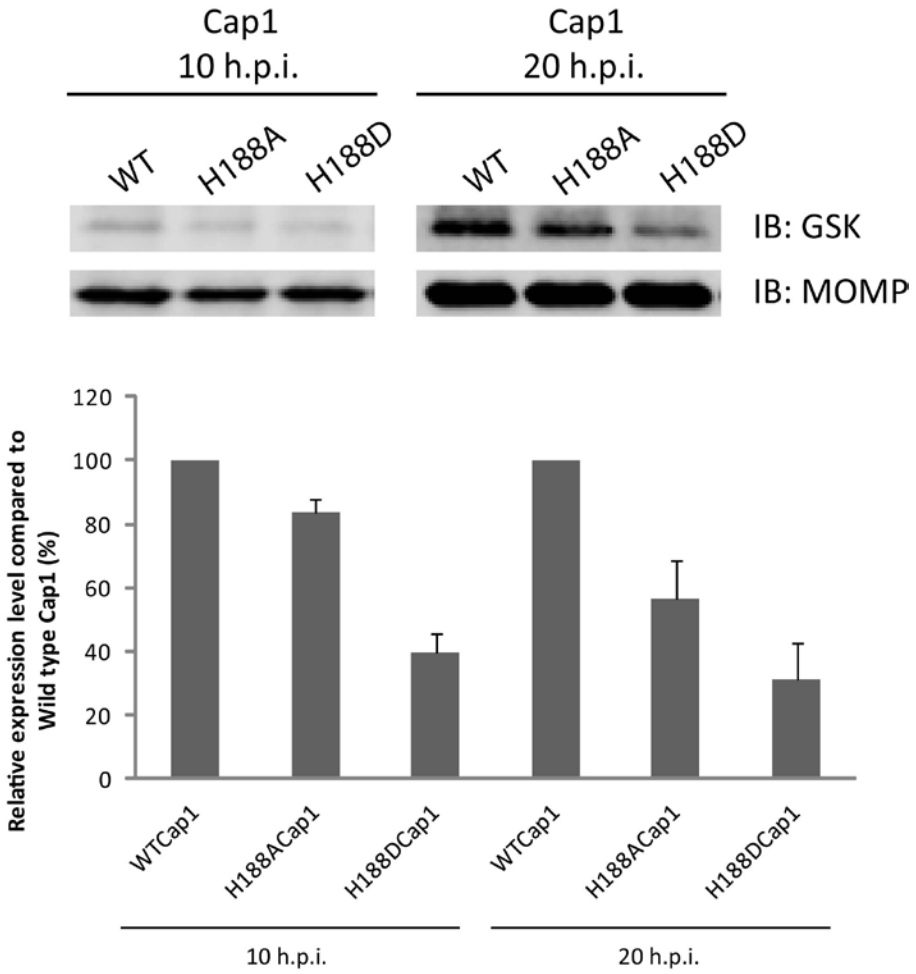

Figure 5: Mcsc binding is important for the stability of recombinant Cap1 in *C. trachomatis*. WT Cap1 and mutant constructs were transformed into *C. trachomatis* L2/434/Bu. Successful transformants were used to infect HeLa cells at an MOI of 200 and cells lysates were collected at 10 and 20 hpi. Samples were subjected to quantitative immunoblot analysis with antibodies against GSK and MOMP. GSK signals were first normalized to the MOMP signal and then compared to WT Cap1 (100%). Results shown were mean and standard deviation from three independent biological replicates.

2.3.4 Chaperone binding enhances recombinant Cap1 secretion *in vivo*

Glycogen synthase kinase (GSK) is a tag not only good for monitoring protein expression but also secretion. This 13 a.a. peptide tag is derived from the human GSK-3β kinase and is

phosphorylated at serine residue by a eukaryotic host kinase (Garcia et al., 2006). Since this tag can only be recognized by eukaryotic kinases, only the protein translocated into host cell cytoplasm is phosphorylated. This provides us a means to examine protein secretion in *Chlamydia*, as has been shown for T3S and T4S systems in other bacteria (Garcia et al., 2006). Based on this assumption, we infected HeLa cells with *Chlamydia* transformants described in the previous section and collected samples at indicated time points and analyzed samples using quantitative immunoblot. In addition to probing with anti-GSK antibody, we also probed the immunoblots with anti-phospho-GSK antibody and determined the ratio of phospho-GSK/GSK signals, which gives a direct degree of secretion. Because the phospho-GSK signals for Ct618 and H188D Cap1 were below the detection limit, we were unable to quantify the ratio. Nevertheless, we observed a 2 fold reduction in the ratio of phospho-GSK/GSK signal in H188A Cap1 compared to wild type Cap1, indicating that Mcsc binding not only stabilizes Cap1, but also enhances its secretion *in vivo* (Fig. 6).

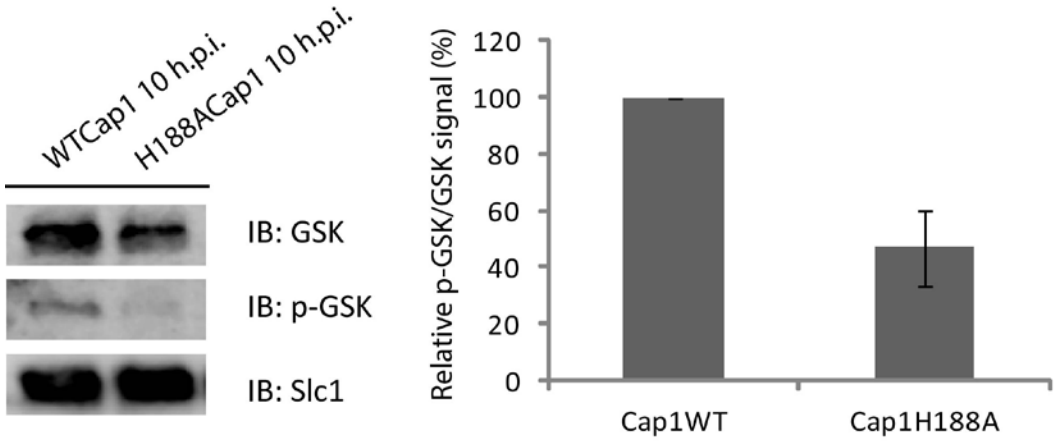

Figure 6: Mcsc binding enhances the secretion of recombinant Cap1 *in vivo*. WT Cap1 and point mutant constructs were transformed into *C. trachomatis* L2/434/Bu. Successful transformants were used to infect HeLa cells at an MOI of 200 and cells lysates were collected at 10 hpi. Samples were subjected to quantitative immunoblot analysis with antibodies against GSK, p-GSK

and MOMP. Phospho-GSK signal was divided by GSK signal and then compared to WT Cap1 (100%). Results shown were mean and standard deviation from three independent biological replicates.

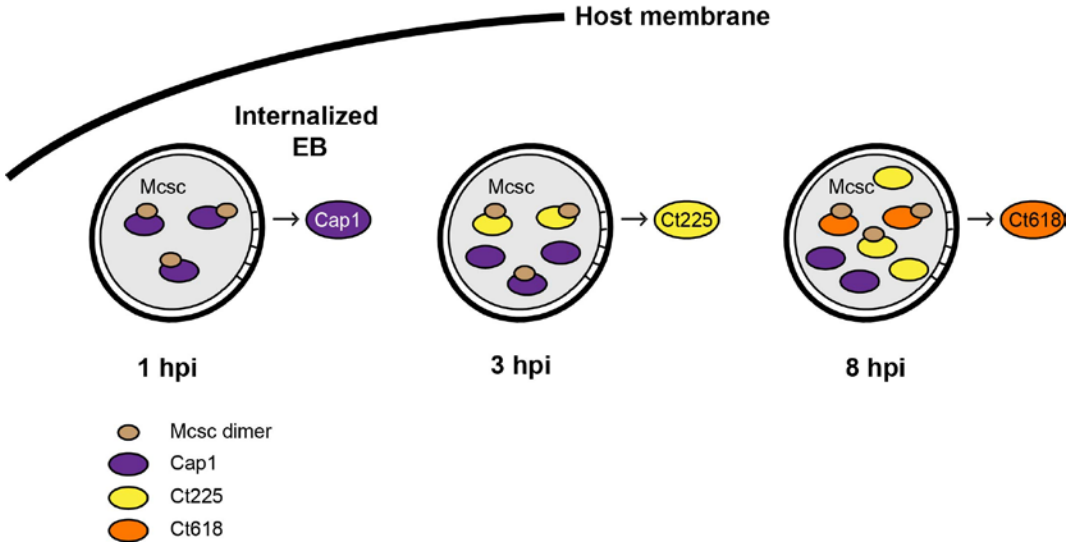

Figure 7: Model of a hierarchical secretion imparted by T3S Chaperone Mcsc during *Chlamydia* Infection. Mcsc, a class IB type III secretion chaperone in *C. trachomatis*, binds to three inclusion membrane proteins, Cap1, Ct225 and Ct618. Genes encoding these three proteins are transcribed and translated at different times post-infection. At early stage of infection, Cap1 is expressed and immediately secreted by T3S system because there is no substrate competition. Later, Ct225 is expressed and starts to compete with Cap1 for Mcsc. Since Ct225 has a higher affinity to Mcsc, Mcsc preferentially binds to Ct225 over Cap1 and the T3S system starts to secret Ct225. Similarly, when Ct618 is expressed, even though both Cap1 and Ct225 are present, because it has the highest affinity toward Mcsc among them, it binds to Mcsc and is secreted by the T3S system. hpi-hour post infection.

2.4 Discussion

New genetic tools have allowed us to examine the function of Mcsc in *Chlamydia*, which previously could only be tested in a heterologous system. By transforming with wild type and mutant effectors that are altered in their ability to bind to their chaperone, we demonstrated that Mcsc helps stabilize and enhance the secretion of at least one of its cargos, Cap1, in *C.*

trachomatis. With this technique, we can now start to ask questions such as what proteins are secreted, how the substrates are recognized and even develop new tools to knockdown target genes specifically.

T3S chaperones have been suggested to play a role in determining secretion hierarchy (Cornelis, 2006). Studies in the *Yersinia* SycE-YopE chaperone-effector system suggests that the complex might form a 3D secretion signal that can be recognized by T3S apparatus preferentially over effector alone and may contribute to the temporal order of secretion (Birtalan et al., 2002; Boyd et al., 2000). This scenario is not only observed in class 1A chaperone, which binds to one cargo, but also in class IB chaperone. Indeed, a real-time analysis of CesT-dependent traslocation revealed a distinct order in the translocation of multiple EPEC effectors, with Tir protein being the first, indicating a translocation hierarchy is established within effectors sharing the same chaperone (Mills, Baruch, Charpentier, Kobi, & Rosenshine, 2008). Since these effectors all bind to the same chaperone, an additional layer of regulation must be involved in this process. However, the source of this regulation is yet unclear. In the case of CesT-Tir in EPEC, it is proposed that temporal coexpression of effectors and chaperones may be the mechanism that confers Tir secretion priority as *cesT* and *tir* genes are cotranscribed and replacing *tir* gene with other effectors enhanced the secretion of those effectors (Thomas et al., 2007). Nevertheless, it is unlikely to be a general mechanism since most class 1B chaperones are unlinked from its cargos in genome location. It is possible that these effectors may be present in different abundances or that the 3D secretion signal is different between each chaperon-effector complex. Our study suggests that the affinity to chaperone might also contribute to this regulation.

Using isothermal titration calorimetry (ITC), Dr. Chul-Jin Lee found that Mcsc has the highest binding affinity to Ct618, then Ct225, and then Cap1 (Table 1). This order is reverse to the timing of gene transcription for these three Incs during *Chlamydia* infection and also our protein expression profile analysis (Bellend 2003) (Figure 3). We reasoned that this inverse correlation is a strategy that *Chlamydial* T3S system uses to ensure correctly ordered secretion of effectors. We proposed a model of a hierarchy secretion imparted by T3S Chaperone Mcsc during *Chlamydia* infection (Fig. 7). In the beginning of infection, because no other substrates are competing with Cap1, it binds to Mcsc and gets secreted right away. Later on when Ct225 is expressed, since some Cap1 is still inside *Chlamydia*, Ct225 will have to compete with Cap1 for limited number of Mcsc molecules. Similarly, when Ct618 is expressed, it now has to compete with both Cap1 and Ct225 for Mcsc. We hypothesized that a higher binding affinity for Mcsc allows the effector expressed later to compete with existing effector to be secreted by the system right after translation. This affinity-based regulation may be especially important for an obligate intracellular parasite like *Chlamydia* since different effectors are translated sequentially and secreted at various stages of infection to establish a suitable replicative niche inside host cells. Similar regulation may also be employed by other pathogenic Gram-negative bacteria since many T3S components are conserved (Buttner, 2012); an evolutionarily conserved mechanism may be shared.

3. Type III Secretion chaperones interact with multiple proteins in the *Chlamydia* elementary body

3.1 Introduction

3.1.1 Functions of Type III Secretion Chaperones

Chlamydia trachomatis, like many Gram-negative bacteria pathogens, use a type III secretion (T3S) system to deliver effector proteins into its mammalian host cells. The secretion of many effectors often requires help of accessory proteins, called T3S chaperones. Depending on the type of their client protein cargos, T3S chaperones can be divided into three classes: class III chaperones prevent pre-oligomerization of needle components in the bacterial cytoplasm before secretion; class II chaperones stabilize translocators by binding their hydrophobic regions, and class I chaperones stabilize and/or enhance effector secretion (Cornelis, 2006). Besides these traditional roles, additional cellular functions have been uncovered for class II and class I chaperones. For instance, SicA, a *Salmonella* T3S chaperone for the effector SipA, directly interacts with the transcriptional activator InvF, and this complex activates the expression of T3S genes (Darwin & Miller, 2001). Similarly, SycD (LcrH), the chaperone for the translocator protein YopD, functions with YopD to represses T3S effector synthesis in *Yersinia pseudotuberculosis* (Francis, Lloyd, & Wolf-Watz, 2001). In *Chlamydia*, the chaperone Scc4 (Ct663) negatively regulates σ^{66}–dependent transcription by directly interacting with both σ^{66} and β subunits of RNA polymerase (Rao et al., 2009). At least one T3S chaperone, the *Shigella* Spa15 protein, is secreted and plays a role in preventing apoptosis of the infected host cell elicited by staurosporine (Faherty & Maurelli, 2009). Furthermore, as discussed in the previous chapter, class I chaperones have been suggested to play a role in determining the secretion hierarchy of their cognate effectors.

3.1.2 *Chlamydia* T3S Chaperones

Based on their primary amino acid sequence, *C. trachomatis* encodes at least six putative T3S chaperones: Slc1(Ct043), Scc1(Ct088), Scc2(Ct576), Scc3(Ct862), Ct274 and Scc4(Ct663) (Fields KA, 2006; Stephens et al., 1998). Several studies have validated their function as chaperones and have identified the substrates they engage. For instance, Slc1 from *C. trachomatis* interacts with TARP and enhances its translocation/secretion in a heterologous *Yersinia* T3S system (Brinkworth et al., 2011; Pais et al., 2013). Scc1 and Scc4 from *C. pneumoniae* enhance the secretion of CopN, whereas Scc3 inhibits CopN secretion (Silva-Herzog et al., 2011). Scc2 is classified as a class II chaperone due to its interaction with CopB and CopD, translocator proteins in *Chlamydia* T3S system (Fields et al., 2005; Spaeth et al., 2009). Additional T3S chaperones have been defined functionally. For example, Mcsc (Multiple Cargo Secretion Chaperone), which does not share any obvious sequence homology with known chaperones, was identified based on its ability to bind and stabilize the inclusion membrane proteins, Cap1 and Ct618 (Spaeth et al., 2009). Moreover, Mcsc shares extensive structural homology to class I chaperones as detailed in chapter 2. In addition, CdsE and CdsG, chaperones of the needle component CdsF, were identified based on their interactions with CdsF and requirements for CdsF stability when expressing in *Escherichia coli* (Betts et al., 2008).

3.1.3 The EB is pre-packed with multiple T3S-related proteins

A quantitative proteomic study indicated that the EB form of *C. trachomatis* is equipped with a complete set of T3S machinery and is pre-packed with an abundant arsenal of putative T3S effectors and chaperones (Saka et al., 2011). In addition to TARP, Ct694 and Ct695, over 50 *Chlamydia*-specific hypothetical proteins lacking signal peptides (~7% of the molar mass of the

EB form) were also identified. Since multiple effectors are likely translocated during invasion, a significant number of these *Chlamydia*-specific proteins may function as effectors with important roles early in infection. Interestingly, the EB form also contains a full complement of known T3S chaperones, with Slc1, Scc2 and Mcsc being the most abundant (Fig. 8A) (Saka et al., 2011). Given their abundance and that genes encoding these chaperones are topologically unlinked from genes for their effector protein cargos; we postulated that Slc1 and Mcsc may engage additional effectors in EBs. In addition, since the homologs of Scc2 in other bacteria have been shown to perturb gene transcription and Scc2 contains tetratricopeptide repeats (TPR), which are implicated in protein-protein interactions other than cargo-chaperone interactions, we hypothesized that Scc2 may interact with other EB proteins and play regulatory roles during *Chlamydia* infection. Hence, we aimed to map the interactome of Slc1, Scc2 and Mcsc, in EBs, to 1) identify potential T3S effectors and 2) uncover additional roles these chaperones may play.

In this study, we immunoprecipitated Slc1, Scc2 and Mcsc from *Chlamydia* EB lysates and identified co-purifying proteins by mass spectrometry. We reported that Scc2 and Slc1 represent central nodes of protein interaction networks. In contrast, only a limited number of interactions were associated with Mcsc in EBs. Scc2 displayed the most extensive set of protein-protein interactions, including the putative T3S translocator proteins, CopB and CopD, proteins with known roles in carbon metabolism, several ORFs of unknown function, and components of the RNA polymerase complex. On the other hand, Slc1 co-precipitated with TARP, an effector essential for EB invasion (Jewett, Miller, Dooley, & Hackstadt, 2010), two known T3S effectors, Ct694 and Ct695, as well as several additional abundant *Chlamydia*-specific EB proteins, including a putative inclusion membrane protein, Ct365, and a hypothetical protein, Ct875. In

this chapter, we provide evidence that Slc1 formed stable complexes with these proteins *in vitro* and enhanced their secretion in a *Yersinia* T3S assay, establishing its role as a *bona fide* multi-cargo T3S chaperone. In the process, we also identified Ct875 as a potential T3S effector due to its capability to be secreted by the *Yersinia* T3S. Immunodepletion of Slc1 from EB lysates led to a co-depletion of TARP and Ct694, indicating that these effectors in EBs are all present in T3S chaperone-containing complexes. We postulate that at the EB stage, a hierarchy in protein secretion is partially imparted by T3S chaperones and that by defining the chaperone-effector landscape in EBs we might be able to assign potential roles to effector protein during invasion, nascent inclusion generation and development of early-stage infection.

3.2 Materials and Methods

3.2.1 Cell lines, bacterial strains and reagents

Chlamydia trachomatis biovar LGV, serotype L2, strain 434/Bu was propagated in HeLa cells or Vero cells maintained in Dulbecco's Modified Eagle Medium (Sigma-Aldrich, St. Louis, Missouri, USA) supplemented with 10% fetal bovine serum (FBS)(Mediatech, Manassas, Virginia, USA). EBs were purified by density gradient centrifugation using Omnipaque 350 (GE Healthcare, Princeton, New Jersey, USA) as previously described (Saka et al., 2011). All recombinant protein expression was performed in *Escherichia coli* strain BL21(DE3). The *Y. pestis* KIM8-E (Δ*ail*) strain (Bartra et al., 2008) used in this study is avirulent and is excluded from the National Select Agent Registry due to the lack of the 102-kb *pgm* locus (Une & Brubaker, 1984). In addition, this strain carries deletions of the *yopE*, *sycE* and *ail* genes and has been cured of the plasminogen activator (Pla)-encoding pPCP1 plasmid. All experiments with *Y. pestis* KIM8-E (Δ*ail*)

were reviewed and approved by the Institutional Biosafety Committee at the University of Miami. All reagents used are of analytical grade.

3.2.2 Generation of antibodies and immunoblot analysis

Antibody generation was performed as described in the previous chapter. Briefly, recombinant proteins: 10His-tagged Slc1 (Ct043), Mcsc (Ct260), and Scc2 (Ct576), and GST-tagged Ct875 were purified on affinity resins and used to immunize New Zealand White rabbits. Anti-GST antibodies were removed by pre-incubation with GST-crosslinked resins, and anti-Ct875 antibodies were affinity purified with Ct875 recombinant protein. Primary antibodies used in immunoblot analysis include anti-Tarp and Ct694 (1:1000) (generated in our laboratory), MOMP (1:2000) (gift from Dr. K. Fields), Ct875, Slc1, Mcsc and Scc2 (1:1000) (generated in this study), CdsD (1:1000) (gift from Dr. K. Fields), CopB (1:1000) (gift from Dr. T. Hackstadt) and RpoB/B' and RpoD (1:1000) (gift from Dr. M. Tan, UC, Irvine).

3.2.3 Identification of proteins that interact with T3S chaperones

Immunoprecipitation (IP). Antibodies against Slc1 and Mcsc were crosslinked separately to protein A/G resins (Pierce, Rockford, Illinois, USA) using 40 mM Dimethyl pimelimidate (Sigma-Aldrich, St. Louis, Missouri, USA) and the reactions were quenched with 40 mM ethanolamine (Sigma-Aldrich, St. Louis, Missouri, USA). Pre-immune serum was also crosslinked to resins and served as a negative control. Approximately $3x10^{10}$ EBs were lyzed by sonication in 1 mL Pierce IP lysis buffer (25 mM Tris, 150 mM NaCl, 1 mM EDTA, 1 % NP-40, 5 % glycerol; pH 7.4)(Pierce, Rockford, Illinois, USA) supplemented with 1 mM phenylmethylsulphonyl fluoride (PMSF) and 1X EDTA-free protease inhibitor cocktail (Roche, Basel, Switzerland). After centrifugation to pellet down insoluble debris, the lysate was incubated with the antibody-

crosslinked resins at 4°C for 4 hours. After 3 washes with IP lysis buffer, the bound proteins were eluted with Pierce Elution buffer (pH 2.8)(Pierce, Rockford, Illinois, USA) and separated via SDS-PAGE on a 4-12 % Bis/Tris gradient gel (Invitrogen, Life Technologies, Carlsbad, CA, USA). Lanes were sliced into 8-10 equivalent sections for in-gel digestion and analyzed by mass spectrometry at the Duke Proteomics Core facility.

Liquid Chromatography Electrospray Ionization Tandem Mass Spectrometry (LC-MS/MS). The in-gel digested peptides from each band were analyzed via LC-MS/MS as follows: Approximately ½ of each digest (5 µL) was first trapped for 5 min on a 5 µm Symmetry C_{18} 180 µm I.D. X 20 mm column at 20 µl/min in 99.9 % mobile phase A, then an analytical separation was performed using a 75 µm x 250 mm BEH C18 column (Waters Corp., Milford, Maryland, USA) with a gradient of 5 to 40 % mobile phase B over 30 minutes, with a flow rate of 0.4 µL/min at 55°C column temperature, using a nanoAcquity liquid chromatograph (Waters Corp., Milford, Maryland, USA). The mobile phase consisted of (A) 0.1 % formic acid in water and (B) 0.1 % formic acid in acetonitrile. Electrospray ionization was used to introduce the sample in real-time to a Synapt G2 Q-Tof mass spectrometer (Waters Corp., Milford, Maryland, USA), collecting data for each sample in data-dependent analysis mode with 0.6 second survey scans and three 0.6-second MS/MS scans in CID mode of the top three most abundant multiply-charged precursor ions. Raw data was processed in Mascot Distiller (v2.3) and searched in Mascot v2.2 (Matrix Science) against a concatenated database containing the deduplicated entries from NCBInr with *Chlamydia trachomatis* taxonomy (http://www.ncbi.nlm.nih.gov/pubmed/). For QToF data, search tolerances in Mascot were 10 ppm on precursor and 0.04 Da on product ions, requiring full trypsin specificity and allowing at most 2 missed cleavages. Carbamidomethylation

(+57.0214 Da, Cys) was included as a fixed modification, and deamidation (Asn and Gln) and oxidation ((+15.9949 Da, Met) were allowed as variable modifications. Scaffold (v3.6.2, Proteome Software Inc.) was used to validate MS/MS based peptide and protein identifications. Peptide identifications were accepted if they could be established at greater than 80% probability as specified by the Peptide Prophet algorithm, and protein identifications were accepted if they could be established at greater than 90% Protein Prophet probability and contained at least 2 identified peptides (Keller, Nesvizhskii, Kolker, & Aebersold, 2002; Nesvizhskii, Keller, Kolker, & Aebersold, 2003). The overall peptide and protein false discovery rate is 0 %. Results were from three independent biological replicates for Slc1 and Mcsc and two independent biological replicates for Scc2.

3.2.4 Co-purification of Slc1 with GST-tagged effectors and Gel Filtration (Size exclusion chromatography)

E. coli BL21(DE3) was co-transformed with a pET24d vector expressing Slc1 and pGEX vector alone or pGEX expressing individual GST-tagged test protein. Protein expression was induced using 0.5 mM isopropyl-1-thio-β-d-galactopyranoside (IPTG) for 3 hours at 37°C. Cells were pelleted and lysed by sonication in binding buffer (1 % Triton X-100, 20 mM Tris, 150 mM NaCl, 1 mM EDTA, 1 mM PMSF, pH 7.4), and GST–tagged proteins were isolated from the supernatant using glutathione-Sepharose beads (GE Healthcare, Pittsburgh, PA, USA). After 4 h incubation, beads were washed 3 times with binding buffer, followed by 3 washes with washing buffer (0.2 % Triton X-100, 300 mM NaCl). Bound proteins were solubilized in 1X Laemmli sample buffer (20 mM Tris-HCl, pH 6.8, 1% SDS, 5% Glycerol, 10 mM DTT, 0.01% bromophenol blue) and resolved by SDS PAGE, followed by immunoblot analysis with anti-Slc1 and –GST antibodies. Gel filtration chromatography was performed on proteins expressed in *E. coli* using a

bi-cistronic vector to co-express untagged Slc1, with His-tagged test proteins. The protein complexes were first purified using a Nickel resin (GE Healthcare, Pittsburgh, PA, USA), eluted with 500 mM imidazole and applied to a Superdex 200 gel filtration column (GE Healthcare, Pittsburgh, PA, USA) for analysis. Fractions from each sample were collected and analyzed by immunoblot with anti-His and anti-Slc1 antibodies. Size markers, alcohol dehydrogenase (150 kDa), Conalbumin (75 kDa) and Carbonic Anhydrase (29 kDa) were purchased from GE (GE Healthcare, Pittsburgh, PA, USA) and Sigma (Sigma-Aldrich, St. Louis, Missouri, USA).

3.2.5 *Yersinia pestis* T3S assays

Yersinia pestis KIM8-E (Δ*ail*) was co-transformed with the compatible plasmids pBAD33 and pBAD24 (Appendix 1) either alone or in combination with pBAD plasmids encoding T3S chaperones and putative effectors. Transformed bacteria were grown overnight at 27°C in TMH media supplemented with ampicillin and chloramphenicol. Overnight cultures were used to inoculate fresh TMH media containing 2.5 mM calcium or without calcium at OD_{620} = 0.2 and incubated for 1 hour at 27°C. L-arabinose was added to 0.2 % final concentration to induce chaperone and effector proteins expression and the culture temperature was shifted to 37°C for 5 hours. Bacteria were harvested by centrifugation and cell pellets were separated from culture supernatants. Proteins in the supernatant fractions were precipitated with 10 % (v/v) trichloroacetic acid, resuspended in 1X SDS-PAGE sample buffer and normalized to the final OD_{620} of the respective culture.

3.3 Results

3.3.1 The type III secretion chaperones Slc1 and Scc2 associate with multiple *C. trachomatis* proteins.

A quantitative proteomics analysis of *C. trachomatis* indicated that around 2% of the EB total mass is composed of T3S chaperones, with Slc1, Mcsc and Scc2 accounting for over 99% of all known T3S chaperones (Fig. 8A) (Saka et al., 2011). Slc1 forms complexes with TARP and enhances TARP translocation into HeLa cells when both proteins are co-expressed in *Yersinia enterocolitica* (Brinkworth et al., 2011; Pais et al., 2013). In EBs, the majority of TARP is in complex with Slc1, and both TARP and Slc1 are present at similar molar concentrations (Saka et al., 2011). However, since *slc1* is located ~500 kb from *tarP*, it is unlikely that Slc1 constitutes a TARP-specific Class IA T3S chaperone. Furthermore, because putative T3S effectors in EBs are present at a 10 fold molar excess over the three major T3S chaperones (Saka et al., 2011), we hypothesized that chaperones like Slc1 and Mcsc must bind multiple effectors. To test this premise we determined the compendium of EB proteins that associate with Slc1 and Mcsc. We immunoprecipitated (IP) Slc1 and Mcsc under native conditions from EB lysates and identified all proteins that associated with each individual chaperone by LC-MS/MS (liquid chromatography-tandem mass spectrometry). As previously reported (Brinkworth et al., 2011; Saka et al., 2011) TARP was one of the major proteins that co-purified with Slc1. In addition, two predicted T3S effectors, Ct694 and Ct695, and two hypothetical proteins, Ct365 and Ct875 co-purified with Slc1 (Fig. 8B). CdsD, a T3S apparatus component, and proteins involved in metabolism were also specifically detected in the Slc1 IP samples (Table 2). Interestingly, both Mcsc and Slc1 mutually co-immunoprecipitated each other. Since these chaperones are not predicted to form

heterodimers (Brinkworth et al., 2011), this result suggests that Slc1 and Mcsc homodimers may co-chaperone the same cargo, presumably Ct365, which was detected in both IP samples.

The same analysis was also performed on a class II T3S chaperone abundant in EBs, Scc2. Scc2 constituted another central hub of the T3S chaperone interactome in EBs. In addition to the known interactors CopB and CopD, the putative T3S translocator proteins in *Chlamydia* (Fields et al., 2005; Spaeth et al., 2009), several membrane-associated proteins were also detected (Fig 8B). Since a portion of Scc2 associates with *Chlamydia* membranes as shown by biochemical fractionation (Fields, Mead, Dooley, & Hackstadt, 2003), interactions with membrane proteins may keep Scc2 in close proximity to membranes. In addition, Scc2 co-precipitated with proteins with known roles in carbon metabolism, several ORFs of unknown function, and components of the RNA polymerase complex (Fig. 8B)(Table 2), implying a potential coupling between T3S activation and metabolic switches and gene transcription during early stages of *Chlamydia* infection.

A

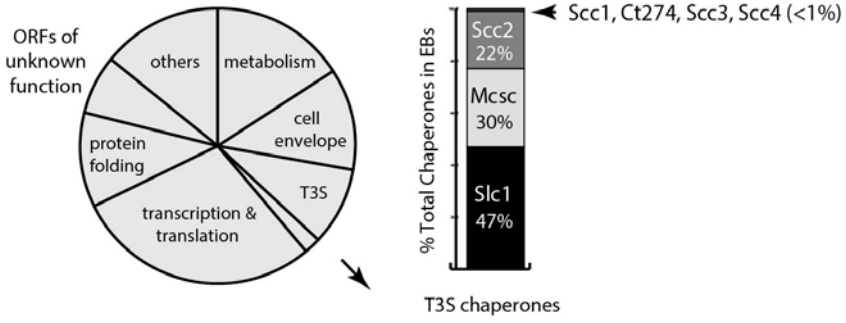

B

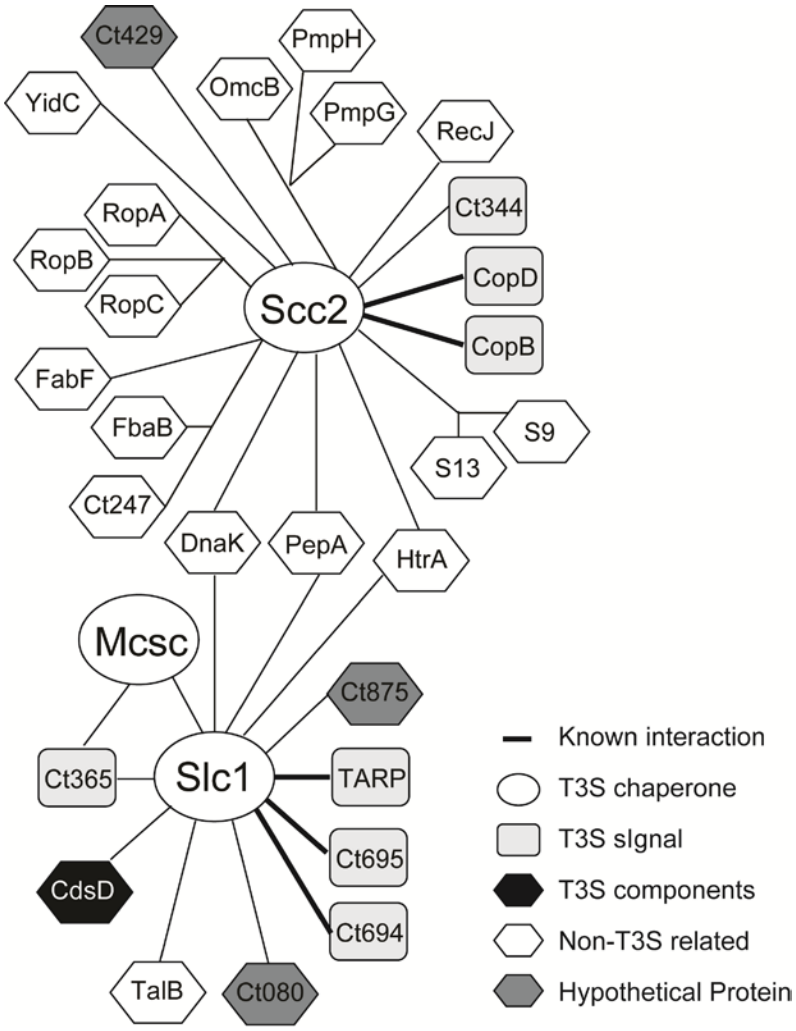

Figure 8: A distinct set of *Chlamydia* proteins associate with Slc1 and Scc2 in the Elementary Body (EB) form. A) Relative protein mass composition of the *C. trachomatis* EB. Approximately 2 % of total EB protein mass is comprised of T3S chaperones, with Slc1, Scc2 and Mcsc accounting for over 99 % of their mass. This figure represents a reanalysis of data reported in (Saka et al., 2011). B) Protein interaction network for Slc1, Scc2 and Mcsc. Cell lysates from gradient purified EBs were incubated with anti-Slc1 antibodies, anti-Scc2 antibodies anti-Mcsc antibodies, or non-specific IgG cross-linked to protein A/G resins. Bound proteins were eluted at low pH, digested with trypsin and identified by liquid chromatography coupled to tandem mass spectrometry (LC-MS/MS) (Table 2). Only proteins that displayed specific interactions are shown.

Table 2: Number of unique spectrum[a] identified by LC-MS/MS from samples immunoprecipitated with anti-Slc1, anti-Scc2 and anti-Mcsc antibodies from *Chlamydia* EBs*.

					Control				Mcsc			Slc1			Scc2	
	Identified Proteins	Accession Number[b]	M.W. (kDa)	Name[c]	Exp. 1	Exp. 2	Exp. 3	Exp. 4	Exp. 1	Exp. 2	Exp. 3	Exp. 1	Exp. 2	Exp. 3	Exp. 1	Exp. 2
1	T3S chaperone	gi|237804605	19	Mcsc (Ct260)	0	0	0	0	7	12	12	0	2	5	0	2
2	T3S chaperone	gi|237804393	18	Slc1 (Ct043)	0	0	0	1	1	1	4	7	22	31	0	1
3	T3S chaperone	gi|165931654	26	Scc2 (Ct576)	0	0	0	1	0	0	0	0	0	0	14	21
4	Putative integral membrane protein	gi|165931439	61	Ct365	0	0	0	0	0	0	8	2	2	11	0	0
5	T3S effector	gi|165930024	35	Ct694	0	0	0	0	0	0	1	6	16	23	0	0
6	T3S effector	gi|165930025	44	Ct695	0	0	0	0	0	0	0	1	8	25	0	0
7	Translocated actin-recruiting phosphoprotein	gi|48869193	103	Tarp (Ct456)	0	0	0	0	0	0	0	9	15	34	0	0
8	Translocated early phosphoprotein	gi|165930209	66	TepP (Ct875)	0	0	1	0	0	0	0	5	7	24	2	2
9	60-kDa cysteine-rich outer membrane protein precursor	gi|144487	56	OmcB (Ct443)	0	0	1	0	0	0	1	0	1	0	10	8
10	DNA-directed RNA polymerase alpha chain	gi|165931585	42	RpoA (Ct507)	0	0	2	3	0	0	3	0	1	0	10	6
11	DNA-directed RNA polymerase beta chain	gi|51538993	140	RpoB (Ct315)	0	0	0	0	0	0	0	0	0	0	20	4
12	DNA-directed RNA polymerase beta-prime chain	gi|165930512	155	RpoC (Ct314)	0	0	0	0	0	0	0	0	0	0	33	9
13	T3S translocon	gi|15605307	50	CopB (Ct578)	0	0	0	0	0	0	0	0	0	0	0	10
14	T3S translocon	gi|165931657	44	CopD (Ct579)	0	0	0	0	0	0	1	0	0	0	3	14
15	Phosphopeptide binding protein (TTS component)	gi|165929994	90	CdsD (Ct664)	0	0	0	0	0	0	0	0	12	13	0	0
16	Chaperone protein	gi|237804743	71	DnaK (Ct396)	0	0	0	0	0	0	0	0	3	10	10	4
17	Serine protease	gi|165931030	53	HtrA (Ct823)	0	0	1	2	0	0	1	0	4	4	8	3
18	Putative aminopeptidase	gi|165931129	54	PepA (Ct045)	0	0	0	0	0	0	0	0	5	3	8	2

19	Dihydrolipoamide acetyltransferase component of pyruvate dehydrogenase complex	gi|165931321	46	Ct247	0	0	0	0	0	0	0	0	1	0	6	6
20	Transaldolase	gi|165931386	36	Ct313	0	0	0	1	0	0	0	3	13	20	2	2
21	Fructose-bisphosphate aldolase	gi|165931288	38	Ct215	0	0	0	1	0	0	3	0	0	0	3	5
22	30S ribosomal protein S9	gi|255310927	15	Ct126	0	0	0	0	0	0	0	0	0	0	5	3
23	SSU ribosomal protein S13P	gi|237804860	14	Ct509	0	0	1	2	0	0	0	0	0	0	4	6
24	Late transcription unit B protein	gi|237804429	11	Ct080	0	0	0	0	0	0	0	0	1	7	0	0
25	Polymorphic membrane protein H	gi|148728350	105	PmpH (Ct872)	0	0	0	0	0	0	0	0	0	0	2	2
26	Polymorphic outer membrane protein G	gi|165931080	107	PmpG (Ct871)	0	0	0	0	0	0	0	1	0	2	4	2
27	Low calcium response protein D	gi|237802522	78	Ct090	0	0	0	1	0	0	0	0	1	1	3	1
28	Single-stranded-DNA-specific exonuclease	gi|165931524	65	RecJ (Ct447)	0	0	0	0	0	0	0	0	0	0	3	5
29	Inner membrane protein (membrane protein insertase)	gi|165931325	88	YidC (Ct251)	0	0	0	0	0	0	0	0	0	0	3	3
30	3-oxoacyl-[acyl-carrier-protein] synthase	gi|165930975	45	FabF (Ct770)	0	0	0	0	0	0	0	0	0	1	2	3
31	Hypothetical protein	gi|14195440	39	Ct429	0	0	0	0	0	0	0	0	0	0	2	3
32	ATP-dependent protease La	gi|165931419	92	Ct344	0	0	0	0	0	0	0	0	0	0	4	1

***Results shown are from three independent experiments of IP, followed by mass spectrometry analysis using control IgG antibodies and antibodies against Mcsc, Slc1 or Scc2.**

***Proteins identified with less than 3 unique spectra or found to be less than 2 fold more abundant than in control IgG samples were not included. Exp -experiment**

[a]**Unique spectrum:** Two spectra are unique if they match different peptides (even if the peptides overlap), or if they match two different charge states of the same peptide, or different modified forms of the same peptide.

[b]**Accession number for NCBI**

[c]**Gene name or CT nomenclature based on *C. trachomatis* serovar D**

3.3.2 Validation of proteomics result by immunoblots

We validated the LC-MS/MS results by immunoblot analysis of the IP materials and immunodepleted flow-through samples with antibodies specific to Slc1, Scc2 and the identified co-precipitating proteins (Fig. 9). We detected TARP, Ct694, Mcsc, CdsD and Ct875 in samples immunoprecipitated with anti-Slc1 antisera but not with pre-immune antisera. In contrast, MOMP, a very abundant EB protein, was not detected in the Slc1 IP samples, highlighting the specificity of the immunoisolations. In addition, Scc2, RpoB/B', RpoD, and CopB were detected in samples immunoprecipitated with anti-Scc2 antisera but not with pre-immune antisera (Fig. 9). As we had previously observed, immunodepletion of Slc1 from EB lysates led to a co-depletion of TARP (Saka et al., 2011). Similarly, Ct694 was also substantially depleted, indicating that these two effectors within EBs are largely present in Sc1-containing complexes. The other co-purifying targets were not efficiently co-depleted which suggest that the complexes were either unstable or present in sub-stoichiometric amounts.

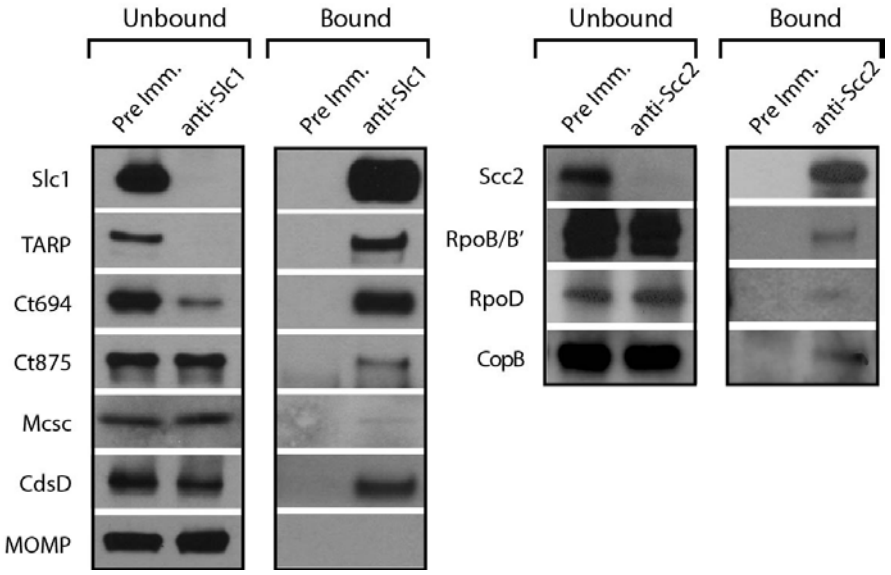

Figure 9: Specificity of Slc1 and Scc2 interactions. EB lysates were incubated with anti-Slc1 antisera, anti-Scc2 antisera or pre-immune sera, and bound proteins were captured on Protein A/G resins. The eluate (bound) and flow through (unbound) from Slc1 IP, Scc2 IP and control IP were analyzed by immunoblot with antibodies against selected proteins. MOMP (major outer membrane protein) is an abundant *Chlamydia* protein that serves as control for the specificity of the interactions shown.

3.3.3 Slc1 forms stable complexes with the effectors TARP, Ct694, Ct695 and Ct875.

We next tested if the major interactions identified for Slc1, especially those with potential T3S effectors, could be recapitulated *in vitro* with recombinant proteins. The most abundant proteins that associated with Slc1 are Ct875, TARP, Ct694, Ct695 and Ct365. We expressed these proteins as GST-tagged fusion proteins together with untagged Slc1 in *E. coli* and tested whether Slc1 would co-purify on glutathione sepharose beads. Because, we could not express the predicted inclusion membrane protein Ct365 (Toh et al., 2003) in *E. coli*, this potential effector was not studied further (data not shown). Pull downs of GST-tagged TARP, Ct694, Ct695 and Ct875 with glutathione beads led to the co-isolation of Slc1. This binding was specific as neither GST nor GST-tagged Ct288, another inclusion membrane protein (Li et al., 2008) that is present in EBs, led to Slc1 co-purification (Fig. 10A). T3S chaperones form stable complexes with a predicted 2:1 stoichiometry of chaperone to effector protein (Feldman & Cornelis, 2003). To test if such larger complexes could form, we co-expressed in *E. coli* untagged Slc1 and hexahistidine-tagged full length TARP, Ct694, Ct695, or Ct875 and isolated protein complexes on nickel resins. The bound material was eluted from the resin with imidazole and analyzed by gel filtration chromatography. All four proteins formed stable complexes with Slc1, with apparent molecular weights above 150 kDa, which are larger than that expected for 2:1

chaperone effector complexes (Fig. 10B). Although gel filtration cannot always accurately predict molecular sizes for non globular proteins (Erickson, 2009), given that TARP forms hexamers and that the oligomerization domain is distinct from the Slc1 binding domain (Brinkworth et al., 2011; Jewett et al., 2010), we postulate that size discrepancies between Slc1/Tarp and the other Slc1/effector complexes represent the formation of higher order oligomeric forms.

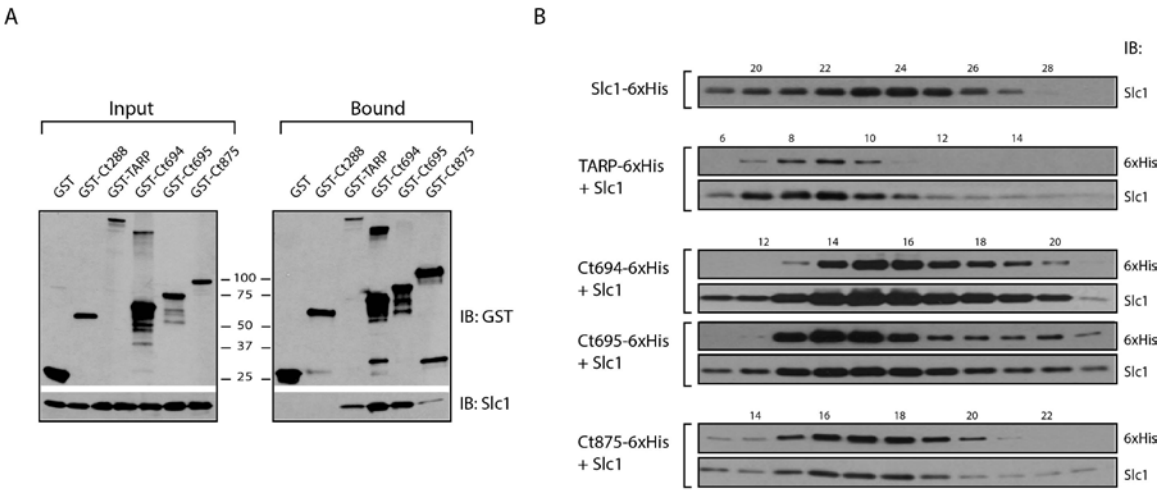

Figure 10: Slc1 associates as stable, multi-protein complexes with TARP, Ct694, Ct695 and Ct875. A-B) Slc1 binds its putative target effectors *in vitro*. Slc1 was co-expressed in *E. coli* with GST-tagged TARP, Ct694, Ct695 and Ct875 fusion proteins. The GST-tagged proteins were isolated from cell lysates with glutathione sepharose beads, and the relative levels of Slc1 co-isolated was assessed by immunoblot analysis (A). GST and GST-288 served as negative controls. To assess the relative size of these complexes, TARP, Ct694, Ct695 and Ct875 were fused to a hexahistidine tag and co-expressed with Slc1. Bound proteins were purified using a Nickel resin, eluted with 500 mM Imidazole, and analyzed by gel filtration chromatography (B). Fraction numbers are provided on the top. Molecular size markers: Alcohol Dehydrogenase (150 kDa), Conalbumin (75 kDa) and Carbonic Anhydrase (29 kDa), peaked at F16-17, F20-21 and F26, respectively. No peak was observed between fractions 8-20 in Slc1-6xHis samples in the absence of co-expressed effectors.

3.3.4 Slc1 enhances the secretion of Ct694, Ct695 and Ct875 in a heterologous T3S system

Based on the gel filtration results we speculated that Slc1, as reported for TARP (Brinkworth et al., 2011), would act as T3S chaperone and enhance the secretion of Ct694, Ct695, and Ct875. To test this premise, we reconstituted chaperone-assisted T3S in *Y. pestis* as previously described (Silva-Herzog et al., 2011). Effectors were expressed in *Y. pestis* as either untagged (Ct694 and Ct875) or FLAG-tagged (Ct695) proteins under the control of an arabinose-inducible promoter in the presence of Slc1 or Mcsc. Upon induction of T3S by calcium chelation, Ct694 and Ct695 were secreted into the supernatants as previously reported (Hower, Wolf, & Fields, 2009). The secretion of Ct694 and Ct695 was enhanced two to three fold when Slc1, but not Mcsc, was co-expressed, suggesting that Slc1 functions as a *bona fide* T3S chaperone specific for these proteins (Fig. 11). Consistent with the known behavior of most T3S chaperones, neither Slc1 nor Mcsc were secreted into supernatants (data not shown). The role of Slc1 in TARP secretion in this system could not be determined as expression of full length TARP in the presence of Slc1 hindered *Y. pestis* T3S (data not shown). Interestingly, full length Ct875 was also a target of secretion by the *Y. pestis* T3S system, even though Ct875 is not predicted to have a T3S signal (Arnold et al., 2009; Saka et al., 2011; Samudrala, Heffron, & McDermott, 2009), and its secretion was enhanced by Slc1. This suggested that Ct875 is a potential T3S effector in *Chlamydia* and Slc1 is its chaperone.

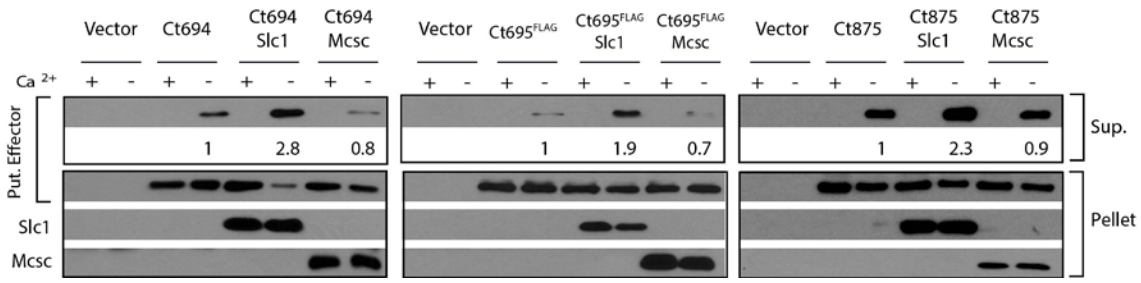

Figure 11: Slc1 enhances the T3S-dependent secretion of Ct694, Ct695 and Ct875. *Y. pestis* KIM8-E (Δ*ail*) was co-transformed with plasmids expressing Ct694, Ct875/TepP and FLAG-tagged Ct695 and untagged Slc1 or Mcsc in the combinations shown. T3S was induced by calcium chelation and the relative amount of protein secreted into the supernatants was assessed by quantitative immunoblots. Sup-cell free supernatant. Mcsc did not enhance the secretion of effectors, indicating that the secretion chaperone activity of Slc1 is specific for its target substrates.

3.4 Discussion

Immunoprecipitation followed by proteomics analysis has given us new insights into the interactome of T3S chaperones *in C. trachomatis* EB. The two most abundant class I T3S chaperones in EBs are the TARP chaperone Slc1 (Brinkworth et al., 2011; Saka et al., 2011) and Mcsc, which engages at least two inclusion membrane proteins during the RB stage (Spaeth et al., 2009). Because the genes encoding Slc1 and Mcsc are unlinked from that of their effectors, we considered the possibility that these chaperones engage multiple effectors in EBs. To test this premise we decided to identify the set of proteins that stably associate with Slc1 and Mcsc at the EB stage by IP coupled to mass spectrometry. We only found a limited number of interactions for Mcsc in EBs, suggesting that Mcsc may function mainly post entry. In contrast, Slc1 engaged at least four new substrates of the T3S system: Ct365, Ct694, Ct695 and Ct875, a protein not previously thought to harbor a T3S signal based on early prediction algorithms (Arnold et al., 2009; Samudrala et al., 2009). We provide evidence that these proteins are T3S

cargos and that Slc1 is a *bona fide* multi-cargo T3S chaperone. Consistent with our findings, Mota's group recently showed that Slc1 can interact with Ct694 and Ct695 *in vitro* and enhances their secretion in *Y. enterocolitica* (Pais et al., 2013).

Although one class 1B T3S chaperone in *Shigella* is secreted during infection (Faherty & Maurelli, 2009), Slc1 itself is unlikely to be a T3S cargo as it was not secreted by *Yersinia* under inducing conditions (data not shown). Nevertheless, we identified several additional proteins that specifically co-IP with Slc1, including the late transcription unit B protein (ltuB, Ct080), a serine protease (HtrA), a putative aminopeptidase (PepA) and a transaldolase (TalB). While not experimentally confirmed, it is unlikely that any of these proteins constitute T3S effectors as computational programs aimed at identifying T3S signals give these proteins very low confidence for T3S (www.effectors.org). Similarly, Scc2, a class II T3S chaperone, pulled down many proteins involved in carbon metabolism and transcription machinery. Since homologs of Scc2 in *Yersinia* (SycD), *Salmonella* (SicA) and *Shigella* (IpgC) contribute to repression (SycD) or activation (SicA & IpgC) of T3S gene expression (Parsot et al., 2003), the associations with components of RNA polymerase complex suggest that Scc2 may play a regulatory role similar to these homologs and modulate T3S gene expression in *Chlamydia*. At present, it is unclear whether these interactions are direct. However, one could envision scenarios wherein chaperones like Slc1 and Scc2 could interact with non-effector proteins to signal the successful entry into a host cell after it is no longer physical bound to an effector. Such a mechanism might be especially important for an intracellular pathogen like *Chlamydia*, where physical engagement of the T3S apparatus may need to be coupled to rapid metabolic adaptations, gene

transcription and post-translational modifications that drive successful colonization of the target cell.

T3S chaperones enhance the secretion of its bound cargos by stabilizing them in the bacterial cytosol or maintaining them in a secretion competent state (Parsot et al., 2003). In addition, T3S chaperones can also prioritize the secretion of cognate effectors as exemplified by YopE, a *Yersinia* T3S effector, whose secretion is severely impaired in the presence of other effectors when lacking a SycE chaperone binding site, indicating that additional secretion signals are either unmasked or conferred by the T3S chaperone (Boyd et al., 2000). Similarly, a real-time analysis of CesT-dependent traslocation revealed a distinct order in the translocation of enteropathogenic *Escherichia coli* effectors and the effector-chaperone interaction is suggested to be one of the determining factors of translocation efficiency (Mills et al., 2008). Based on these findings, we hypothesized that T3S chaperones would play a prominent role in establishing a hierarchy to the secretion of effectors by *Chlamydia* EBs. The most abundant T3S chaperone in EBs is Slc1, which, like CesT, engages multiple effectors. TARP, one of Slc1s' cargoes (Brinkworth et al., 2011), is secreted within 5 min upon EB attachment to epithelial cells (Clifton et al., 2004). Interestingly, the majority of TARP in EBs is found pre-complexed with Slc1 (Fig. 9) (Saka et al., 2011), implying that this pre-engagement with its chaperone could prime TARP for rapid secretion. Similarly, a significant proportion of Ct694 within EBs is pre-complexed with Slc1 (Fig. 9), suggesting that Ct694 may be also secreted very early during infection, possibly at the same time as TARP. In contrast, only a minor portion of Ct875 was present in complexes with Slc1 in EBs, even though Ct875 is more abundant than TARP and Ct694 (Saka et al., 2011). Given these observations, we considered a model wherein T3S

substrates pre-bound by Slc1 in EBs, such as TARP and Ct694, will be delivered first, followed by Ct875 and potentially others effectors which do not exist as pre-formed chaperone complexes in EBs.

4. Identification of TepP as a new tyrosine-phosphorylated T3S effector that mediates a host scaffolding protein recruitment to nascent inclusions and host innate immune signaling

4.1 Introduction

4.1.1 T3S effectors in *Chlamydia*

Like many Gram-negative bacterial pathogens, *Chlamydia* uses a type III secretion (T3S) system to deliver effector proteins into their target host cells (reviewed in (Peters et al., 2007)). These effectors interfere with diverse host cellular processes including signaling, cytoskeletal rearrangements, and vesicle trafficking to enhance bacterial entry, establish a replicative niche and evade innate immunity (Betts et al., 2009). At early stage of infection, the Translocated Actin Recruiting Protein (TARP) is delivered into the host cytoplasm after bacterial attachment (Clifton et al., 2004). TARP facilitates invasion by mediating actin re-arrangements through the direct nucleation of F-actin polymerization and the recruitment of Rac-specific guanine nucleotide exchange factors (Jewett et al., 2010; Lane, Mutchler, Al Khodor, Grieshaber, & Carabeo, 2008). Another T3S effector, Ct694, is delivered into host cells during *Chlamydia* entry where it engages the cytoskeletal organizing protein AHNAK (Hower et al., 2009). After entry, a new set of T3S effectors are synthesized and translocated to the inclusion membrane (Inc proteins) (Rockey, Scidmore, Bannantine, & Brown, 2002) where they mediate the recruitment of host proteins such as SNAREs, 14-3-3β, Rab proteins, signaling molecules and lipid transporters (Delevoye et al., 2008; Derre et al., 2011; Rzomp et al., 2006; Scidmore & Hackstadt, 2001). At later stages of infection, *Chlamydia* protein associating with death domains (CADD), is translocated into the host cell cytoplasm and interacts with death domains of tumor necrosis factor (TNF) family receptors and potentially induces apoptosis of infected cells

(Stenner-Liewen et al., 2002). In addition, Ct847, a mid-cycle gene product, interacts with host Grap2 cyclin D-interacting protein (GCIP), a multifunctional protein involved in cell cycle which is degraded in a proteasome-dependent pathway during *Chlamydia* infection (Chellas-Gery, Linton, & Fields, 2007). Depletion of GCIP by siRNA prior to infection confers a growth advantage to *C. trachomatis* L2; nevertheless, whether Ct847 directly mediates GCIP degradation is still unclear.

Although T3S effectors share a signal sequence at their N-terminus, these signals are relatively unstructured and poorly conserved, rendering computational prediction difficult. Although two algorithms are now available to predict T3S substrate, the prediction power is limited and has a high error rate (Mueller et al., 2013). Because until recently *Chlamydia* could not be readily manipulated with molecular genetic tools, most approaches to identify effectors have been indirect and relied on heterologous expression systems (Valdivia, 2008). In this manner, it is predicted that approximately 5-8 % of the *C. trachomatis* genome, or 45-70 genes, encode proteins for T3S. However, few effectors have been confirmed as secreted and even fewer have described functions. This is especially true for the early stage of infection, in which only two effectors, TARP and Ct694, have been experimentally validated in *C. trachomatis* to date (Clifton et al., 2004; Hower et al., 2009). Given the complexity of this early stage of infection, which comprises invasion and establishment of the early replicative niche, more effectors are expected to be involved in this process and await discovery.

4.1.2 Bacterial effector proteins are subjected to tyrosine-phosphorylation upon translocation into their target host cells

Through co-evolution with their hosts, pathogens have evolved many mechanisms to hijack host cellular processes. One common strategy is to commandeer host signaling pathways through routes such as relocating host signaling molecules and inducing post-translational modifications (PTM) of host proteins or effectors themselves (Ribet & Cossart, 2010). An emerging field of bacteria-associated PTM is tyrosine phosphorylation as exemplified by Tir and CagA in Enteropathogenic *Escherichia coli* (EPEC) and *Helicobactor pylori*, respectively (Backert & Selbach, 2005). Tir (translocated intimin receptor) is secreted by the EPEC T3S system and inserts itself into the host plasma membrane. After binding to the bacterial outer membrane protein, intimin, Tir is phosphorylated at tyrosine residue by multiple host kinases, triggering actin nucleation and pedestal formation beneath adherent bacteria (Kenny, 1999). On the other hand, CagA from *H. pylori* is tyrosine-phosphorylated upon translocation to host cells by T4S and this phosphorylation induces global cytoskeletal rearrangements, leading to cell scattering and elongation (Backert, Moese, Selbach, Brinkmann, & Meyer, 2001; Moese et al., 2004). In the case of *C. trachomatis*, TARP is tyrosine-phosphorylated after translocation and this phosphorylation is important for interactions with guanine nucleotide exchange factors, Sos1 and Vav2, and subsequent actin remodeling (Lane et al., 2008). Additionally, phosphorylated TARP interacts with SHC1, a host adaptor protein that regulates apoptosis and growth-related genes (Mehlitz et al., 2010). SHC1 is phosphorylated and activated during *Chlamydia* infection in a phospho-TARP-dependent manner and SHC1 knockdown sensitized infected host cell to apoptosis, suggesting SHC1 activation stimulates survival signals to host cells. Significantly, phosphotyrosine immunoblot of cells early after *Chlamydia* infection indicates that multiples

proteins besides TARP are tyrosine-phosphorylated (Birkelund, Johnsen, & Christiansen, 1994; Fawaz, van Ooij, Homola, Mutka, & Engel, 1997). Two studies reported that host proteins, cortactin and ezrin, contribute to the observed signals (Fawaz et al., 1997; Swanson, Crane, & Caldwell, 2007). Nevertheless, since the molecular weights of these proteins only partially overlap the observed signals, additional unidentified proteins must exist.

In chapter 3, we immunoprecipited Slc1 from *Chlamydia* EB lysates and identified co-purifying proteins by mass spectrometry. In this manner, we determined that Slc1 is in complex with multiple T3S effectors and that co-expression of Slc1 enhanced the secretion of these effectors in *Yersinia pestis*. In this chapter, we describe how, based on this information, we identified and characterized a new effector, TepP (Translocated early phosphoprotein – Ct875), which is tyrosine-phosphorylated upon translocation into host cells. Given that TepP phosphorylation at Tyr residues occurs later with respect to TARP phosphorylation, we postulate that TARP may be secreted before TepP. We further show that phosphorylated TepP associates with host scaffolding proteins Crk-I and Crk-II and that the recruitment of Crk proteins to nascent inclusions is absent in cells infected with a *Chlamydia* mutant harboring a *tepP* null allele and is restored in complemented strain. In addition, endocervical epithelial cells infected with this mutant exhibited transcriptional changes in a subset of innate immunity-related genes and different cell morphology compared to cells infected with complemented strain. We propose a model wherein TepP acts downstream of TARP to recruit scaffolding proteins that initiate and amplify signaling cascades important for establishing a replicative niche for *Chlamydia* within the infected host.

4.2 Materials and Methods

4.2.1 Cell lines, bacterial strains and reagents

Chlamydia trachomatis biovar LGV, serotype L2, strain 434/Bu was propagated in HeLa cells or Vero cells maintained in Dulbecco's Modified Eagle Medium (Sigma-Aldrich, St. Louis, Missouri, USA) supplemented with 10% fetal bovine serum (FBS) (Mediatech, Manassas, Virginia, USA). Human endocervical epithelial A2EN cells (Buckner et al., 2011) were maintained in keratinocyte-SFM medium (Gibco, Life Technologies corp., Grand Island, NY, USA) supplemented with 10 % FBS, 0.5 ng/mL human recombinant epidermal growth factor and 50 µg/mL bovine pituitary extract. EBs were purified by density gradient centrifugation using Omnipaque 350 (GE Healthcare, Princeton, New Jersey, USA) as previously described (Saka et al., 2011). All recombinant protein expression was performed in *Escherichia coli* strain BL21(DE3).

4.2.2 Indirect immunofluorescence staining

Approximately $5x10^4$ HeLa cells/well were seeded onto glass coverslips placed in a 24 well plate. The following day, cells were incubated with LGV-L2 EBs at an MOI of 20 and infections were synchronized by centrifugation (3000 rpm for 30 min) at 10°C followed by transferring the plates to a 37°C, 5 % CO_2 humidified incubator. At the indicated time points, the coverslips were fixed either with 100% methanol on ice for 15 min or with 3% formaldehyde/0.025% glutaraldehyde at room temperature for 20 min. Cells were then permeabilized with 0.2 % Triton in phosphate buffer saline solution (PBS), blocked with 3 % BSA in PBS for 30 min and stained with antibodies against TepP (1:10), mouse LPS (1:250)(EV1-H1), rabbit MOMP (1:250)(gift from K. A. fields), phosphotyrosine (1:100) (Cell signaling #9411), Slc1

(1:100), Crk (1:10)(BD Transduction Laboratories 610035 clone 22). DAPI (Invitrogen Life Technologies, Carlsbad, CA, USA) was used for staining nucleic acids. To permeabilize EBs at very early time points, 0.005% SDS in PBS was used. The images were further deconvolved using Huygens software (Scientific Volume Imaging, Hilversum, Netherlands).

4.2.3 Protein lysates and IP of effector proteins

For small-scale infections, ~10^5 HeLa cells were seeded per well in 24-well plates the day before experiment. Cells were incubated with LGV-L2 or its mutant derivatives at a MOI of 100 and infections were synchronized by centrifuging at 3000 rpm for 30 min at 10°C, followed by a shift to 37°C. Samples were collected at indicated time points by washing the well once with PBS followed by adding 90 µl 2X Laemmli sample buffer. For IPs of effector proteins, ~$5x10^6$ HeLa cells were pre-seeded into a 10-cm cell culture dish the day before infections and cells were incubated with LGV-L2 or its mutant derivatives at a MOI of 100. Infections were synchronized by pre-incubation for 1 hour at 4°C in Hanks balanced salt solution, followed by the addition of DMEM media pre-warmed to 37°C. At the indicated time points, infected cells were washed two times with ice-cold PBS and lyzed in 1 mL Pierce IP lysis buffer supplemented with 1 mM PMSF, protease inhibitor cocktail and Halt phosphatase inhibitor (Pierce, Rockford, Illinois, USA). After sonication and high speed centrifugation to remove insoluble debris, antibodies against TARP (Jorgensen et al., 2011) or TepP were added to cell lysates and incubated for 3 hours at 4°C. Protein A resin was added to isolate immunocomplexes, washed thoroughly with Pierce IP lysis buffer, and bound proteins were resolved by SDS PAGE and subjected to immunoblot analysis. Primary antibodies used in immunoblot include IFIT2

antibody (Sigma-Aldrich #SAB1405991), phosphotyrosine (Cell signaling #9411), and Crk (BD Transduction Laboratories 610035 clone 22) with 1:1000 dilution in 3% BSA/TBST.

4.2.4 *In vitro* GST-Crk binding assay

Hexahistidine-tagged TepP was purified on Nickel resin (Qiagen, Valencia, CA, USA) and beads with bound TepP were aliquoted into three tubes. Two tubes were incubated with HeLa cell lysates for *in vitro* phosphorylation for 1 hour at 4°C and one of the tubes was further treated with Alkaline Phosphatase, Calf Intestinal (CIP)(New England BioLabs, Ipswich, MA, USA) 50 Unit/rxn to reverse phosphorylation reactions at 37°C for 40 min in NEB buffer 3. To prepare HeLa cell lysates for *in vitro* phosphorylation, around $3x10^6$ HeLa cells were lyzed in *in vitro* kinase buffer (100 mM KCl, 10 mM HEPES, pH 7.7, 2 mM $MaCl_2$ and 2 mM ATP) supplemented with PMSF, Halt phosphatase inhibitor (Pierce, Rockford, Illinois, USA) and protease inhibitor cocktail (Roche, Basel, Switzerland). Cell debris was removed by centrifugation. The last tube was incubated with *in vitro* kinase buffer only as a control. Purified GST and GST-Crk were added to tubes containing TepP, phospho-TepP or CIP-treated TepP and incubated in the cold room for 2 hours. After washing resins four times with Pierce IP lysis buffer (25 mM Tris, 150 mM NaCl, 1 mM EDTA, 1 % NP-40, 5 % glycerol; pH 7.4)(Pierce, Rockford, Illinois, USA), bound proteins were denatured in sample buffer and analyzed by immunoblots with anti-GST, -Crk, -TepP and -p-Tyr antibodies.

4.2.5 Identification of TepP phosphorylation sites by LC-MS/MS

IP. Two 15-cm cell culture dishes of confluent HeLa cells were infected with LGVL-2 at a MOI of 100 as described above. Another two dishes of confluent HeLa cells were mock-infected. Four hours post treatment, cells were collected, washed twice with PBS and lyzed as previously

described (Tsai & Carstens, 2006) to generate cytosolic and nuclear/EB fraction. After clarifying the cytosolic fraction by high speed centrifugation, antibodies against TepP were added to the infected and control cell lysates and incubated for 3 hours at 4°C with continuous mixing. Immunocomplexes were purified with protein A resin and bound proteins were solubilized in SDS sample buffer.

Phosphopeptide Sample Preparation and Nano-Flow LC-MS/MS Analysis. Following 1D-SDS-PAGE separation, the molecular weight region corresponding to that of TepP was excised and subjected to an in-gel trypsin digestion as previously described (Wilm et al., 1996). Extracted peptides were brought to dryness using vacuum centrifugation and resuspended in 100 µL 80 % acetonitrile, 1 % TFA, 50 mg/mL MassPrep Enhancer, pH 2.5 (Waters Corp., Milford, Maryland, USA). Phosphopeptides were enriched using a 200 µL TiO2 Protea Tip (Protea Bio., Morgantown, WV, USA) and subsequently washed with 200 µL 80 % acetonitrile, 1 % TFA, 50 mg/mL MassPrep Enhancer followed by 200 µL 80 % acetonitrile, 1 % TFA. Peptides were eluted in 50 µL 20 % acetonitrile, 5 % aqueous ammonia, pH 10.5 and then acidified to pH 2.5 with formic acid prior to drying using vacuum centrifugation.

Samples were resuspended in 10 µL 2 % acetonitrile, 0.1 % formic acid, 10 mM citric acid and subjected to chromatographic separation on a Waters NanoAquity UPLC, in the same manner as described for the immunoprecipitation samples, with the following exceptions: the analytical column was held at 5 % B for 5 min at the beginning of the analytical separation, prior to a linear elution gradient of 5 % B to 40 % B over 30 min. The analytical column was connected to a fused silica PicoTip emitter (New Objective, Cambridge, MA) with a 10 µm tip orifice and

coupled to an LTQ-Orbitrap XL mass spectrometer through an electrospray interface. The instrument was set to acquire a precursor MS scan in the Orbitrap from *m/z* 400-2000 with r = 60,000 at *m/z* 400 and a target AGC setting of 1e6 ions. In a data-dependent mode of acquisition, MS/MS spectra of the three most abundant precursor ions were acquired in the linear ion trap with a target AGC setting of 5e3 ions. Max fill times were set to 1000 ms for full MS scans and 250 ms for MS/MS scans with minimum MS/MS triggering thresholds of 5000 counts. For all experiments, fragmentation occurred in the LTQ linear ion trap with a collision-induced dissociation (CID) energy setting of 35% and a dynamic exclusion of 60 s was employed for previously fragmented precursor ions.

Qualitative Identifications and residue specific phosphorylation localization from Raw LC-MS/MS Data. Raw data was processed in Mascot Distiller (v2.3) and searched in Mascot v2.2 (Matrix Science) against a concatenated database containing the deduplicated entries from NCBInr with *Chlamydia trachomatis* taxonomy. Search tolerances for LTQ-Orbitrap XL data were 10 ppm for precursor ions and 0.8 Da for product ions using trypsin specificity with up to two missed cleavages. Carbamidomethylation (+57.0214 Da, C) was set as a fixed modification, whereas oxidation (+15.9949 Da, M) and phosphorylation (+79.9663 Da, S, T, and Y) were considered a variable modifications. All searched spectra were imported into Scaffold and confidence thresholds were set using the PeptideProphet and ProteinProphet algorithms which yielded a peptide and a protein false discovery rate of 0% (Keller et al., 2002; Nesvizhskii et al., 2003). Phosphorylation site localization was assessed by exporting peak lists directly from Scaffold into the online AScore algorithm (*ascore.med.harvard.ed)(Beausoleil, Villen, Gerber, Rush, & Gygi, 2006).*

4.2.6 Identification and whole genome sequencing of a TepP-deficient LGV-L2 strain.

A strain containing a *G309A* (W103*) null allele in *tepP* was initially identified by whole genome sequencing of a collection of ethyl methyl sulfonate (EMS)-mutagenized and plaque-purified *C. trachomatis* LVG-L2 strains generated as previously described (Nguyen & Valdivia, 2012)(Bastidas R. J. and Valdivia R. H. unpublished results). Strain CTL2-M062 harboring *tepP G309A* was identified from a pool of 20 mutants by Sanger sequencing of the *tepP* locus (CTL0255). CTL2-MO62 was recovered in sucrose-phosphate-glutamate (SPG) buffer (0.22 M sucrose, 0.01 M potassium phosphate, 0.005 M L-glutamic acid, pH 7.0) after hypotonic lysis of a monolayer of infected HeLa cells grown in a 10-cm^2 cell culture dish. Lysates were sonicated (2 x 10 seconds in ice water) and bacterial cells were spun down at 14,000 rpm, for 15 minutes at 4 °C, and resuspended in 1X DNAse I buffer (New England Biolabs, Ipswich, MA, USA). Cell suspensions were treated with 4 Units of DNAse 1 (New England Biolabs, Ipswich, MA, USA) for 1 hour at 37 °C to deplete contaminating host DNA. Following a wash with PBS buffer, total DNA was isolated with a DNA isolation kit (DNeasy tissue and blood kit, Qiagen, Valencia, CA, USA) as described by the manufacturer.

For whole genome sequencing, 1 μg of CTL2-M062 enriched DNA was fragmented with an Adaptive Focused Acoustics S220 instrument (Covaris, Inc. Woburn, MA, USA), and DNA sequencing libraries were prepared with a library construction kit (TruSeq DNA Sample Preparation Kit v2, Illumina, Inc. San Diego, CA, USA) according to the manufacturer's instructions. Libraries were sequenced in a MiSeq DNA Sequencing Platform (Illumina, Inc. San Diego, CA, USA) at the Duke University IGSP DNA Sequencing Core facility. Genome assembly

and single nucleotide variant (SNV) identification was performed with Geneious Software version 6 (Biomatters - http://www.geneious.com/). The *C. trachomatis* L2 434/Bu genome (GenBank no. NC_010287) was used as reference sequence. All non synonymous SNVs identified in CTL2-M062 (Table 3) were independently verified by Sanger sequencing.

4.2.7 Generation of *Chlamydia* Recombinant strains

Chlamydia recombinants were generated as previously described (Nguyen & Valdivia, 2012). Briefly, confluent Vero cells grown on a 24-well plate were co-infected with CTL2-MO62 (Rifampin resistant, Rif^R) and a Spectinomycin resistant mapping strain (Spc^R) at a ratio of 2:4 and recombinant progeny were selected from among plaques that formed in the presence of Rif (200 ng/mL) and Spc (200 µg/mL). Plaque-purified recombinants were further expanded in Vero cells and genotyped with SNV specific primers.

4.2.8 *Chlamydia* Transformation

The gene encoding TepP and its predicted promoter region (300 bp upstream of the TepP start codon) was amplified by PCR from LGV-L2 genomic DNA and inserted into the *E. coli-Chlamydia* shuttle vector p2TK2-SW2 (Agaisse & Derre, 2013). The recombinant $TepP^{W103*}$ strains (G1) were transformed with either empty vector or vector harboring wild type TepP as previously described with some modifications (Wang et al., 2011). Briefly, around $4x10^6$ Vero cells treated with transformation buffer (10 mM Tris pH 7.4 in 50 mM $CaCl_2$) were infected with G1 pre-incubated with around 6 µg plasmid in transformation buffer. Transformed *Chlamydia* was selected under 1U of penicillin G (Sigma P3032) for several passages. After initial selections, transformed *Chlamydia* was maintained in the presence of 10U penicillin G. TepP expression was confirmed by immunoblot analysis.

4.2.9 Infectious Forming Unit (IFU) assay

Confluent monolayers of HeLa cells were infected with various *Chlamydia* strains at an MOI < 1. Bacteria in infected cells were harvested at 28 hpi by hypotonic lysis as previously described (Nguyen & Valdivia, 2013). Serial dilutions of the cell lysates were used to infect a new monolayer of HeLa cells and inclusions were detected by immunostaining with anti-Slc-1 antibodies at 24 hpi. The number of inclusions was counted under a fluorescence microscope. The total number of IFUs obtained at 28h (output) was divided by the number of input bacteria to derive number of infectious progeny per input bacteria.

4.2.10 Crk siRNA knockdowns

HeLa cells were transfected either with siRNAs designed against Crk (Qiagen Cat. No. 1027416) or with negative control siRNA (Qiagen Cat. No. 1027280) using Lipofectamine RNAiMAX reagent (Invitrogen, Life Technologies, Carlsbad, CA, USA). At 48 h post transfection, cells were harvested and analyzed by immunoblot with anti-Crk and anti-Nup62 (loading control) (Mab414, Covance, Princeton, NJ, USA). For IFU assay, cells were infected with wild type LGV-L2 at an MOI < 1 for 28 hr after 48 hr of siRNA transfection. IFU was determined as described above.

4.2.11 Microarray analysis

Approximately 0.8 x 10^6 A2EN cells were seeded per well in 6-well plates the day before experiment. Duplicate cells samples were mock infected, or infected with the *tepP* mutant strain transformed with empty vector or the vector harboring wild type *tepP* at an MOI of 10. Infections were synchronized by centrifugation at 3000 rpm for 30 min at 10°C, followed by an immediate shift to 37°C with pre-warmed cell culture media. Samples were collected at 4 hpi

using QIAGEN RNeasy Plus Mini Kit (QIAGEN, Valencia, CA, USA) as described by the manufacturer. RNA integrity was assessed with Agilent 2100 Bioanalyzer G2939A (Agilent Technologies, Santa Clara, CA, USA) and quantified with a Nanodrop 8000 spectrophotometer (Thermo Scientific/Nanodrop, Wilmington, DE, USA). Hybridization targets were prepared with MessageAmp Premier RNA Amplification Kit (Applied Biosystems/Ambion, Austin, TX, USA) from total RNA, hybridized to GeneChip Human Genome U133A 2.0 arrays in Affymetrix GeneChip hybridization oven 645, washed in Affymetrix GeneChip Fluidics Station 450 and scanned with Affymetrix GeneChip Scanner 7G according to standard Affymetrix GeneChip Hybridization, Wash, and Stain protocols (Affymetrix, Santa Clara, CA, USA). Data analysis was performed using Partek Genomic Suite 6.6 (Partek Inc., Saint Louis, MO, USA).

4.2.12 Quantitative real-time PCR (Q-PCR)

Q-PCR was performed using *Power* SYBR Green RNA-to-C_T 1-*Step* Kit and StepOne Real-Time PCR system as described by the manufacturer (Applied Biosystems, Grand Island, NY, USA). Primers specific for IL-6, CXCL3, MAP3k8, IFIT1, IFIT2, and Actin were designed using Roche Universal Probe Library (http://www.roche-applied-science.com) and are listed in Appendix 2. Primers against *Chlamydia* 16S rRNA were used to quantify the amount of bacteria in each sample (Appendix 2).

4.2.13 GFP-TepP pulldown

A stable cell line constitutively expressing GFP-TepP was made using retrovirus packed with pLEGFP-C1/TepP. Virus packaging was achieved by co-transfecting GP2-293 cell line (Clontech Laboratories, Inc. Mountain View, CA, USA) with both pVSV-G and pLEGFP-C1/TepP using FuGENE6 (Promega, Madison, WI, USA). HeLa cells were transduced with virus, followed

by 400 µg/mL Geneticin (G418) (Gibco, Life Technologies corp., Grand Island, NY, USA) selection. The cell line was further sorted by fluorescence-activated cell sorting (FACS) to enrich GFP-TepP expressing cells. Four confluent T175 flasks (around 6 x 10^7 cells) were used for pull-down. Another four T175 flasks of confluent cells expressing GFP alone were used as a control. Cell lysates were incubated with GFP-Trap_A beads (Chromotek, Martinsried, Germany) and bound proteins were eluted with 70 µl Pierce elution buffer (pH 2.8) and added with 20 µl 5X Laemmli Sample Buffer. Samples were analyzed by SDS page and stained with colloidal blue staining kit (Novex, Life Technologies, Carlsbad, CA, USA). Areas between 25 kDa and 188 kDa were sliced into five gels for each sample and submitted for mass spectrometry analysis.

4.2.14 Cell morphology analysis after infection

Confluent A2EN cells in a 24-well plate were infected with either CTL2-M062G1+pV or CTL2-M062G1+pTepP with an MOI of 50 by centrifuging at 3000 rpm for 30 min at 10°C. Images for cell morphology were taken 1 hour after shifting to 37°C using DIC (differential interference contrast)(Carl Zeiss, Oberkochen, Germany). For immunoblot analysis, samples were collected at 8 hpi and probed with anti-TepP, MOMP and actin antibodies.

4.3 Results

4.3.1 Ct875 (TepP) is translocated early during *Chlamydia* infection.

Ct875 is the most abundant *Chlamydia*-specific hypothetical protein pre-packed in EBs (Saka et al., 2011). As described in the sections below, we renamed Ct875 as TepP to reflect the new functions for this protein defined in this study. Since this protein can be secreted by *Yersinia* T3S system as shown in the previous chapter (Fig. 11), we speculated that this potential

T3S effector is secreted early during EB attachment to cells and that it plays a role in invasion and/or establishment of the nascent inclusion. Consistent with this, an analysis of Ct875/TepP localization by immunofluorescence microscopy indicated a close association of Ct875/TepP with EBs by 2 hours post infection (hpi) in HeLa cells (Fig. 12 upper panel). However, the localization of Ct875/TepP was distinct from that of chlamydial LPS, suggesting translocation of Ct875/TepP from the EB at attachment sites. This localization pattern is similar to what has been described for TARP and Ct694 (Hower et al., 2009), and is clearly distinct from that of Slc1 which is mostly localized to the bacterial cytosol (Fig. 12 lower panel). Overall, these findings provide experimental evidence that Ct875/TepP is a new T3S effector translocated early during EB entry into epithelial cells.

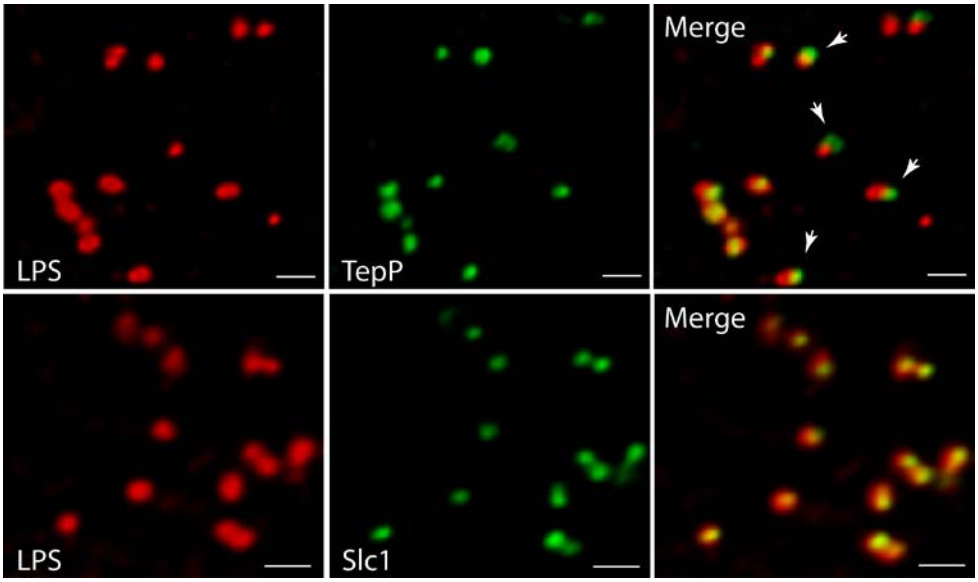

Figure 12: Ct875/TepP is secreted at *Chlamydia* entry sites. Ct875/TepP is secreted from EBs early during infection. HeLa cells were infected with LGV-L2 at an MOI of 20 for 2 hr. Cells were fixed, permeabilized and immunostained with antibodies against *Chlamydia* LPS (red), Ct875/TepP (green) and Slc1 (green). Scale bar: 1 μm.

4.3.2 TepP (Ct875) is phosphorylated upon infection with kinetics distinct from TARP.

Approximately 5-6 distinct proteins are tyrosine-phosphorylated early upon infection with *C. trachomatis* (Birkelund et al., 1994; Fawaz et al., 1997). Most of these proteins were originally assumed to be host proteins that were phosphorylated as a consequence of the activation of multiple kinase signaling pathways by *Chlamydia*, until TARP was identified as one of these major tyrosine-phosphorylated proteins (Clifton et al., 2004). Because Ct875/TepP has a molecular weight of 65 kDa, similar to one of the major tyrosine-phosphorylated protein detected within 15 min of *C. trachomatis* LGV-L2 infection (Birkelund et al., 1994)(Fig. 13A), we considered the possibility that Ct875/TepP is also tyrosine-phosphorylated. Consistent with this, analysis by indirect immunofluorescence microscopy indicated that anti-Ct875/TepP and anti-phosphotyrosine signals co-localized around bacteria at 2 hpi (Fig. 13B). Next, we determined that Ct875/TepP immunoprecipitated from infected HeLa cell lysates, but not from EBs lysates, was detected by anti-phosphotyrosine antibodies in immunoblot analysis, suggesting that Ct875/TepP is tyrosine-phosphorylated upon association with host cells (Fig. 13C). Phosphorylation of TepP provided us an opportunity to monitor the kinetics of its translocation into cells. EB infections were synchronized at 4^{o}C and shifted to 37^{o}C for various time intervals within a 1 h span. Infected samples were lysed, split in two and TARP and TepP were immunoprecipitated. Total TARP, TepP and tyrosine-phosphorylated protein in the IP material was monitored with specific antibodies. We observed that tyrosine phosphorylation of TepP was delayed with respect to TARP by ~10 min (Fig. 13D), suggesting either that kinases responsible for TepP phosphorylation are recruited with delayed kinetics to EB entry sites or that TARP translocation from EBs precedes TepP. However, TepP might not be the major ~65-70

kDa phosphoprotein since the TepP band only partly overlapped with the major ~65-70 kDa phosphotyrosine protein bands in dual labeling immunoblots (Fig. 13E).

We proceeded to map the phosphorylation sites on translocated Ct875/TepP by mass spectrometry. Infections were scaled up and Ct875/TepP was IP at 4 hpi in the presence of phosphatase inhibitors and processed for phospho-proteomics analysis. Four phospho-peptides were detected in the sample: two contained phosphorylated tyrosine (Y43 and Y496) and two phosphorylated serine residues (S410 and S415) (Fig. 14). Because the peptide spanning Y496 is part of a tandem repeat (ASD**Y**DLPR), it is unclear if one or both tyrosine residues (Y496 and Y504) are phosphorylated. Overall, these results indicate that Ct875/TepP is phosphorylated at multiple residues during infection and thus we renamed this protein as TepP for translocated early phosphoprotein.

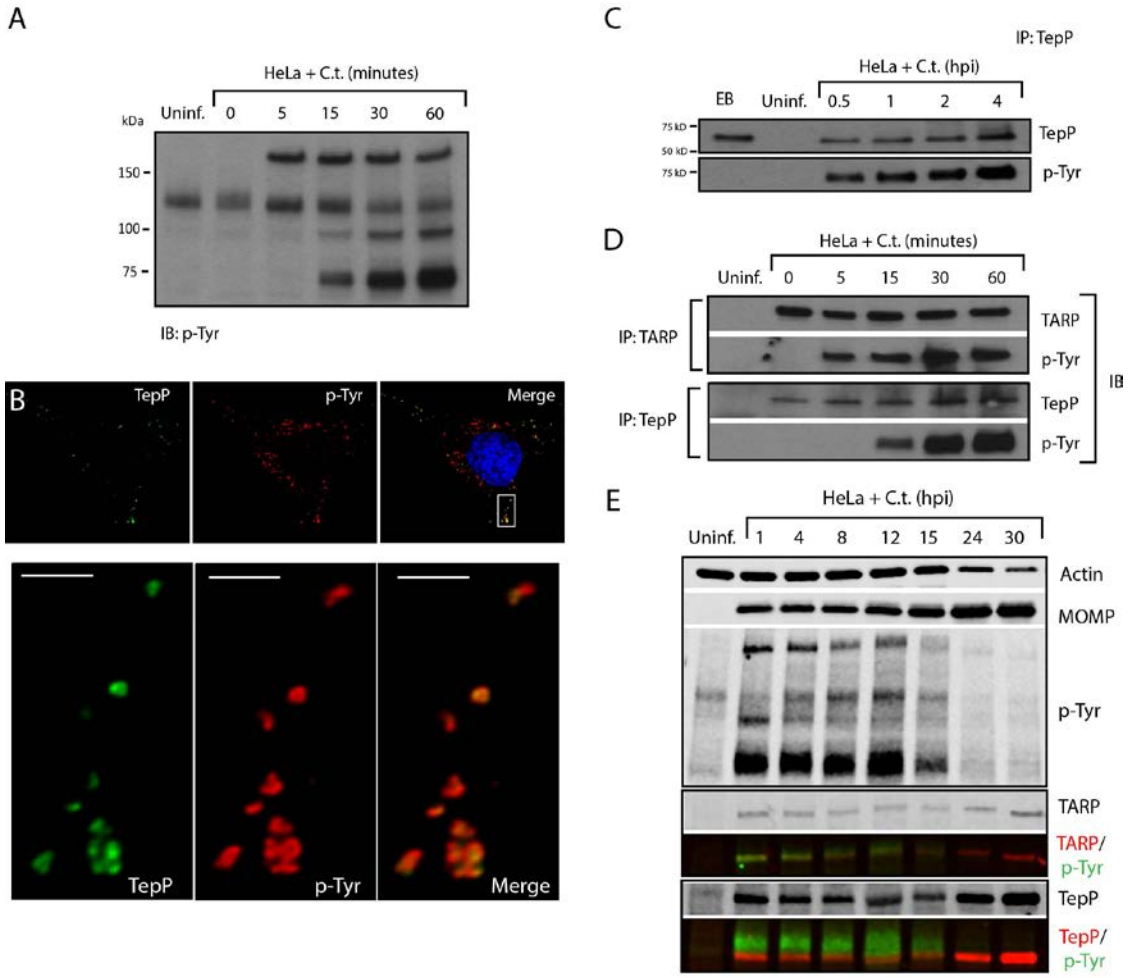

Figure 13: TepP/Ct875 is phosphorylated upon translocation. A) Immunoblot analysis of total cell lysates of *Chlamydia* infected cells shows the appearance of at least three major tyrosine-phosphorylated proteins (>150 kDa, 100 kDa, and 65-70 kDa) within 1 hpi. B) TepP colocalizes with anti-phospho-Tyr signals at *Chlamydia* entry sites. HeLa cells were infected as in A) and immunostained with anti-TepP (green) and anti-p-Tyr (red) antibodies. Host and bacterial DNA were stained with DAPI (blue). Scale bar: 10 µm (upper panel); 2 µm (lower panel). C) TepP is phosphorylated at tyrosine residues upon EB association with host cells. Cells were infected as in A) with an MOI of 100 for the indicated times and TepP was immunoprecipitated from cell lysates and analyzed by immunoblotting with anti-TepP and anti p-Tyr antibodies. TepP was recognized by anti p-Tyr antibodies only upon association with host cells. D-E) TARP and TepP are tyrosine-phosphorylated at different rates during *Chlamydia* infection. HeLa cells were infected as in A) and total protein lysates were generated at 0, 5, 15, 30 min and 1 hpi and TepP and TARP was IP as above with anti-TARP or anti-TepP antibodies followed by immunoblot analysis with anti-TARP, -TepP and p-Tyr antibodies (D). Note there is a relative delay in TepP tyrosine phosphorylation with respect to TARP. The prominent higher molecular weight tyrosine-phosphorylated band corresponds to Tarp, as assessed by 2-color

immunofluorescence-detection. In contrast, TepP only partially overlaps with the major 65-70 kDa tyrosine-phosphorylated proteins (E). MOMP: major outer membrane protein, Uninf: uninfected.

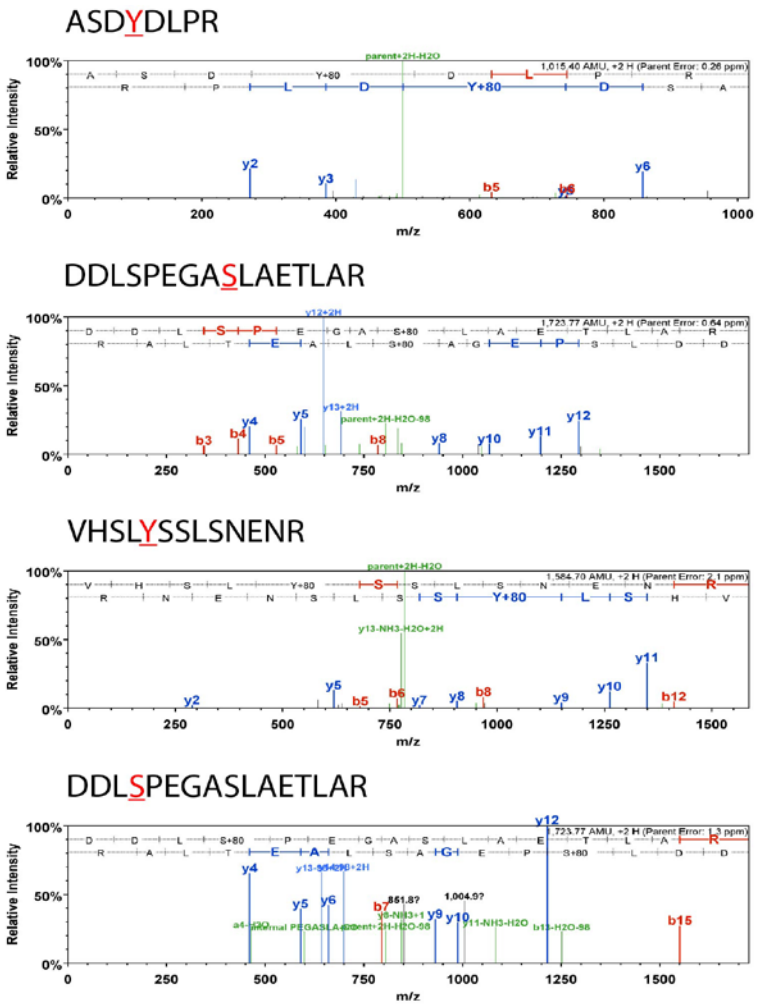

Figure 14: M/Z spectra of TepP phosphopeptides. Endogenous TepP was immunoprecipitated at 4 hpi. The corresponding TepP band was excised from the gel, digested with trypsin and phosphopeptides were enriched on a titanium dioxide affinity column, prior to elution and analysis by LC-MS/MS. Four phospho-peptides were detected: two phosphoserine and two phosphotyrosine. Detected peptides were shown above each spectrum and detected phosphorylation site was underlined. Y-axis is the relative intensity of peaks. X-axis is mass-to-charge ratio (m/z).

4.3.3 Crk, an adaptor protein, associates with TepP and is recruited to nascent inclusions.

Protein tyrosine phosphorylation plays an important role in signal transduction by mediating the recruitment of proteins containing Src homology 2 (SH2) and/or phosphotyrosine binding (PTB) domains to target proteins (Backert & Selbach, 2005). Analysis of the TepP phosphopeptides using NetPhorest (http://netphorest.info/) (Miller et al., 2008) indicated the presence of a consensus pYxxP binding site (ASD**Y**DL**P**R) for the scaffolding protein Crk (Fig. 15A) (Songyang et al., 1993). Crk is an adaptor protein that mediates phosphorylation-mediated regulation of cytoskeletal dynamics, cell adhesion and migration, phagocytosis, immune response and tumorogenesis (Birge, Kalodimos, Inagaki, & Tanaka, 2009; Liu, 2013). Mammals express Crk-I and Crk-II, two alternatively spliced forms of *CRK*, and the Crk-like protein, Crk-L. Crk proteins contain SH2 and SH3 domains, which mediate binding to phosphorylated tyrosine residues and proline-rich domains, respectively (Birge et al., 2009). To test if TepP translocated by EBs associated with Crk proteins, we performed a time course of infection and immunoprecipitated TepP in the presence of phosphatase inhibitors. *Chlamydia* infection did not alter the steady state levels of CrkI-II (Fig. 15E); whereas increasing amounts of CrkI and CrkII co-IP with TepP as the infection progressed (Fig. 15B), indicating that these proteins are part of a complex. By immunofluorescence microscopy, we further observed endogenous Crk recruited to bacteria as early as 1 hpi and that this association continued past 8 hours, a point at which nascent inclusions have migrated to the microtubule organizing center (Fig. 15C). To test if the association of TepP with Crk is direct, we next examined if recombinant TepP could bind to Crk *in vitro*. We found that the binding between TepP and GST-Crk was significantly enhanced by *in vitro* phosphorylation of TepP and reduced after phosphatase treatment (Fig. 15D), suggesting

that TepP phosphorylation is important for the recruitment of Crk. Together, these data are consistent with a model wherein TepP, after being secreted into host cells, is tyrosine-phosphorylated and recruits Crk to nascent inclusions, presumably through interactions with its SH2 domain.

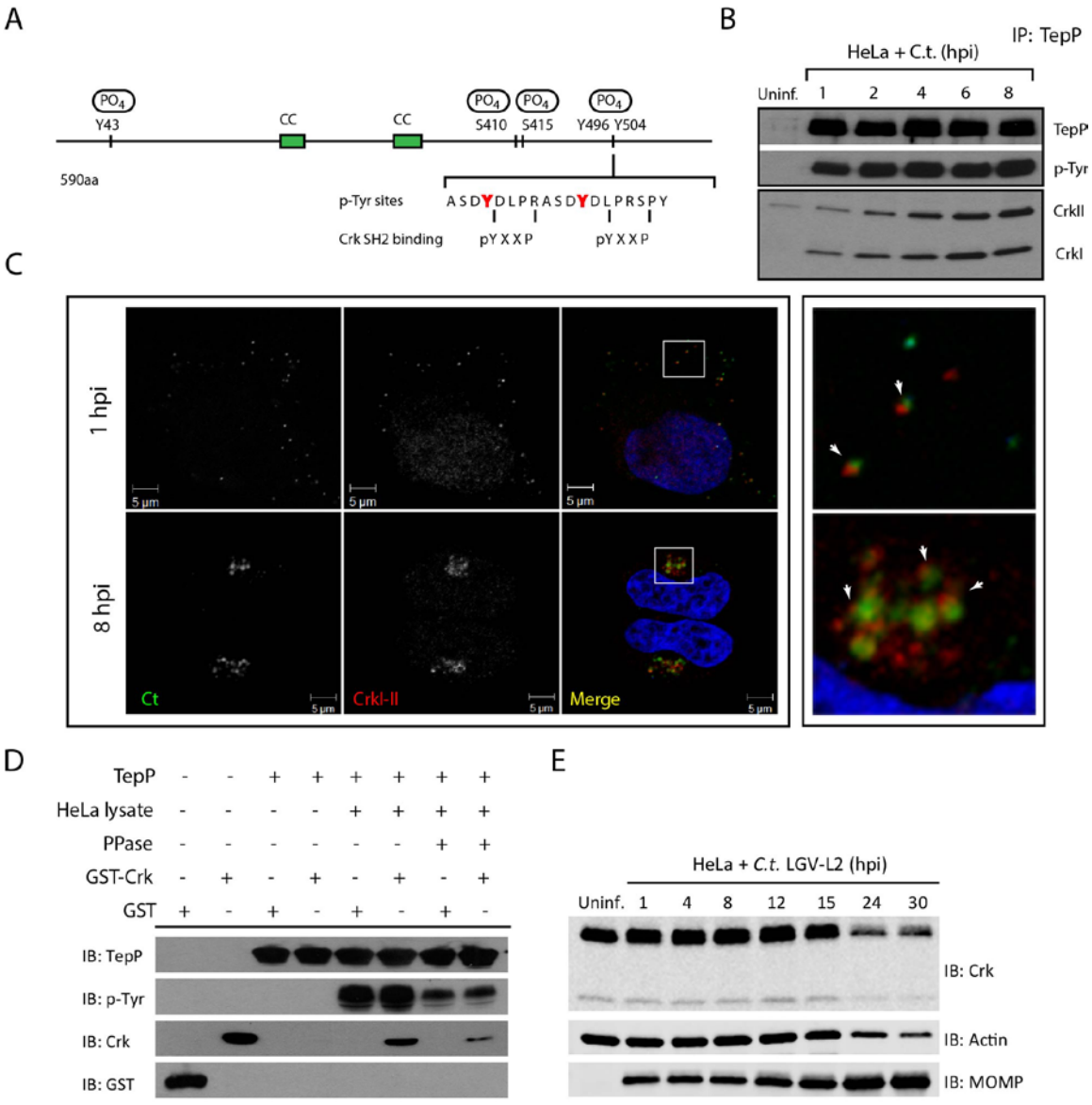

Figure 15: Crk-I and Crk-II bind to tyrosine-phosphorylated TepP and are recruited to nascent inclusions early during infection. A) Cartoon schematic of TepP phosphorylation sites identified by mass spectrometry (Fig. 14). B) CrkI and CrkII co-IP with TepP. HeLa cells were infected with

L2 at MOI of 100 for 1, 2, 4, 6 and 8 hours. Cell lysates were immunoprecipitated with anti-TepP antibodies and the bound proteins were analyzed by immunoblot with anti-Crk, TepP and p-Tyr antibodies. Both isoforms of Crk, CrkI (lower band) and CrkII (upper band), co-IP with TepP. Uninf-uninfected. C) CrkI-II is recruited to *Chlamydia* entry sites and nascent inclusions. HeLa cells were infected with L2 at an MOI of 20 for 1 and 8 hours. Cells were fixed and stained with anti-MOMP (green) and anti-Crk (red) antibodies. Left panels are magnified images form boxed areas. Examples of sites of association between bacteria and Crk are marked by arrows. DAPI was used to stain nucleic acids. CrkI-II was recruited to *Chlamydia* entry sites by 1 hpi and this association continued after the nascent inclusion had trafficked to the host cells' perinuclear region. D) Recombinant TepP interacts with GST-Crk in a phosphorylation-dependent manner. Purified GST or GST-Crk was incubated with purified TepP-6xHis or purified TepP-6xHis that had been phosphorylated *in vitro.* One sample of phosphorylated TepP-6xHis was treated with Calf intestinal Alkaline Phosphatase (PPase). The efficiency of TepP co-precipitation with GST-Crk increased after *in vitro* phosphorylation. Dephosphorylation with PPase decreased the efficiency of GST-Crk co-precipitation. E) Crk levels remain constant throughout infection. Confluent monolayer of HeLa cells were infected with wild type LGV-L2 at an MOI of 50 and collected at indicated time points. Samples were subjected to immunoblot analysis with antibodies against Crk, Actin and MOMP. Uninf: control uninfected cells.

4.3.4 TepP is required for the recruitment of Crk to nascent inclusions

Although *Chlamydia* spp. lacks a system for performing targeted gene disruptions, chemically-derived mutants can be readily generated and loss-of-function mutations can be identified by whole genome sequencing (Nguyen & Valdivia, 2012). Using such an approach, our group has recently generated and sequenced a comprehensive collection of ethyl methyl sulfonate (EMS)-derived mutants of *C. trachomatis* LGV-L2 (unpublished results). We identified 6 strains with mutations in TepP, including strain CTL2-M062, bearing a G to A transversion that led to a premature stop codon at amino acid 103 (W103*) (Fig. 16A). By immunoblot analysis, EBs from CTL2-M062 lacked any detectable full length TepP, suggesting that the truncated form of TepP was either unstable or not properly expressed (Fig. 16B). Interestingly, even though TepP is not the predominant ~65-70 kDa tyrosine-phosphorylated protein observed early during *C. trachomatis* infection, these phosphorylated species were no longer detected when cells

were infected with the TepP-deficient CTL2-M062 mutant (Fig. 16C); whereas the levels of the phospho-TARP band (~150 kDa) were unaltered. These results indicate that TepP may induce the phosphorylation of additional host and or secreted bacterial proteins at the early stages of infection. Next, we determined whether Crk association with nascent inclusions was dependent on TepP. HeLa cells were infected with either wild type or the TepP-deficient *C. trachomatis* mutant and the co-localization of bacteria with Crk was assessed by immunofluorescence microscopy. Crk was no longer associated with intracellular CTL2-M062 by 8 hpi (Fig. 16D).

The original TepP deficient isolate carried an additional 11 EMS-induced single nucleotide variants (SNVs) (Fig. 16A; Table 3) (Whole genome sequencing was performed by Dr. Robert Bastidas). To exclude the possibility that these SNVs contributed to the lack of Crk recruitment to nascent inclusions, we generated recombinant strains between the TepP deficient isolate (generated in a Rif^R background) and a spectinomycin (Spc^R) LGV-L2 strain by co-infection of cells as previously described (Nguyen & Valdivia, 2012). Double drug resistant recombinants were plaque purified and screened by allele-specific PCR to determine the relative segregation of mutations present in the original TepP-deficient isolate. A total of 200 recombinants were screened and four co-isogenic strains were identified where various assortment of mutations were present (Fig. 17A and 17B). The marked reduction of the ~65-70 kDa signal in phosphotyrosine immunoblots was only observed in the strain lacking TepP (Fig. 17C). Similarly, Crk recruitment to nascent inclusions was only impaired in strains encoding the $TepP^{W103*}$ variant (Fig. 17D), providing further genetic support to the notion that TepP is directly responsible for the recruitment of Crk to inclusions.

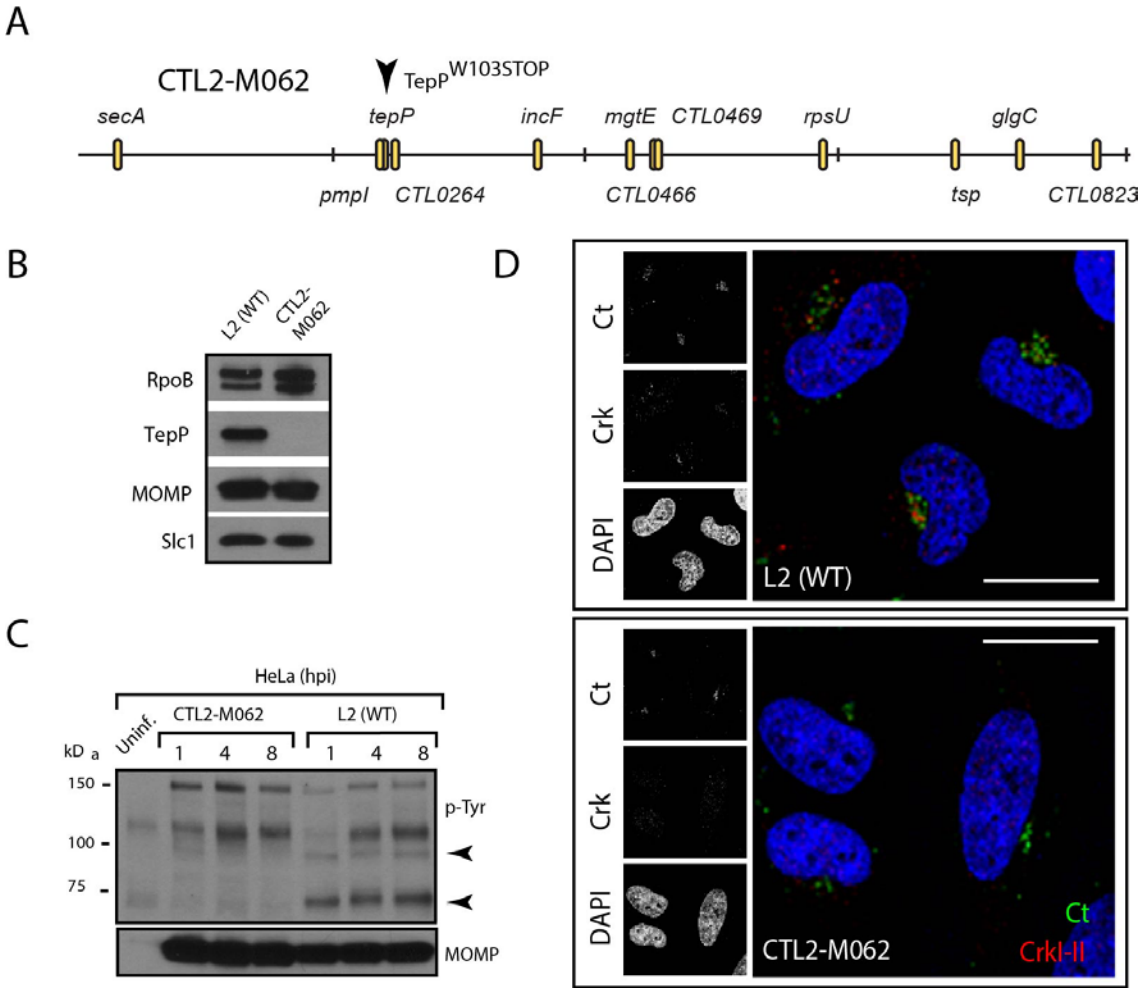

Figure 16: A TepP mutant failed to recruit Crk to nascent inclusions. A) Physical map of single nucleotide variants identified in strain CTL2-M062, a chemically derived LGV-L2 mutant containing a nonsense mutation in the codon for amino acid 103 of TepP. Non synonymous mutations were identified by whole genome sequencing and verified by Sanger sequencing. Key differences from the parental reference strain are highlighted. B-C) TepP is required for the accumulation of major tyrosine-phosphorylated proteins in *Chlamydia* infected cells. Immunoblot analysis of the EB lysate of CTL2-M062 showed no detectable levels of TepP compared to wild type LGV-L2 (WT) (B). HeLa cells were infected with wild type LGV-L2 (WT) or CTL2-M062 at an MOI of 50 and samples were collected at indicated time points and analyzed by immunoblot with antibodies against p-Tyr and MOMP. MOMP (*Chlamydia* major outer membrane protein) is a loading control for bacteria loads. Arrows indicate major TepP-dependent tyrosine-phosphorylated proteins (C). D) Crk does not associate with nascent inclusions in CTL2-M062 infected cells. Immunofluorescence staining of HeLa cells infected with wild type LGV-L2 and CTL2-M062 for 8 h. Cells were stained with anti-Crk (red) and anti-MOMP (green) antibodies, and with DAPI (blue). Crk recruitment was absent in a TepP deficient strain. Scale bar: 20 μm.

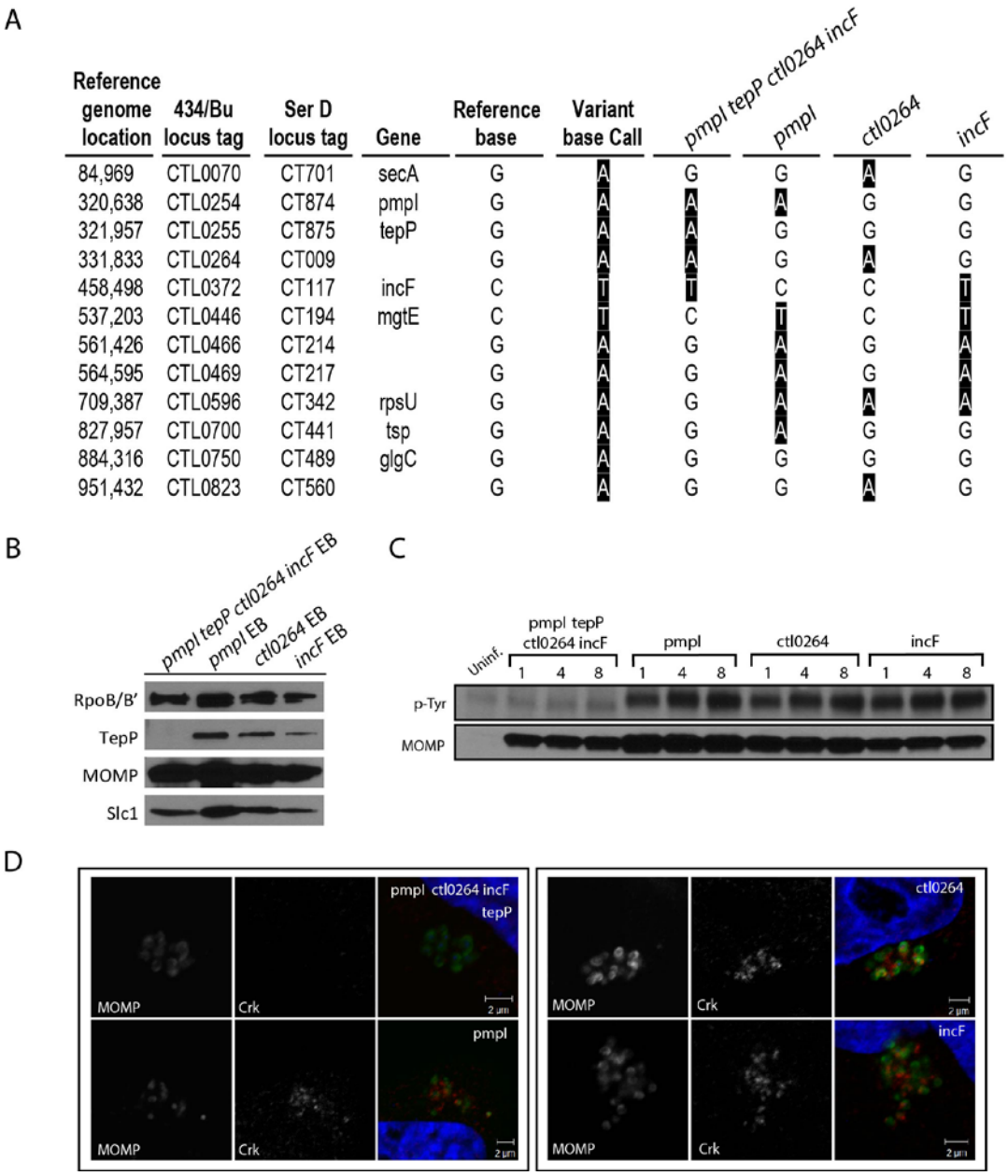

Figure 17: TepP is required for the recruitment of Crk to nascent inclusions. A) Genotype of recombinant strains harboring products of a CTL2-M062 (Rif^r) and a LGV-L2 Spc^r co-infection. Black shading indicates single nucleotide variants (SNV) present in CTL2-M062. Each SNV was verified by Sanger sequencing. B) *C. trachomatis* recombinant harboring a *tepP* null allele (*tepP* W103*) does not express full length TepP. EBs of four recombinants were selected from a co-infection setting between CTL2-M062 (Rif^r) and a Spc^r LGV-L2 variant. Recombinants were isolated by plaquing on Vero cell monolayers in the presence of rifampin and spectinomycin. Individual plaques were amplified on Vero cells, and EBs from recombinants with the genotypes shown were harvested and purified on density gradients. EBs were lyzed in SDS sample buffer,

and subjected to immunoblot analysis with antibodies against TepP and RpoB/B', MOMP and Slc1. C-D) The *tepP* mutation is genetically linked to the lack of the infection-induced p65-70 kDa tyrosine-phosphorylated proteins and the loss of Crk recruitment to nascent inclusions. Various recombinant strains generated from a cross between CTL2-M062 and wild type LGV-L2 were tested for the presence of the p65-70 kDa p-Tyr proteins (C) and recruitment of Crk to nascent inclusions (D).

Table 3: Single nucleotide variants identified in strain CTL2-M062 by whole genome sequencing (Table was constructed by Dr. Robert Bastidas).

Reference genome location	Reference Base	Variant Base Call	Codon change	Amino Acid Change	Variant type	Gene	434/Bu locus tag	Ser D locus tag	Product	Coverage	Strand-Bias	Variant Frequency
84,969	G	A	G514A	G172R	Non synonymous	secA	CTL0070	CT701	preprotein translocase subunit SecA	523	58%	100%
145,291	G	A	G1797A		Synonymous		CTL0113	CT744	hypothetical protein	462	60%	100%
192,335	C	T	G2187A		Synonymous	priA	CTL0147	CT778	primosome assembly protein PriA	556	50%	100%
192,335	C	T	C1128T		Synonymous	bioF	CTL0146	CT777	8-amino-7-oxononanoate synthase	556	50%	100%
c216,843	C	T			Non coding					616	50%	99%
320,638	G	A	C737T	S246F	Non synonymous	pmpI	CTL0254	CT874	polymorphic outer membrane protein	386	51%	100%
321,957	G	A	G309A	W103*	Non sense	tepP	CTL0255	CT875	translocated early phospho protein	328	51%	100%
331,833	G	A	G213A	M71I	Non synonymous		CTL0264	CT009	hypothetical protein	470	57%	100%
335,058	G	A	G528A		Synonymous		CTL0267	CT012	putative integral membrane protein	613	54%	100%
444,524	C	T	C1650T		Synonymous		CTL0360	CT105	hypothetical protein	604	51%	100%
458,498	C	T	C230T	T77I	Non synonymous	incF	CTL0372	CT117	inclusion membrane protein F	553	51%	100%
480,180	G	A	G480A		Synonymous		CTL0395	CT140	exported protein	474	53%	99%
514,164	C	T	G521A		Synonymous		CTL0425	CT140	hypothetical protein	659	50%	100%
537,203	C	T	G541A	V181I	Non synonymous	mgtE	CTL0446	CT194	magnesium transport protein	569	53%	100%
558,011	C	T	C1153T		Synonymous	hemL	CTL0462	CT210	glutamate-1-semialdehyde aminotransferase	566	53%	100%
561,426	G	A	C185T	P62L	Non synonymous		CTL0466	CT214	hypothetical protein	490	65%	99%
564,595	G	A	G128A	G43D	Non synonymous		CTL0469	CT217	hypothetical protein	486	52%	100%
604,651	C	T	C471T		Synonymous		CTL0506	CT254	inner membrane protein	676	53%	100%
689,168	G	A	G423A		Synonymous	xseA	CTL0583	CT329	exodeoxyribonuclease VII large subunit	572	58%	100%
709,387	G	A	C140T	A47V	Non synonymous	rpsU	CTL0596	CT342	30S ribosomal protein S21	496	58%	100%
726,889	C	T	G717A		Synonymous		CTL0610	CT356	hypothetical protein	393	55%	100%
826,893	C	T	G243A		Synonymous	rpsL	CTL0698	CT439	30S ribosomal protein S12	529	51%	100%

827,957	G	A	G85A	D29N	Non synonymous	tsp	CTL0700	CT441	carboxy-terminal processing protease	509	51%	100%
846,119	C	T	C567T		Synonymous	plsC	CTL0713	CT453	1-acyl-sn-glycerol-3-phosphate acyltransferase	521	60%	99%
884,316	G	A	C458T	S153L	Non synonymous	glgC	CTL0750	CT489	glucose-1-phosphate adenylyltransferase	660	50%	100%
951,432	G	A	G408A	M136I	Non synonymous		CTL0823	CT560	hypothetical protein	459	55%	100%
123,163	C	A	C -> A		Non coding					423	52%	100%
127,338	T	A	T657A		Synonymous		CTL0103	CT734	putative lipoprotein	369	54%	100%
435,453	G	A	C743T	A248V	Non synonymous	nusA	CTL0352	CT097	transcription elongation factor NusA	630	55%	100%
448,523	G	A	C110T	A37V	Non synonymous		CTL0364	CT109	hypothetical protein	587	65%	100%
616,827	C	T	G315A		Synonymous		CTL0518	CT266	hypothetical protein	616	52%	100%
637,039	C	T	C610T	R204C	Non synonymous	clpC	CTL0538	CT286	ATP-dependent Clp protease	698	54%	100%
638,353	T	C	T1924C	F642L	Non synonymous	clpC	CTL0538	CT286	ATP-dependent Clp protease	548	56%	100%
675,519	G[§]	A[§]	C1411T	H471Y	Non synonymous	rpoB	CTL0567	CT315	DNA-directed RNA polymerase subunit beta	585	51%	100%
693,265	G	A	G473A	S158N	Non synonymous	pykF	CTL0586	CT332	pyruvate kinase	649	51%	100%
798,820	G	A	G470A	G157E	Non synonymous	pmpC	CTL0671	CT414	polymorphic outer membrane protein	600	56%	100%
929,717	C	A	C -> A		Non coding					544	53%	100%

*Single nucleotide variants in black are variants identified in CTL2M062.

*Single nucleotide variants in gray are strain background variants differing from 434/Bu reference sequence.

[§] Variant leading to rifampin resistance.

*All non-parental non synonymous variants were verified by Sanger sequencing.

4.3.5 Complementation of the TepP mutant restores the pattern of tyrosine phosphorylation induced by *Chlamydia* and rescue Crk recruitment

Finally, to provide final genetic confirmation of the role of TepP in mediating these events, we took advantage of recent developments in DNA transformation in *C. trachomatis* (Wang et al., 2011). We transformed the recombinant TepP^{W103*} strain with a *C. trachomatis-E. coli* shuttle plasmid expressing the *tepP* gene under the control of its endogenous promoter or the empty vector control and selected for stable transformants in the presence of penicillin. The transformed strains expressed TepP to a similar level as wild type strains (Fig. 18A). An immunoblot analysis of infected cells showed the restoration of the ~65-70 kDa phosphotyrosine immunosignals in TepP complemented strains but not in strains transformed with the empty vector (Fig. 18B). In addition, Crk recruitment to nascent *Chlamydia* inclusions was restored (Fig. 18C). Similar results were observed when using A2EN cells, a newly derived human endocervical epithelial cell line (Buckner et al., 2011) (Fig. 18D and 18E). Taken together, our results confirm that TepP is the major contributor, either directly or indirectly, to the tyrosine-phosphorylation of multiple proteins early during *C. trachomatis* infection and the subsequent recruitment of Crk to nascent inclusions.

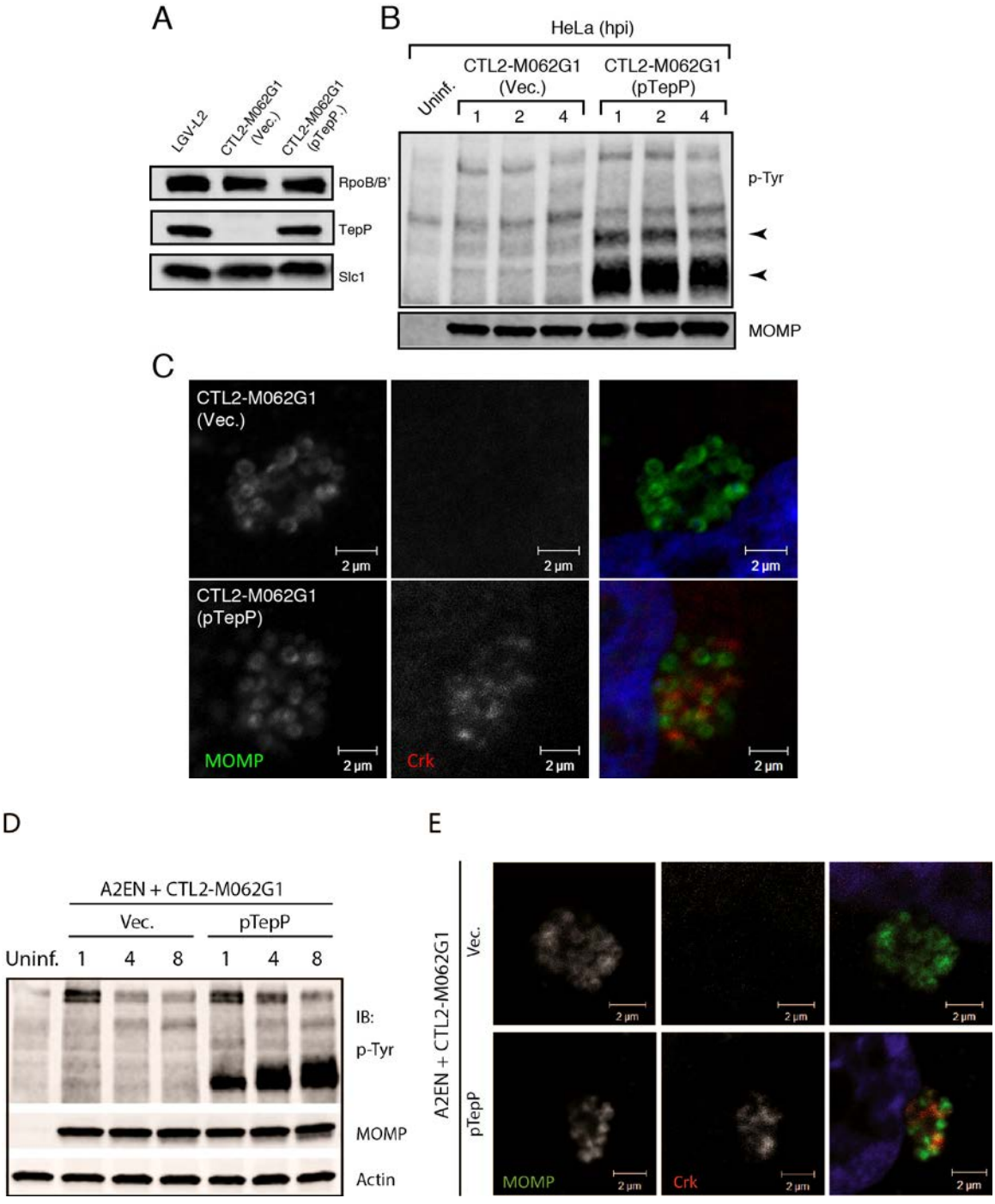

Figure 18: Genetic complementation of a *Chlamydia tepP* mutant restores the normal tyrosine-phosphorylation pattern of multiple proteins and rescues Crk recruitment to nascent inclusions. A) The recombinant TepP^{W103*} strain CTL2-M062G1 was transformed with an empty vector (Vec.) or a vector harboring the wild type *tepP* gene (pTepP). Immunoblot analysis of EBs

derived from these strains with anti-TepP antibodies confirmed the complementation of TepP expression to wild type levels (LGV-L2). Slc1 and RpoB/B' levels were shown as loading controls. B) The complemented recombinant TepP^{W103*} strains restored the pattern of tyrosine-phosphorylation induced during *Chlamydia* infection. Confluent HeLa cells were infected with CTL2-M062G1 strains described in (A) at an MOI of 50 and total protein lysates were collected at indicated time points. Samples were subjected to immunoblot analysis with antibodies against p-Tyr and MOMP. C) The complemented recombinant TepP^{W103*} strain rescued Crk recruitment to nascent *Chlamydia* inclusions. HeLa cells were infected for 8 h with CTL2-M062G1 strains described in (A) at an MOI of 20, and immunostained with anti-Crk (red) and anti-MOMP (green) antibodies, and DAPI (blue). D-E) Similar results were observed in A2EN cells, a newly derived human endocervical epithelial cell line.

4.3.6 TepP and Crk are not essential for *Chlamydia* growth in Tissue culture model.

Although the CTL2-M062 had a ~ 15 fold growth defect compared to the wild type parental strain, we could not unambiguously link this growth defect to strains bearing the *tepP* mutant allele (data not shown). To address whether TepP played a role in promoting *C. trachomatis* replication or infectivity, we compared the ability of the *tepP* mutants transformed with the *tepP* expressing plasmid or plasmid alone to generate infectious progeny. We observed no differences in the generation of EBs among these strains in either HeLa cells (Fig. 19D) or in A2EN cells (data not shown). Similarly, silencing of Crk, a major TepP-binding partner, with siRNAs in HeLa cells did not impact *C. trachomatis* replication (Fig. 19A-C).

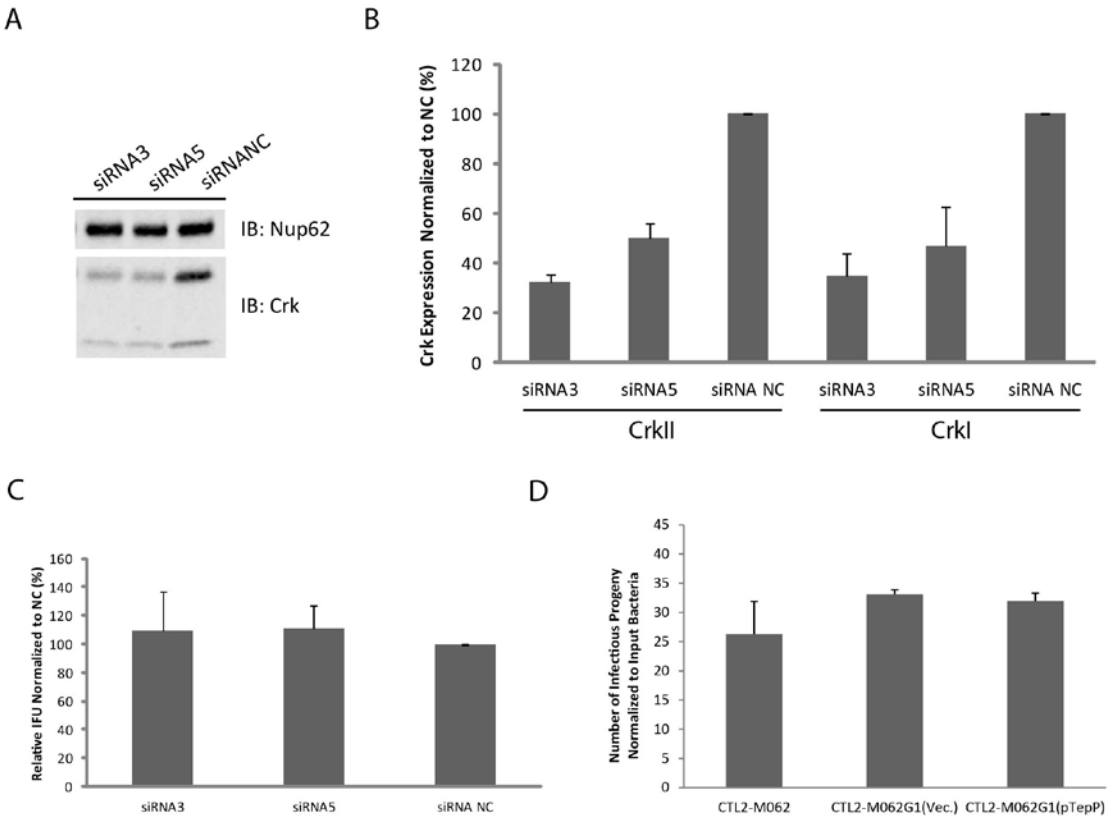

Figure 19: Replication potential of LGV-L2 in Crk knockdown cells and *tepP* mutants in epithelial cells. A) Transfection of Crk siRNAs decreased the expression level of both CrkI and CrkII in HeLa cells. Upper panel is the immunoblot analysis of HeLa cells transfected with two different Crk siRNAs (3 and 5) or negative control siRNA (NC) for 48 h. Total cell lysates were probed with anti-Crk and anti-Nup62 (loading control) antibodies. B) Quantification of siRNA-mediated decreased levels of Crk protein expression as assessed by quantitative immunoblots on a LI-COR imager. CrkI and CrkII expression level was decreased around 50% after siRNA treatment. C) Crk siRNA knockdown does not affect *C. trachomatis* growth as assessed by IFU assay. IFUs were normalized to growth in cells treated with control siRNA (NC). D) Comparison of IFU burst between the *tepP* mutant CTL2-MO62G1, and its derivatives transformed with empty vector or pTepP. HeLa cells were infected for 28 h at an MOI < 1. The resulting infectious progeny were titered in HeLa cells as described in Material and Methods, and normalized to input number of bacteria. All data shown were as means ± standard deviations from experiments performed in triplicate.

4.3.7 TepP regulates the expression of genes associated with innate immune responses.

These observations suggest that TepP is not essential for *C. trachomatis* replication in cell culture models of infection, although we cannot rule out a role for TepP in promoting invasion or intracellular survival in other cell types or in the context of intact tissues and an active immune system. However, given the observation that TepP recruits Crk, a scaffolding protein important in cell signaling and TepP mediates multiple tyrosine phosphorylations, we hypothesized that the presence of TepP should lead to defined transcriptional response by the infected cell. We compared the global transcriptional profile of mock infected A2EN cells or A2EN cells infected with the *tepP* mutant and its complemented counterpart for 4 h (RNA samples were collected by Victoria Carpenter). A microarray analysis revealed 33 genes displaying greater than 1.5 fold changes in gene expression levels (Fig. 20A and Table 3). A Gene Ontology (GO) analysis of these differentially expressed genes revealed an enrichment for genes with immunity-related functions (data not shown). We next validated by quantitative-PCR, the expression of five of these genes: IL-6 and CXCL3, and MAP3k8, IFIT1 and IFIT2, whose mRNA levels decrease and increase, respectively, depending on the presence of TepP (Fig. 20B). Interestingly, the fold-change for IFIT1 and IFIT2 changed from 2 fold to more than 10 fold by 8 hpi; whereas the level of fold-change for MAP3k8 did not (Fig. 20C). The change in transcript levels also reflected in protein levels. IFIT2 protein was detected 24 hpi and this induction was TepP-dependent, as shown by immunoblot of *Chlamydia* infection time course probed with anti-IFIT2 antibody (Fig 20D). These data suggest that one of the functions of TepP is to modulate gene expression in the early stages of infection, presumably to impact the type and magnitude of the ensuing innate immune response.

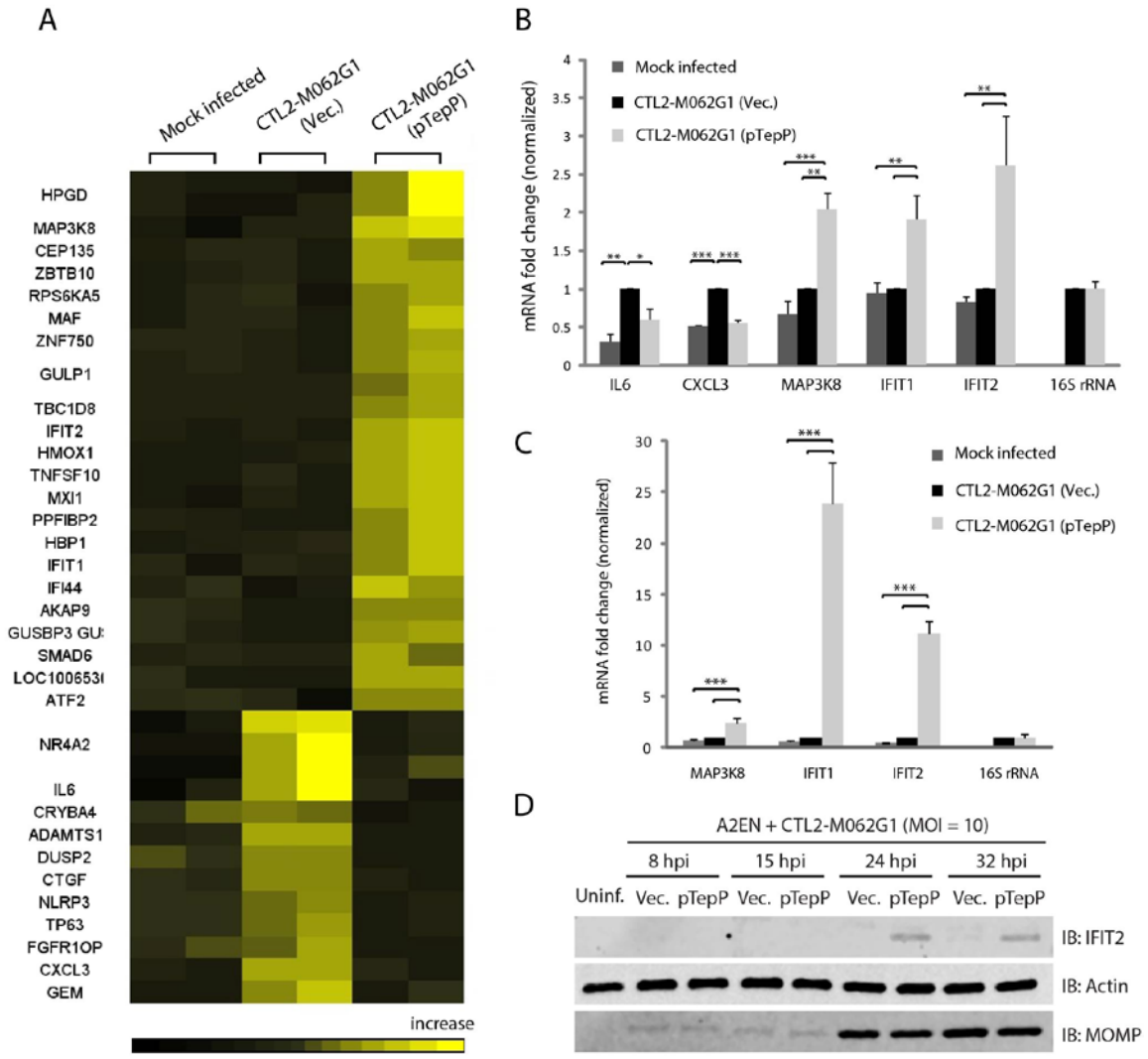

Figure 20: Global transcriptional profiling links TepP function to immune-related responses. A) Microarray analysis identified 33 host genes that have >1.5 fold-change in transcript levels between recombinant TepP^{W103*} strains (CTL2-M062G1) transformed with empty vector (Vec) and vector containing wild type *tepP* gene (pTepP). A2EN epithelial cells were infected for 4 h. Results shown were from duplicate biological samples. B) Q-PCR results validated transcript level changes observed for 5 immune-related genes at 4 hpi. Fold-change in mRNA abundance was normalized to CTL2-M062G1 (Vec). The amount of bacteria in each sample is indicated by 16S rRNA. C) TepP-dependent elevation of IFIT transcript levels at 8 hpi. Q-PCR results of MAP3k8, IFIT1 and IFIT2 mRNA in A2EN cells infected as in (A). All data shown were as means ± standard deviations from three independent biological replicates. *, $P < 0.05$; **, $P < 0.01$; ***, $P < 0.001$ (one-way analysis of variance and Tukey's multiple-comparison test). D) IFIT2 protein levels increased in a TepP-dependent manner during *Chlamydia* infection. A2EN epithelial cells were infected with CTL2-M062G1 transformed with empty vector (Vec) and vector containing wild type *tepP* gene (pTepP) at an MOI of 10. Samples were collected at indicated time points

and analyzed by immunoblot with antibodies against IFIT2, Actin and MOMP. Actin is a loading control for host cell and MOMP is a loading control for bacteria.

Table 4: List of genes in A2EN cells that display greater than 1.5 fold change in transcription upon infection with the *tepP* mutant vs its complemented counterpart at 4 hpi.

Column ID[a]	Gene Symbol	Gene Title	RefSeq Transcript ID	p-value[b] V[c] vs. TepP[d]	Fold-Change V vs. TepP	Description	p-value[b] Uninf[e] vs. TepP	Fold-Change Uninf vs. TepP	Description	p-value[b] Uninf vs. V	Fold-Change Uninf vs. V	Description
204794_at	DUSP2	dual specificity phosphatase 2	NM_004418	0.001	1.531	V up vs TepP	0.003	1.263	Uninf up vs TepP	0.005	-1.213	Uninf down vs V
222162_s_at	ADAMTS1	ADAM metallopeptidase with thrombospondin type 1 motif, 1	NM_006988	0.001	1.726	V up vs TepP	0.021	1.173	Uninf up vs TepP	0.002	-1.472	Uninf down vs V
205027_s_at	MAP3K8	mitogen-activated protein kinase kinase kinase 8	NM_005204	0.002	-1.857	V down vs TepP	0.001	-2.244	Uninf down vs TepP	0.051	-1.209	Uninf down vs V
215483_at	AKAP9	A kinase (PRKA) anchor protein (yotiao) 9	NM_005751	0.001	-1.544	V down vs TepP	0.006	-1.301	Uninf down vs TepP	0.019	1.186	Uninf up vs V
209101_at	CTGF	connective tissue growth factor	NM_001901	0.001	1.562	V up vs TepP	0.015	1.213	Uninf up vs TepP	0.007	-1.288	Uninf down vs V
214329_x_at	TNFSF10	tumor necrosis factor (ligand) superfamily, member 10	NM_003810	0.003	-1.709	V down vs TepP	0.002	-1.848	Uninf down vs TepP	0.273	-1.081	Uninf down vs V
207850_at	CXCL3	chemokine (C-X-C motif) ligand 3	NM_002090	0.003	1.570	V up vs TepP	0.465	-1.041	Uninf down vs TepP	0.002	-1.634	Uninf down vs V
203665_at	HMOX1	heme oxygenase (decycling) 1	NM_002133	0.003	-1.739	V down vs TepP	0.003	-1.783	Uninf down vs TepP	0.721	-1.025	Uninf down vs V
202364_at	MXI1	MAX interactor 1	NM_005962	0.004	-1.763	V down vs TepP	0.003	-1.910	Uninf down vs TepP	0.343	-1.083	Uninf down vs V
217502_at	IFIT2	interferon-induced protein with tetratricopeptide repeats 2	NM_001547	0.004	-1.682	V down vs TepP	0.003	-1.768	Uninf down vs TepP	0.496	-1.051	Uninf down vs V
204526_s_at	TBC1D8	TBC1 domain family, member 8 (with GRAM domain)	NM_007063	0.004	-1.603	V down vs TepP	0.004	-1.576	Uninf down vs TepP	0.776	1.018	Uninf up vs V
215599_at	GUSBP3 / GUSBP9	glucuronidase, beta pseudogene 3 / glucuronidase, beta pseudogene 9	NR_027386	0.003	-1.636	V down vs TepP	0.009	-1.412	Uninf down vs TepP	0.079	1.159	Uninf up vs V
214657_s_at	LOC100653017	uncharacterized	NR_002802	0.004	-1.808	V down vs	0.008	-1.596	Uninf down	0.198	1.133	Uninf up vs

	/ MIR612 / NEAT1	LOC100653017 / microRNA 612 / nuclear paraspeckle assembly transcri				TepP			vs TepP			V
209102_s_at	HBP1	HMG-box transcription factor 1	NM_012257	0.008	-1.577	V down vs TepP	0.005	-1.759	Uninf down vs TepP	0.232	-1.115	Uninf down vs V
212841_s_at	PPFIBP2	PTPRF interacting protein, binding protein 2 (liprin beta 2)	NM_003621	0.008	-1.756	V down vs TepP	0.010	-1.678	Uninf down vs TepP	0.640	1.047	Uninf up vs V
207069_s_at	SMAD6	SMAD family member 6	NM_005585	0.007	-1.517	V down vs TepP	0.012	-1.406	Uninf down vs TepP	0.310	1.079	Uninf up vs V
219995_s_at	ZNF750	zinc finger protein 750	NM_024702	0.009	-1.603	V down vs TepP	0.019	-1.437	Uninf down vs TepP	0.254	1.115	Uninf up vs V
216015_s_at	NLRP3	NLR family, pyrin domain containing 3	NM_004895	0.008	1.525	V up vs TepP	0.051	1.236	Uninf up vs TepP	0.052	-1.234	Uninf down vs V
204235_s_at	GULP1	GULP, engulfment adaptor PTB domain containing 1	NM_016315	0.013	-1.505	V down vs TepP	0.013	-1.505	Uninf down vs TepP	0.999	1.000	Uninf up vs V
211834_s_at	TP63	tumor protein p63	NM_001114978	0.008	1.514	V up vs TepP	0.047	1.246	Uninf up vs TepP	0.062	-1.216	Uninf down vs V
216248_s_at	NR4A2	nuclear receptor subfamily 4, group A, member 2	NM_006186	0.034	1.985	V up vs TepP	0.441	-1.179	Uninf down vs TepP	0.020	-2.339	Uninf down vs V
204621_s_at	NR4A2	nuclear receptor subfamily 4, group A, member 2	NM_006186	0.007	1.965	V up vs TepP	0.143	-1.221	Uninf down vs TepP	0.003	-2.400	Uninf down vs V
204622_x_at	NR4A2	nuclear receptor subfamily 4, group A, member 2	NM_006186	0.041	1.741	V up vs TepP	0.073	-1.544	Uninf down vs TepP	0.009	-2.687	Uninf down vs V
214059_at	IFI44	Interferon-induced protein 44	NM_006417	0.010	-1.847	V down vs TepP	0.024	-1.550	Uninf down vs TepP	0.189	1.192	Uninf up vs V
219312_s_at	ZBTB10	zinc finger and BTB domain containing 10	NM_023929	0.017	-1.627	V down vs TepP	0.015	-1.675	Uninf down vs TepP	0.792	-1.030	Uninf down vs V
204237_at	GULP1	GULP, engulfment adaptor PTB domain containing 1	NM_016315	0.014	-1.576	V down vs TepP	0.020	-1.496	Uninf down vs TepP	0.599	1.053	Uninf up vs V
206843_at	CRYBA4	crystallin, beta A4	NM_001886	0.017	1.562	V up vs TepP	0.032	1.424	Uninf up vs TepP	0.390	-1.097	Uninf down vs V
207286_at	CEP135	centrosomal protein 135kDa	NM_014645	0.020	-1.572	V down vs TepP	0.026	-1.513	Uninf down vs TepP	0.727	1.039	Uninf up vs V
209348_s_at	MAF	v-maf musculoaponeurotic fibrosarcoma oncogene homolog (avian)	NM_005360	0.026	-1.619	V down vs TepP	0.024	-1.645	Uninf down vs TepP	0.903	-1.016	Uninf down vs V
211548_s_at	HPGD	hydroxyprostaglandin dehydrogenase 15-(NAD)	NM_000860	0.021	-2.021	V down vs TepP	0.032	-1.820	Uninf down vs TepP	0.556	1.110	Uninf up vs V
203914_x_at	HPGD	hydroxyprostaglandin dehydrogenase 15-(NAD)	NM_000860	0.049	-1.984	V down vs TepP	0.051	-1.969	Uninf down vs TepP	0.974	1.008	Uninf up vs V

204472_at	GEM	GTP binding protein overexpressed in skeletal muscle	NM_005261	0.042	1.585	V up vs TepP	0.357	-1.157	Uninf down vs TepP	0.020	-1.834	Uninf down vs V
205587_at	FGFR1OP	FGFR1 oncogene partner	NM_007045	0.019	1.528	V up vs TepP	0.077	1.274	Uninf up vs TepP	0.140	-1.199	Uninf down vs V
203153_at	IFIT1	interferon-induced protein with tetratricopeptide repeats 1	NM_001548	0.050	-1.510	V down vs TepP	0.029	-1.669	Uninf down vs TepP	0.495	-1.105	Uninf down vs V
205207_at	IL6	interleukin 6 (interferon, beta 2)	NM_000600	0.050	2.017	V up vs TepP	0.485	-1.192	Uninf down vs TepP	0.029	-2.403	Uninf down vs V
204635_at	RPS6KA5	ribosomal protein S6 kinase, 90kDa, polypeptide 5	NM_004755	0.037	-1.596	V down vs TepP	0.044	-1.547	Uninf down vs TepP	0.827	1.032	Uninf up vs V
212984_at	ATF2	activating transcription factor 2	NM_001256090	0.049	-1.560	V down vs TepP	0.196	-1.257	Uninf down vs TepP	0.216	1.241	Uninf up vs V

[a]probeset ID on Affymetrix human genome U133A 2.0 array

[b]p-value was calculated using ANOVA analysis

[c]V- CTL2-M062G1 transformed with empty vector

[d] TepP- CTL2-M062G1 transformed with vector containing wild type tepP gene

[e]Uninf - uninfected A2EN cells

4.3.8 GFP-TepP pull down multiple actin-related proteins

Protein homology searches and functional domain predictions revealed limited information for TepP. To decipher the function of TepP, we decide to identify the potential interacting partners in host cells using GFP IP followed by mass spectrometry. To obtain enough material for mass spectrometry analysis, we constructed a stable HeLa cell line that constitutively expressed GFP-TepP and enriched GFP-TepP by GFP-Trap, a GFP-binding protein crosslinked agarose beads. The same procedure was performed on a stable HeLa cell line that expressed GFP as a control. Interestingly, multiple proteins involved in actin cytoskeletal dynamics were specifically detected in the GFP-TepP sample, indicating that TepP could modulate host actin cytoskeletal rearrangements (Table 5).

Table 5: Number of unique spectrum[a] identified by LC-MS/MS from samples immunoprecipitated with GFP-Trap from cell lysate containing GFP or GFP-TepP.

					IP Sample	
	Identified Proteins	Accession Number	M.W. (kDa)	Taxonomy	GFP	GFP-TepP
1	Caldesmon (CALD1)	Q05682|CALD1	93	Human	0	15
2	Tropomyosin beta chain (TPM2)	P07951|TPM2	33	Human	0	15
3	Myosin-10 (MYH10)	P35580|MYH10	229	Human	0	12
4	Fascin (FSCN1)	Q16658|FSCN1	55	Human	0	11
5	Glyceraldehyde-3-phosphate dehydrogenase (GAPDH)	P04406|G3P	36	Human	0	8
6	2-oxoglutarate dehydrogenase E1 component, mitochondrial (OGDH)	Q02218|ODO1	116	Human	0	9
7	Phostensin (KIAA1949)	Q6NYC8|PHTNS	68	Human	0	7
8	Plastin-3 (PLS3)	P13797|PLST	71	Human	0	7
9	Conserved hypothetical protein Ct875 (TepP) [Chlamydia trachomatis 434/Bu]	gi|165930209	66	C. trachomatis	0	7
10	Ankycorbin (RAI14)	Q9P0K7|RAI14	110	Human	0	6
11	Histone deacetylase 6 (HDAC6)	Q9UBN7|HDAC6	131	Human	0	5
12	Erythrocyte band 7 integral membrane protein (STOM)	P27105|STOM	32	Human	0	5
13	Prohibitin-2 (PHB2)	Q99623|PHB2	33	Human	0	5

14	Junction plakoglobin (JUP)	P14923|PLAK	82	Human	0	5
15	Aminopeptidase N (ANPEP)	P15144|AMPN	110	Human	0	5
16	Guanine nucleotide-binding protein G(I)/G(S)/G(T) subunit beta-2 (GNB2)	P62879|GBB2	37	Human	0	3
17	Brain acid soluble protein 1 (BASP1)	P80723|BASP1	23	Human	0	4
18	EF-hand domain-containing protein D2 (EFHD2)	Q96C19|EFHD2	27	Human	0	4
19	A-kinase anchor protein 2 (AKAP2)	Q9Y2D5|AKAP2	95	Human	0	4
20	Guanine nucleotide-binding protein G(i), alpha-2 subunit (GNAI2)	P04899|GNAI2	40	Human	0	4
21	L-lactate dehydrogenase B chain (LDHB)	P07195|LDHB	37	Human	0	4
22	Voltage-dependent anion-selective channel protein 1 (VDAC1)	P21796|VDAC1	31	Human	0	3
23	Dolichol-phosphate mannosyltransferase (DPM1)	O60762|DPM1	30	Human	0	3
24	F-actin-capping protein subunit alpha-2 (CAPZA2)	P47755|CAZA2	33	Human	0	3
25	Dihydrolipoyllysine-residue succinyltransferase component of 2-oxoglutarate dehydrogenase complex, mitochondrial (DLST)	P36957|ODO2	49	Human	0	3
26	PDZ and LIM domain protein 7 (PDLIM7)	Q9NR12|PDLI7	50	Human	0	3
27	Annexin A5 (ANXA5)	P08758|ANXA5	36	Human	0	3
28	60S ribosomal protein L7a (RPL7A)	P62424|RL7A	30	Human	0	3
29	Dihydrolipoyl dehydrogenase, mitochondrial (DLD)	P09622|DLDH	54	Human	0	3
30	Band 4.1-like protein 2 (EPB41L2)	O43491|E41L2	113	Human	0	3
31	Filamin-B (FLNB)	O75369|FLNB	278	Human	0	3
32	3-hydroxyacyl-CoA dehydrogenase type-2 (HSD17B10)	Q99714|HCD2	27	Human	0	3
33	Ras GTPase-activating-like protein IQGAP1 (IQGAP1)	P46940|IQGA1	189	Human	2	34
34	Coronin-1C (CORO1C)	Q9ULV4|COR1C	53	Human	2	18
35	Filamin-A (FLNA)	P21333|FLNA	281	Human	3	14
36	Tropomyosin alpha-3 chain (TPM3)	P06753|TPM3	33	Human	1	14
37	Serine/threonine-protein phosphatase PP1-gamma catalytic subunit (PPP1CC)	P36873|PP1G	37	Human	1	14
38	Cytospin-A (CYTSA)	Q69YQ0|CYTSA	125	Human	1	13
39	Protein phosphatase 1 regulatory subunit 12A (PPP1R12A)	O14974|MYPT1	115	Human	2	10
40	Nexilin (NEXN)	Q0ZGT2|NEXN	81	Human	2	6
41	40S ribosomal protein S3 (RPS3)	P23396|RS3	27	Human	1	8
42	Cytospin-B (CYTSB)	Q5M775|CYTSB	119	Human	1	5
43	78 glucose-regulated protein (HSPA5)	P11021|GRP78	72	Human	1	7
44	Nucleolin (NCL)	P19338|NUCL	77	Human	1	5
45	L-lactate dehydrogenase A chain (LDHA)	P00338|LDHA	37	Human	1	5
46	40S ribosomal protein S4, X isoform (RPS4X)	P62701|RS4X	30	Human	1	5
47	Tropomyosin alpha-4 chain (TPM4)	P67936|TPM4	29	Human	1	4
48	Cell division control protein 2 homolog (CDC2)	P06493|CDC2	34	Human	1	4

49	40S ribosomal protein S2 (RPS2)	P15880|RS2	31	Human	1	4
50	Supervillin (SVIL)	O95425|SVIL	248	Human	1	4
51	14-3-3 protein theta (YWHAQ)	P27348|1433T	28	Human	1	3
52	Spectrin alpha chain, brain (SPTAN1)	Q13813|SPTA2	285	Human	34	93
53	Alpha-actinin-4 (ACTN4)	O43707|ACTN4	105	Human	37	91
54	Alpha-actinin-1 (ACTN1)	P12814|ACTN1	103	Human	19	39
55	Spectrin beta chain, brain 1 (SPTBN1)	Q01082|SPTB2	275	Human	10	34
56	Myosin-Ic (MYO1C)	O00159|MYO1C	122	Human	16	34
57	Myosin-Ib (MYO1B)	O43795|MYO1B	132	Human	13	31
58	Myosin phosphatase Rho-interacting protein (MPRIP)	Q6WCQ1|MPRIP	117	Human	11	29
59	LIM domain and actin-binding protein 1 (LIMA1)	Q9UHB6|LIMA1	85	Human	6	18
60	Uncharacterized protein C19orf21	Q8IVT2|CS021	75	Human	6	15
61	Protein flightless-1 homolog (FLII)	Q13045|FLII	145	Human	4	10
62	ATPase family AAA domain-containing protein 3A (ATAD3A)	Q9NVI7|ATD3A	71	Human	2	5
63	F-actin-capping protein subunit beta (CAPZB)	P47756|CAPZB	31	Human	2	5

***Results shown are from GFP and GFP-TepP IP using GFP-Trap, followed by mass spectrometry analysis.**

***Proteins identified with less than 3 unique spectra or found to be less than 2 fold more abundant than in control GFP samples were not included.**

[a]**Unique spectrum:** Two spectra are unique if they match different peptides (even if the peptides overlap), or if they match two different charge states of the same peptide, or different modified forms of the same peptide.

[b]**Accession number for NCBI**

4.3.9 TepP induces cell morphology changes after *Chlamydia* infection

The results described thus far address the potential functions of TepP during infection on a molecular level. To get a broader view of functions on a cellular level, we decided to look at cell morphology after infection. Confluent A2EN cells were infected with either CTL2-M062G1+pV or CTL2-M062G1+pTepP with an MOI of 50. Surprisingly, cells started to clump together and form 'islands' within 1 hpi after infected with complement strain; whereas the cells infected with tepP-deficient mutant had morphology similar to uninfected cells (Fig 21A).

Immunoblot analysis of samples collected at later time point (8 hpi) showed no difference in global actin levels (Fig 21B), suggesting that the observed space between cells was not due to cell loss but cell structural changes. Interestingly, this morphology changes were not apparent in HeLa cells or Vero cells and did not happen when using MOI less than 10 (data not shown), indicating that this morphology change is evident in cell lines with architecture closer to the natural context of infection.

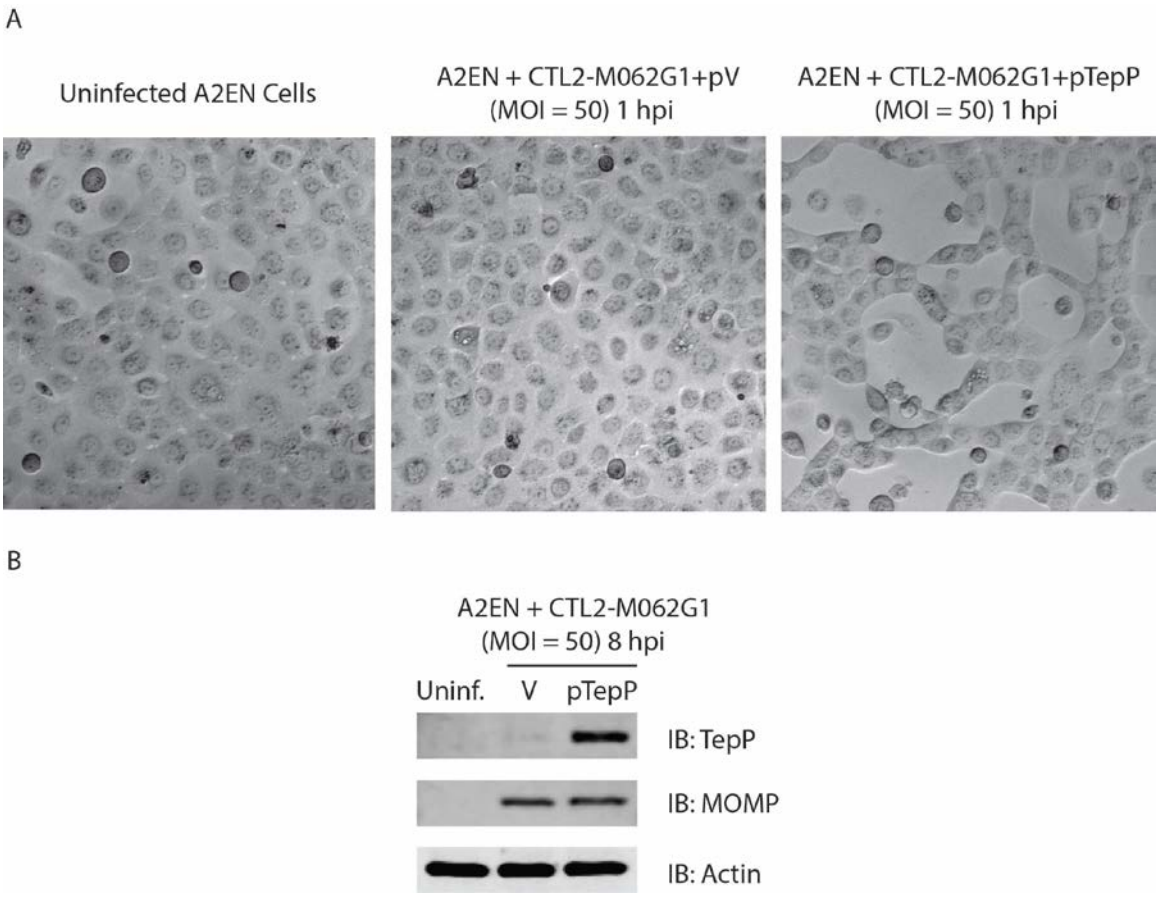

Figure 21: TepP-induced cell morphology changes. A) A2EN epithelial cells were infected with CTL2-M062G1 transformed with empty vector (Vec) and vector containing wild type *tepP* gene (pTepP) at an MOI of 50. Cell clumping was observed in cells infected with complement strain, whereas cells infected with mutant strain showed no difference from uninfected cells. Images were acquired by differential interference contrast (DIC) after 1 hpi. B) Total actin levels did not change between cell monolayers infected with mutant and complemented strains. A2EN epithelial cells were infected as in (A). Protein samples were collected at 8 hpi and analyzed by

immunoblot with antibodies against TepP, MOMP and Actin. Actin is a loading control for host cell and MOMP is a loading control for bacteria.

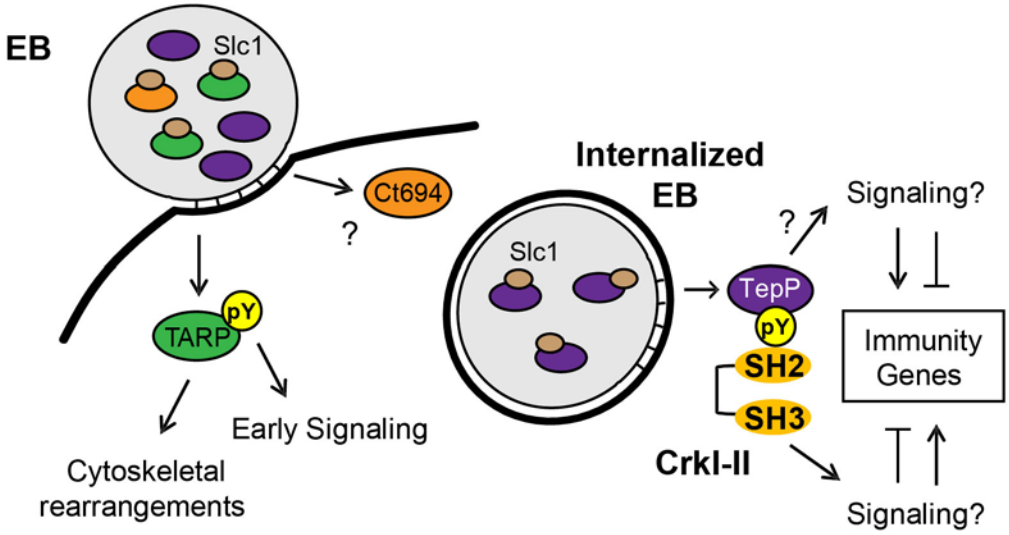

Figure 22: Model of the regulation and function of early effectors in signaling events occurring during the establishment of a nascent *Chlamydia* inclusion. The EB form of *C. trachomatis* is pre-loaded with multiple T3S effectors and chaperones. The majority of TARP and Ct694, two known early effectors, are pre-complexed with their cognate chaperone, Slc1, whereas only a small portion of TepP is in complex with Slc1. Upon *Chlamydia* attachment, TARP and Ct694 are translocated into host cell cytoplasm, freeing Slc1 to associate with TepP and enhance its secretion. TepP is translocated across membranes and phosphorylated by host tyrosine kinases. Phospho-TepP then recruits the host scaffolding protein, Crk, through interacting with the SH2 domain of Crk. The SH3 domain of Crk then recruits other host proteins to the nascent inclusion to initiate signaling cascades within the infected cell. TepP may also recruit additional proteins to initiate signaling responses independent of Crk.

4.4 Discussion

Our findings indicate that TepP is a novel *C. trachomatis* effector that is targeted for tyrosine phosphorylation upon delivery into epithelial cells. TepP is phosphorylated at both tyrosine and serine residues (Fig. 14 and Fig. 15A), with a phosphotyrosine residue mapping to the peptide ASD**Y**DLPR, which is repeated in tandem between amino acids 496-504. This phosphorylation site matches the pYxxP consensus binding site for the host adaptor proteins

Crk-I and Crk-II (Songyang et al., 1993). Indeed, we found that both Crk proteins co-IP with endogenous TepP during the early stages of EB infection (Fig. 15B). This interaction is likely to be direct and dependent on tyrosine phosphorylation since recombinant TepP only interacts with GST-CrK upon *in vitro* phosphorylation (Fig. 15D). Consistent with these observations, CrkI-II associated with EBs at entry sites and nascent inclusions (Fig. 15C). Importantly, the lack of CrkI-II association with nascent inclusions in a *tepP* null mutant strain and restoration after complementation provided genetic confirmation that TepP is required for Crk recruitment.

CrkI-II are well-characterized scaffolding proteins that organize cytoskeletal rearrangement and signal transduction events (Birge et al., 2009). The SH2 domain of Crk interacts with tyrosine-phosphorylated proteins. The SH3 domain, in turn, can interacts with multiple proteins including guanine nucleotide exchange factors (GEFs) such as C3G, Sos1 and Dock180, and c-Abl and PI3K (p85 subunit), a protein and lipid kinase (reviewed in (Birge et al., 2009)). The manipulation of Crk function by bacterial effectors is not unprecedented. In *Helicobactor pylori*, CagA, a Type IV secretion effector, is tyrosine-phosphorylated upon translocation and interacts with Crk (Suzuki et al., 2005). This interaction then triggers downstream signaling events of Crk, including SoS1/H-Ras/Raf1, C3G/Rap1/B-Raf and Dock180/ELMO pathway, resulting in CagA-specific cell responses such as epithelial cell scattering and cell-cell dissociation (Suzuki et al., 2005). In *Pseudomonas aeruginosa*, exoenzyme T (ExoT) ADP-ribosylates both CrkI and CrkII, preventing the binding of Crk SH2 domain to focal adhesion complex proteins, paxillin and $p130^{cas}$ (Deng, Sun, & Barbieri, 2005). This leads to uncoupling of integrin signaling and results in actin depolymerization and potentially contributes to the anti-phagocytic activity of this opportunistic pathogen. The function of Crk in *C. trachomatis* infection is less clear. Because the Crk partner Sos1 and

Dock180 activate Rac1 (Kiyokawa et al., 1998; Nimnual, Yatsula, & Bar-Sagi, 1998) and Rac1 activation is partially required for *C. trachomatis* invasion (Carabeo, Grieshaber, Hasenkrug, Dooley, & Hackstadt, 2004), it is possible that TepP, in addition to TARP (Lane et al., 2008), contributes to Rac1 activation at bacteria entry sites through its recruitment of Crk. However, since TepP is not essential for bacterial entry or establishment of the replicative vacuole within epithelial cells (Fig. 19D), we see a limited role for this effector in the activation of these pathways. Similarly, RNAi-mediated silencing of CrkI-II in HeLa cells did not affect the ability of bacteria to enter and replicate in these cells (Fig. 19A-C). These findings are in contrast to observations made in *Drosophila* S2 cells where Crk was identified as a potential host factor important for *C. muridarum* growth (Elwell, Ceesay, Kim, Kalman, & Engel, 2008), and suggest possible differences in cell lines or *Chlamydia* strains used. At this stage we do not know the full compendium of proteins recruited to nascent inclusions via TepP and Crk-mediated protein scaffolding. However, it is clear from the number of proteins that are tyrosine-phosphorylated in a TepP-dependent manner that TepP contributes to multiple signaling events during *Chlamydia* invasion.

Since signaling events often lead to changes in gene transcription, we performed a microarray analysis to compare the global transcript level response of A2EN cells to infection with *tepP* mutants versus their complemented counterparts. Interestingly, many immune-related genes showed a TepP- dependent activation. Among them, the most striking changes were observed for IFIT1 and IFIT2 with a fold-change more than 10 fold by 8 hpi (Fig. 20C). IFIT1 and IFIT2 belong to a family of interferon-induced protein with tetratricopeptide repeats (IFITs) that have a well-established role in host anti-viral defense. IFIT proteins repress the translation

of viral genes by binding to eIF3, a translation initiation factor, and virus RNA bearing 5'-triphosphate, leading to suppression of virus replication (Hui, Terenzi, Merrick, & Sen, 2005; Pichlmair et al., 2011; Terenzi, Hui, Merrick, & Sen, 2006). In addition, ectopic overexpression of IFIT2 promotes cell death by a mitochondrial pathway, revealing another potential anti-viral mechanism for these proteins (Stawowczyk, Van Scoy, Kumar, & Reich, 2011). The role of IFIT proteins in bacterial infections is less clear. In murine macrophages, overexpression of IFIT2 represses lipopolysaccharide (LPS) induced TNF- α and IL-6 expression (Berchtold et al., 2008). In contrast, IFIT2$^{-/-}$ mice display reduced TNF- α and IL-6 in serum and LPS-mediated lethality in an endotoxic shock model, suggesting IFIT2 is a critical mediator for the secretion of LPS-induced proinflammatory cytokines (Siegfried et al., 2013). In *C. trachomatis*, both IFIT1 and IFIT2 genes were reported to be up-regulated more than 10-fold in HeLa 229 cells by 16 hpi (Lad, Fukuda, Li, de la Maza, & Li, 2005). Our study shows that in the absence of TepP, the transcript level of IFIT1 and IFIT2 is similar to the level of uninfected A2EN cells, implying that TepP-mediated signaling regulates the expression of these genes during *C. trachomatis* infection. IFIT1 and IFIT2 can be induced directly by type I interferon (IFN -α/β) (Der, Zhou, Williams, & Silverman, 1998). In addition, binding of host pattern recognition receptors (PRRs), including Toll-like receptors, retinoic acid-inducible gene I-like receptors, and DNA-dependent activators of IRFs, to the microbial nucleic acids and other macromolecules, such as LPS, could also induce transcription of IFIT1/2 IFIT1 (Reich, 2013). Since *Chlamydia* infection induces type I IFN secretion in host cells, either *Chlamydia*-induced IFN or *Chlamydia* LPS or both may contribute to this up-regulation. We are currently investigating what TepP-mediated signal transduction pathways may mediate the change of IFIT transcripts and other genes early in infection and the consequences of these events in colonization of the host.

In addition to the effects in molecular levels, TepP is also responsible for a drastic cell morphology change induced by *Chlamydia* infection (Fig. 21). This phenomenon only happens when using high MOI, which may not be the case during the primary infection within the host. However, during secondary infections, when newly-generated EBs are released from infected cells, the surrounding cells will be exposed to a relatively high amount of *Chlamydia* – effectively a high MOI. We hypothesize that this destruction of cell monolayers may help *Chlamydia* dissemination in the genital tract because *Chlamydia* could better access cells in deeper layers when upper monolayers are destroyed. This destruction is likely to be mediated by the actin-remodeling potential of TepP. Nevertheless, this hypothesis will require further animal experiments to support.

Taken together, our data is consistent with a model in which TepP acts as a scaffolding protein that upon tyrosine phosphorylation, recruits additional scaffolding proteins like Crk, which in turn recruit more proteins to nascent inclusions, presumably to help establish an early niche for replication within the host (Fig. 22). In addition, the transcriptional response of host cells to infection with *tepP* mutants suggest that there is a distinct gene expression program that is dependent on TepP-mediated signaling events. We hypothesize that the compendium of genes activated and repressed in a TepP-dependent manner are important in establishing an immune environment within infected tissues that is more conducive to *C. trachomatis* colonization, survival and/or dissemination.

5. Concluding remarks

Despite the immense health cost burden associated with *Chlamydia* infections, little is known about its pathogenesis. Our understanding of the mechanisms that drive pathogenesis is limited by the dearth of molecular genetic tools available for manipulating chlamydial genomes and its complex parasitic and biphasic developmental cycle. Approximately 5-10% of the *C. trachomatis* genome is predicted to encode proteins with putative T3S signals (Arnold et al., 2009; Samudrala et al., 2009). These potential effector proteins are presumably translocated into host epithelial cells at various stages of infection to mediate epithelial cell invasion, establishment of a protected replicative vacuole, and evasion of innate immune responses (reviewed in (Betts et al., 2009)). Because *Chlamydia* cannot be readily manipulated with molecular genetic tools, most approaches for identifying effectors have been indirect and relied on heterologous expression systems (Valdivia, 2008). To date, only two effectors that are secreted in the early stage of infection, TARP and Ct694, have been experimentally validated in *C. trachomatis* (Clifton et al., 2004; Hower et al., 2009). Given the complexity of interactions with the host cell during *Chlamydia* entry and nascent inclusion development, we expected additional effectors to be secreted upon the association of the EB with its target epithelial cell and that most of these effectors are pre-loaded in EBs. Indeed, a quantitative analysis of the *C. trachomatis* EB proteome (Saka et al., 2011) suggested the presence of at least 20 abundant hypothetical proteins with putative T3S signals. EBs are also pre-loaded with most of the predicted T3S chaperones encoded by the *Chlamydia* genome. However, putative T3S effectors are in molar excess to that of available T3S chaperones, which led us to speculate that these chaperones may engage multiple effectors. Indeed, by coupling immunoprecipitation of these

chaperones in EBs with mass spectrometry, we identified several potential T3S effectors that may function early during infection. We further showed that one of the candidates, Ct875 (TepP), is a T3S effector that is secreted early during *Chlamydia* infection. A similar methodology may be applied to identify potential T3S effector in pathogens that are not genetically tractable.

Usurping host cellular signaling pathways by effector tyrosine phosphorylation is an emerging theme among bacterial pathogens. Examples have been found in *Enteropathogenic Escherichia coli*, *Helicobactor pylori* and *Bartonella henselae* and the list is still growing (Backert & Selbach, 2005). Since protein tyrosine phosphorylation often results in recruitment of SH2 (Src homology 2) and PTB (phosphotyrosine binding) domains containing proteins and initiates signaling cascades in eukaryotes, *Chlamydia* may develop multiple strategies to exploit this pathway to recruits different layers of host proteins during infection. Indeed, *Chlamydia* infection induces multiple protein tyrosine-phosphorylations at early stage of infection (Birkelund et al., 1994; Fawaz et al., 1997). Nevertheless, only two proteins, TARP (Clifton et al., 2004) and Ezrin (Swanson et al., 2007) have been experimentally validated so far. Our study identified the third one, TepP (Ct875). Interestingly, cells infected with a TepP mutant strain only elicits phosphorylation of the 150 kDa protein, which is TARP, suggesting TepP is the critical mediator of the other phosphorylation events. Future direction can be aimed at addressing the identities of these proteins and host signaling events they may target

In the battlefield between pathogen and host, using the right weapon at the right time is the key to succeed. The temporal manner in which effectors are secreted is likely to be

important for the proper manipulation of host cell functions. This is especially vital for an obligate intracellular pathogen like *Chlamydia*, whose propagation is entirely reliant on host cells. However, how the hierarchy of effector secretion is determined remains a mystery. One possibility is that the regulation relies on the transcription and translation of T3S effector and the apparatus transport whatever is available. The other possibility is that bacterial regulatory proteins shuttle destined cargo to secretion apparatuses at the correct time. In the later hypothesis, it is likely that chaperones provide this regulatory function. In *Chlamydia*, both Mcsc and Slc1 are classified as class IB chaperones and bind multiple effectors. In both cases, we observed a differential binding preference of these chaperones to their cognate cargos, suggesting a hierarchy in effector translocation that may be partially imparted by chaperone. In the case of Mcsc, it binds to three inclusion membrane proteins with an order of affinity reversely correlated to the timing of their protein expressions. This strategy may ensure that late expressed effectors can be secreted in a timely manner and exert their functions (Fig. 7).

At the EB stage, the majority of TARP and Ct694 are found pre-complexed with Slc1, whereas only a minor portion of TepP is present in complexes with Slc1 (Fig. 9), even though TepP is more abundant than TARP and Ct694 in EBs (Saka et al., 2011). This implies that this pre-engagement with its chaperone could prime Tarp and Ct694 for rapid secretion upon attachment. Given these observations, we considered a model wherein T3S substrates pre-bound by Slc1 in EBs, such as TARP and Ct694, will be delivered first, followed by TepP and potentially others effectors which do not exist as pre-formed chaperone complexes in EBs. Consistent with this model, TepP was tyrosine-phosphorylated later than TARP (Fig. 13D). Although we cannot exclude the possibility that TepP-specific tyrosine kinases are recruited later

than those that phosphorylate TARP, our preliminary results indicate that TepP is phosphorylated by kinases that also target TARP (Victoria Carpenter, unpublished data), making this possibility less likely. Overall, the delayed phosphorylation of TepP, coupled with the relative abundance of Slc1-Tarp as compared to Slc1-TepP complexes within EBs lead us to propose that Slc1 imparts a hierarchy to the translocation of effectors during *Chlamydia* invasion (Fig. 22). Since many T3S components are conserved among many pathogenic Gram-negative bacteria, including *Yersinia*, *Salmonella* and *Shigella* species (Cornelis, 2006), T3S systems might share an evolutionarily conserved mechanism. Therefore, this study on the chlamydial T3S system may also be applicable to the T3S systems in these pathogens and might help develop better strategies for treatment.

Appendix 1: Plasmid constructs used in this study.

Vector	Insert
Yeast two Hybrid	
pGBT9	Cap1(Ct529)(1-254 a.a.)(1-20 a.a.)(1-50 a.a.) (1-100 a.a.)(100-176 a.a.)(100-224 a.a.)(176-224 a.a.)
pGBT9	Ct618(1-214 a.a.)(1-20 a.a.)(1-50 a.a.) (1-100 a.a.)(100-140 a.a.)(100-193 a.a.)(140-193 a.a.)
pGAD424	Mcsc(FL) (Ct260)
Crystallography	
pET30-GBF*usion*1 (pGBF1OPT)/TEV	Cap1(176-224 a.a.)
pET30-GBF*usion*3 (pGBF3OPT)/TEV	Ct618(140-193 a.a.)
pET30-GBF*usion*3 (pGBF3OPT)/TEV	Ct225(69-122 a.a.)
***In vivo* stability/secretion assay**	
p2TK2-SW2	WTCap1 (1-224 a.a.)-GSK
p2TK2-SW2	H188ACap1 (1-224 a.a.)-GSK
p2TK2-SW2	H188DCap1 (1-224 a.a.)-GSK
p2TK2-SW2	WTCt618 (1-214 a.a.)-GSK
p2TK2-SW2	H156ACt618 (1-214 a.a.)-GSK
p2TK2-SW2	H156DCt618 (1-214 a.a.)-GSK
***Yersinia* T3S system**	
pBAD24	Mcsc(FL)
pBAD24	Slc1(FL)
pBAD33	Ct694 (FL)
pBAD33	Ct695(FL)-FLAG
pBAD33	TepP(FL) (Ct875)
GST pulldown	
pET24d	Slc1(FL)
pGEX	GST
	GST-Ct288 (305 - 560 a.a.)
	GST-TARP(FL)
	GST-Ct694(FL)
	GST-Ct695(FL)
	GST-TepP(FL)

Gel filtration	
pET24d	Slc1(FL)-6His Slc1/TARP(FL)-6His Slc1/Ct694(FL)-6His Slc1/Ct695(FL)-6His Slc1/TepP(FL)-6His
***Chlamydia* Transformation**	
p2TK2-SW2	TepP(FL)

***FL-full length**

Appendix 2: Primer sequences used for Q-PCR

Primer	Sequence (5' - 3')
IL-6 Forward	gatgagtacaaaagtcctgatcca
IL-6 Reverse	ctgcagccactggttctgt
CXCL3 Forward	aaatcatcgaaaagatactgaacaag
CXCL3 Reverse	ggtaagggcagggaccac
MAP3k8 Forward	cgcaagaggctgctgagt
MAP3k8 Reverse	ttcctgtgcacgaagaatca
IFIT1 Forward	agccagatctcagaggagcc
IFIT1 Reverse	ccatttgtactcatggttgctgtaa
IFIT2 Forward	tggtggcagaagaggaagat
IFIT2 Reverse	gtaggctgctctccaaggaa
Actin Forward	ccaaccgcgagaagatga
Actin Reverse	ccagaggcgtacagggatag
16S rRNA Forward	ggaggctgcagtcgagaatct
16S rRNA Reverse	ttacaaccctagagccttcatcaca

References

Abby, S. S., & Rocha, E. P. (2012). The non-flagellar type III secretion system evolved from the bacterial flagellum and diversified into host-cell adapted systems. *PLoS Genet, 8*(9), e1002983. doi: 10.1371/journal.pgen.1002983

Abdelrahman, Y. M., & Belland, R. J. (2005). The chlamydial developmental cycle. *FEMS Microbiol Rev, 29*(5), 949-959. doi: 10.1016/j.femsre.2005.03.002

Agaisse, H., & Derre, I. (2013). A *C. trachomatis* cloning vector and the generation of *C. trachomatis* strains expressing fluorescent proteins under the control of a *C. trachomatis* promoter. *PLoS One, 8*(2), e57090. doi: 10.1371/journal.pone.0057090

Akeda, Y., & Galan, J. E. (2005). Chaperone release and unfolding of substrates in type III secretion. *Nature, 437*(7060), 911-915. doi: 10.1038/nature03992

Arnold, R., Brandmaier, S., Kleine, F., Tischler, P., Heinz, E., Behrens, S., . . . Rattei, T. (2009). Sequence-based prediction of type III secreted proteins. *PLoS Pathog, 5*(4), e1000376. doi: 10.1371/journal.ppat.1000376

Backert, S., Moese, S., Selbach, M., Brinkmann, V., & Meyer, T. F. (2001). Phosphorylation of tyrosine 972 of the *Helicobacter pylori* CagA protein is essential for induction of a scattering phenotype in gastric epithelial cells. *Mol Microbiol, 42*(3), 631-644.

Backert, S., & Selbach, M. (2005). Tyrosine-phosphorylated bacterial effector proteins: the enemies within. *Trends Microbiol, 13*(10), 476-484. doi: 10.1016/j.tim.2005.08.002

Bannantine, J. P., Griffiths, R. S., Viratyosin, W., Brown, W. J., & Rockey, D. D. (2000). A secondary structure motif predictive of protein localization to the chlamydial inclusion membrane. *Cell Microbiol, 2*(1), 35-47.

Barta, M. L., Hickey, J., Kemege, K. E., Lovell, S., Battaile, K. P., & Hefty, P. S. (2013). Structure of CT584 from *Chlamydia trachomatis* refined to 3.05 A resolution. *Acta Crystallogr Sect F Struct Biol Cryst Commun, 69*(Pt 11), 1196-1201. doi: 10.1107/S1744309113027371

Bartra, S. S., Styer, K. L., O'Bryant, D. M., Nilles, M. L., Hinnebusch, B. J., Aballay, A., & Plano, G. V. (2008). Resistance of *Yersinia pestis* to complement-dependent killing is mediated by the Ail outer membrane protein. *Infect Immun, 76*(2), 612-622. doi: 10.1128/IAI.01125-07

Beausoleil, S. A., Villen, J., Gerber, S. A., Rush, J., & Gygi, S. P. (2006). A probability-based approach for high-throughput protein phosphorylation analysis and site localization. *Nat Biotechnol, 24*(10), 1285-1292. doi: 10.1038/nbt1240

Belland, R. J., Zhong, G., Crane, D. D., Hogan, D., Sturdevant, D., Sharma, J., . . . Caldwell, H. D. (2003). Genomic transcriptional profiling of the developmental cycle of *Chlamydia trachomatis*. *Proc Natl Acad Sci U S A, 100*(14), 8478-8483. doi: 10.1073/pnas.1331135100

Berchtold, S., Manncke, B., Klenk, J., Geisel, J., Autenrieth, I. B., & Bohn, E. (2008). Forced IFIT-2 expression represses LPS induced TNF-alpha expression at posttranscriptional levels. *BMC Immunol, 9*, 75. doi: 10.1186/1471-2172-9-75

Betts-Hampikian, H. J., & Fields, K. A. (2010). The Chlamydial Type III Secretion Mechanism: Revealing Cracks in a Tough Nut. *Front Microbiol, 1*, 114. doi: 10.3389/fmicb.2010.00114

Betts, H. J., Twiggs, L. E., Sal, M. S., Wyrick, P. B., & Fields, K. A. (2008). Bioinformatic and biochemical evidence for the identification of the type III secretion system needle protein of *Chlamydia trachomatis*. *J Bacteriol, 190*(5), 1680-1690. doi: 10.1128/JB.01671-07

Betts, H. J., Wolf, K., & Fields, K. A. (2009). Effector protein modulation of host cells: examples in the *Chlamydia spp*. arsenal. *Curr Opin Microbiol, 12*(1), 81-87. doi: 10.1016/j.mib.2008.11.009

Birge, R. B., Kalodimos, C., Inagaki, F., & Tanaka, S. (2009). Crk and CrkL adaptor proteins: networks for physiological and pathological signaling. *Cell Commun Signal, 7*, 13. doi: 10.1186/1478-811X-7-13

Birkelund, S., Johnsen, H., & Christiansen, G. (1994). *Chlamydia trachomatis* serovar L2 induces protein tyrosine phosphorylation during uptake by HeLa cells. *Infect Immun, 62*(11), 4900-4908.

Birtalan, S. C., Phillips, R. M., & Ghosh, P. (2002). Three-dimensional secretion signals in chaperone-effector complexes of bacterial pathogens. *Mol Cell, 9*(5), 971-980.

Boyd, A. P., Lambermont, I., & Cornelis, G. R. (2000). Competition between the Yops of *Yersinia enterocolitica* for delivery into eukaryotic cells: role of the SycE chaperone binding domain of YopE. *J Bacteriol, 182*(17), 4811-4821.

Brinkworth, A. J., Malcolm, D. S., Pedrosa, A. T., Roguska, K., Shahbazian, S., Graham, J. E., . . . Carabeo, R. A. (2011). *Chlamydia trachomatis* Slc1 is a type III secretion chaperone that enhances the translocation of its invasion effector substrate TARP. *Mol Microbiol, 82*(1), 131-144. doi: 10.1111/j.1365-2958.2011.07802.x

Brown, A. a. T., M. (1998). *Yeast Gene Analysis*. London: Academic Press.

Buckner, L. R., Schust, D. J., Ding, J., Nagamatsu, T., Beatty, W., Chang, T. L., . . . Quayle, A. J. (2011). Innate immune mediator profiles and their regulation in a novel polarized

immortalized epithelial cell model derived from human endocervix. *J Reprod Immunol, 92*(1-2), 8-20. doi: 10.1016/j.jri.2011.08.002

Buttner, D. (2012). Protein export according to schedule: architecture, assembly, and regulation of type III secretion systems from plant- and animal-pathogenic bacteria. *Microbiol Mol Biol Rev, 76*(2), 262-310. doi: 10.1128/MMBR.05017-11

Campbell, L. A., & Kuo, C. C. (2004). *Chlamydia pneumoniae*--an infectious risk factor for atherosclerosis? *Nat Rev Microbiol, 2*(1), 23-32. doi: 10.1038/nrmicro796

Carabeo, R. A., Grieshaber, S. S., Hasenkrug, A., Dooley, C., & Hackstadt, T. (2004). Requirement for the Rac GTPase in *Chlamydia trachomatis* invasion of non-phagocytic cells. *Traffic, 5*(6), 418-425. doi: 10.1111/j.1398-9219.2004.00184.x

Carabeo, R. A., Mead, D. J., & Hackstadt, T. (2003). Golgi-dependent transport of cholesterol to the *Chlamydia trachomatis* inclusion. *Proc Natl Acad Sci U S A, 100*(11), 6771-6776. doi: 10.1073/pnas.1131289100

Centers for Disease Control and Prevention, C. (Producer). (2013). *Chlamydia* Profiles, 2011. Retrieved from http://www.cdc.gov/std/chlamydia2011/default.htm

Chellas-Gery, B., Linton, C. N., & Fields, K. A. (2007). Human GCIP interacts with CT847, a novel *Chlamydia trachomatis* type III secretion substrate, and is degraded in a tissue-culture infection model. *Cell Microbiol, 9*(10), 2417-2430. doi: 10.1111/j.1462-5822.2007.00970.x

Chellas-Gery, B., Wolf, K., Tisoncik, J., Hackstadt, T., & Fields, K. A. (2011). Biochemical and localization analyses of putative type III secretion translocator proteins CopB and CopB2 of *Chlamydia trachomatis* reveal significant distinctions. *Infect Immun, 79*(8), 3036-3045. doi: 10.1128/IAI.00159-11

Clausen, J. D., Christiansen, G., Holst, H. U., & Birkelund, S. (1997). *Chlamydia trachomatis* utilizes the host cell microtubule network during early events of infection. *Mol Microbiol, 25*(3), 441-449.

Clifton, D. R., Fields, K. A., Grieshaber, S. S., Dooley, C. A., Fischer, E. R., Mead, D. J., . . . Hackstadt, T. (2004). A chlamydial type III translocated protein is tyrosine-phosphorylated at the site of entry and associated with recruitment of actin. *Proc Natl Acad Sci U S A, 101*(27), 10166-10171. doi: 10.1073/pnas.0402829101

Cornelis, G. R. (2006). The type III secretion injectisome. *Nat Rev Microbiol, 4*(11), 811-825. doi: 10.1038/nrmicro1526

Darwin, K. H., & Miller, V. L. (2001). Type III secretion chaperone-dependent regulation: activation of virulence genes by SicA and InvF in *Salmonella typhimurium*. *EMBO J, 20*(8), 1850-1862. doi: 10.1093/emboj/20.8.1850

Delevoye, C., Nilges, M., Dehoux, P., Paumet, F., Perrinet, S., Dautry-Varsat, A., & Subtil, A. (2008). SNARE protein mimicry by an intracellular bacterium. *PLoS Pathog, 4*(3), e1000022. doi: 10.1371/journal.ppat.1000022

Deng, Q., Sun, J., & Barbieri, J. T. (2005). Uncoupling Crk signal transduction by *Pseudomonas* exoenzyme T. *J Biol Chem, 280*(43), 35953-35960. doi: 10.1074/jbc.M504901200

Der, S. D., Zhou, A., Williams, B. R., & Silverman, R. H. (1998). Identification of genes differentially regulated by interferon alpha, beta, or gamma using oligonucleotide arrays. *Proc Natl Acad Sci U S A, 95*(26), 15623-15628.

Derre, I., Swiss, R., & Agaisse, H. (2011). The lipid transfer protein CERT interacts with the *Chlamydia* inclusion protein IncD and participates to ER-*Chlamydia* inclusion membrane contact sites. *PLoS Pathog, 7*(6), e1002092. doi: 10.1371/journal.ppat.1002092

Elwell, C. A., Ceesay, A., Kim, J. H., Kalman, D., & Engel, J. N. (2008). RNA interference screen identifies Abl kinase and PDGFR signaling in *Chlamydia trachomatis* entry. *PLoS Pathog, 4*(3), e1000021. doi: 10.1371/journal.ppat.1000021

Engstrom, P., Nguyen, B. D., Normark, J., Nilsson, I., Bastidas, R. J., Gylfe, A., . . . Bergstrom, S. (2013). Mutations in hemG mediate resistance to salicylidene acylhydrazides, demonstrating a novel link between protoporphyrinogen oxidase (HemG) and *Chlamydia trachomatis* infectivity. *J Bacteriol, 195*(18), 4221-4230. doi: 10.1128/JB.00506-13

Erickson, H. P. (2009). Size and shape of protein molecules at the nanometer level determined by sedimentation, gel filtration, and electron microscopy. *Biol Proced Online, 11*, 32-51. doi: 10.1007/s12575-009-9008-x

Faherty, C. S., & Maurelli, A. T. (2009). Spa15 of *Shigella flexneri* is secreted through the type III secretion system and prevents staurosporine-induced apoptosis. *Infect Immun, 77*(12), 5281-5290. doi: 10.1128/IAI.00800-09

Fawaz, F. S., van Ooij, C., Homola, E., Mutka, S. C., & Engel, J. N. (1997). Infection with *Chlamydia trachomatis* alters the tyrosine phosphorylation and/or localization of several host cell proteins including cortactin. *Infect Immun, 65*(12), 5301-5308.

Feldman, M. F., & Cornelis, G. R. (2003). The multitalented type III chaperones: all you can do with 15 kDa. *FEMS Microbiol Lett, 219*(2), 151-158.

Fields, K. A., Fischer, E. R., Mead, D. J., & Hackstadt, T. (2005). Analysis of putative *Chlamydia trachomatis* chaperones Scc2 and Scc3 and their use in the identification of type III secretion substrates. *J Bacteriol, 187*(18), 6466-6478. doi: 10.1128/JB.187.18.6466-6478.2005

Fields, K. A., & Hackstadt, T. (2000). Evidence for the secretion of *Chlamydia trachomatis* CopN by a type III secretion mechanism. *Mol Microbiol, 38*(5), 1048-1060.

Fields, K. A., & Hackstadt, T. (2002). The chlamydial inclusion: escape from the endocytic pathway. *Annu Rev Cell Dev Biol, 18*, 221-245. doi: 10.1146/annurev.cellbio.18.012502.105845

Fields KA, H. T. (2006). The *Chlamydia* Type III Secretion System: Structure and Implications for Pathogenesis. In P. B. W. Patrik M. Bavoil (Ed.), *Chlamydia: Genomics And Pathogenesis* (pp. 222-223). Norfolk, UK: Horizon Bioscience.

Fields, K. A., Mead, D. J., Dooley, C. A., & Hackstadt, T. (2003). *Chlamydia trachomatis* type III secretion: evidence for a functional apparatus during early-cycle development. *Mol Microbiol, 48*(3), 671-683.

Fling, S. P., Sutherland, R. A., Steele, L. N., Hess, B., D'Orazio, S. E., Maisonneuve, J., . . . Starnbach, M. N. (2001). CD8+ T cells recognize an inclusion membrane-associated protein from the vacuolar pathogen *Chlamydia trachomatis*. *Proc Natl Acad Sci U S A, 98*(3), 1160-1165. doi: 10.1073/pnas.98.3.1160

Francis, M. S., Lloyd, S. A., & Wolf-Watz, H. (2001). The type III secretion chaperone LcrH co-operates with YopD to establish a negative, regulatory loop for control of Yop synthesis in *Yersinia pseudotuberculosis*. *Mol Microbiol, 42*(4), 1075-1093.

Galan, J. E., & Wolf-Watz, H. (2006). Protein delivery into eukaryotic cells by type III secretion machines. *Nature, 444*(7119), 567-573. doi: 10.1038/nature05272

Garcia, J. T., Ferracci, F., Jackson, M. W., Joseph, S. S., Pattis, I., Plano, L. R., . . . Plano, G. V. (2006). Measurement of effector protein injection by type III and type IV secretion systems by using a 13-residue phosphorylatable glycogen synthase kinase tag. *Infect Immun, 74*(10), 5645-5657. doi: 10.1128/IAI.00690-06

Gregory, W. W., Gardner, M., Byrne, G. I., & Moulder, J. W. (1979). Arrays of hemispheric surface projections on *Chlamydia psittaci* and *Chlamydia trachomatis* observed by scanning electron microscopy. *J Bacteriol, 138*(1), 241-244.

Grieshaber, S. S., Grieshaber, N. A., & Hackstadt, T. (2003). *Chlamydia trachomatis* uses host cell dynein to traffic to the microtubule-organizing center in a p50 dynamitin-independent process. *J Cell Sci, 116*(Pt 18), 3793-3802. doi: 10.1242/jcs.00695

Hackstadt, T., Rockey, D. D., Heinzen, R. A., & Scidmore, M. A. (1996). *Chlamydia trachomatis* interrupts an exocytic pathway to acquire endogenously synthesized sphingomyelin in transit from the Golgi apparatus to the plasma membrane. *Embo Journal, 15*(5), 964-977.

Heinzen, R. A., Scidmore, M. A., Rockey, D. D., & Hackstadt, T. (1996). Differential interaction with endocytic and exocytic pathways distinguish parasitophorous vacuoles of *Coxiella burnetii* and *Chlamydia trachomatis*. *Infect Immun, 64*(3), 796-809.

Ho, T. D., & Starnbach, M. N. (2005). The S*almonella enterica serovar typhimurium*-encoded type III secretion systems can translocate *Chlamydia trachomatis* proteins into the cytosol of host cells. *Infect Immun, 73*(2), 905-911. doi: 10.1128/IAI.73.2.905-911.2005

Hower, S., Wolf, K., & Fields, K. A. (2009). Evidence that CT694 is a novel *Chlamydia trachomatis* T3S substrate capable of functioning during invasion or early cycle development. *Mol Microbiol, 72*(6), 1423-1437. doi: 10.1111/j.1365-2958.2009.06732.x

Hu, V. H., Holland, M. J., & Burton, M. J. (2013). Trachoma: protective and pathogenic ocular immune responses to *Chlamydia trachomatis*. *PLoS Negl Trop Dis, 7*(2), e2020. doi: 10.1371/journal.pntd.0002020

Hui, D. J., Terenzi, F., Merrick, W. C., & Sen, G. C. (2005). Mouse p56 blocks a distinct function of eukaryotic initiation factor 3 in translation initiation. *J Biol Chem, 280*(5), 3433-3440. doi: 10.1074/jbc.M406700200

Hybiske, K., & Stephens, R. S. (2007). Mechanisms of host cell exit by the intracellular bacterium *Chlamydia*. *Proc Natl Acad Sci U S A, 104*(27), 11430-11435. doi: 10.1073/pnas.0703218104

Izore, T., Job, V., & Dessen, A. (2011). Biogenesis, regulation, and targeting of the type III secretion system. *Structure, 19*(5), 603-612. doi: 10.1016/j.str.2011.03.015

Jewett, T. J., Miller, N. J., Dooley, C. A., & Hackstadt, T. (2010). The conserved Tarp actin binding domain is important for chlamydial invasion. *PLoS Pathog, 6*(7), e1000997. doi: 10.1371/journal.ppat.1000997

Johnson, D. L., & Mahony, J. B. (2007). *Chlamydophila pneumoniae* PknD exhibits dual amino acid specificity and phosphorylates Cpn0712, a putative type III secretion YscD homolog. *J Bacteriol, 189*(21), 7549-7555. doi: 10.1128/JB.00893-07

Johnson, D. L., Stone, C. B., & Mahony, J. B. (2008). Interactions between CdsD, CdsQ, and CdsL, three putative *Chlamydophila pneumoniae* type III secretion proteins. *J Bacteriol, 190*(8), 2972-2980. doi: 10.1128/JB.01997-07

Jorgensen, I., Bednar, M. M., Amin, V., Davis, B. K., Ting, J. P., McCafferty, D. G., & Valdivia, R. H. (2011). The *Chlamydia* protease CPAF regulates host and bacterial proteins to maintain pathogen vacuole integrity and promote virulence. *Cell Host Microbe, 10*(1), 21-32. doi: 10.1016/j.chom.2011.06.008

Keller, A., Nesvizhskii, A. I., Kolker, E., & Aebersold, R. (2002). Empirical statistical model to estimate the accuracy of peptide identifications made by MS/MS and database search. *Anal Chem, 74*(20), 5383-5392.

Kenny, B. (1999). Phosphorylation of tyrosine 474 of the enteropathogenic *Escherichia coli* (EPEC) Tir receptor molecule is essential for actin nucleating activity and is preceded by additional host modifications. *Mol Microbiol, 31*(4), 1229-1241.

Kim, J. F. (2001). Revisiting the chlamydial type III protein secretion system: clues to the origin of type III protein secretion. *Trends Genet, 17*(2), 65-69.

Kiyokawa, E., Hashimoto, Y., Kobayashi, S., Sugimura, H., Kurata, T., & Matsuda, M. (1998). Activation of Rac1 by a Crk SH3-binding protein, DOCK180. *Genes Dev, 12*(21), 3331-3336.

Lad, S. P., Fukuda, E. Y., Li, J., de la Maza, L. M., & Li, E. (2005). Up-regulation of the JAK/STAT1 signal pathway during *Chlamydia trachomatis* infection. *J Immunol, 174*(11), 7186-7193.

Lane, B. J., Mutchler, C., Al Khodor, S., Grieshaber, S. S., & Carabeo, R. A. (2008). Chlamydial entry involves TARP binding of guanine nucleotide exchange factors. *PLoS Pathog, 4*(3), e1000014.

Li, Z., Chen, C., Chen, D., Wu, Y., Zhong, Y., & Zhong, G. (2008). Characterization of fifty putative inclusion membrane proteins encoded in the *Chlamydia trachomatis* genome. *Infect Immun, 76*(6), 2746-2757. doi: 10.1128/IAI.00010-08

Lilic, M., Vujanac, M., & Stebbins, C. E. (2006). A common structural motif in the binding of virulence factors to bacterial secretion chaperones. *Mol Cell, 21*(5), 653-664. doi: 10.1016/j.molcel.2006.01.026

Liu, D. (2013). The adaptor protein Crk in immune response. *Immunol Cell Biol*. doi: 10.1038/icb.2013.64

Lorenz, C., Hausner, J., & Buttner, D. (2012). HrcQ provides a docking site for early and late type III secretion substrates from *Xanthomonas*. *PLoS One, 7*(11), e51063. doi: 10.1371/journal.pone.0051063

Low, N., Cassell, J. A., Spencer, B., Bender, N., Hilber, A. M., van Bergen, J., . . . Stephenson, J. M. (2012). *Chlamydia* control activities in Europe: cross-sectional survey. *Eur J Public Health, 22*(4), 556-561. doi: 10.1093/eurpub/ckr046

Lower, M., & Schneider, G. (2009). Prediction of type III secretion signals in genomes of gram-negative bacteria. *PLoS One, 4*(6), e5917. doi: 10.1371/journal.pone.0005917

Lutter, E. I., Barger, A. C., Nair, V., & Hackstadt, T. (2013). *Chlamydia trachomatis* inclusion membrane protein CT228 recruits elements of the myosin phosphatase pathway to regulate release mechanisms. *Cell Rep, 3*(6), 1921-1931. doi: 10.1016/j.celrep.2013.04.027

Malhotra, M., Sood, S., Mukherjee, A., Muralidhar, S., & Bala, M. (2013). Genital *Chlamydia trachomatis*: an update. *Indian J Med Res, 138*(3), 303-316.

Markham, A. P., Jaafar, Z. A., Kemege, K. E., Middaugh, C. R., & Hefty, P. S. (2009). Biophysical characterization of *Chlamydia trachomatis* CT584 supports its potential role as a type III secretion needle tip protein. *Biochemistry, 48*(43), 10353-10361. doi: 10.1021/bi901200y

Mehlitz, A., Banhart, S., Maurer, A. P., Kaushansky, A., Gordus, A. G., Zielecki, J., . . . Meyer, T. F. (2010). Tarp regulates early *Chlamydia*-induced host cell survival through interactions with the human adaptor protein SHC1. *J Cell Biol, 190*(1), 143-157. doi: 10.1083/jcb.200909095

Miller, M. L., Jensen, L. J., Diella, F., Jorgensen, C., Tinti, M., Li, L., . . . Linding, R. (2008). Linear motif atlas for phosphorylation-dependent signaling. *Sci Signal, 1*(35), ra2. doi: 10.1126/scisignal.1159433

Mills, E., Baruch, K., Charpentier, X., Kobi, S., & Rosenshine, I. (2008). Real-time analysis of effector translocation by the type III secretion system of enteropathogenic *Escherichia coli*. *Cell Host Microbe, 3*(2), 104-113. doi: 10.1016/j.chom.2007.11.007

Moese, S., Selbach, M., Kwok, T., Brinkmann, V., Konig, W., Meyer, T. F., & Backert, S. (2004). *Helicobacter pylori* induces AGS cell motility and elongation via independent signaling pathways. *Infect Immun, 72*(6), 3646-3649. doi: 10.1128/IAI.72.6.3646-3649.2004

Morita-Ishihara, T., Ogawa, M., Sagara, H., Yoshida, M., Katayama, E., & Sasakawa, C. (2006). *Shigella* Spa33 is an essential C-ring component of type III secretion machinery. *J Biol Chem, 281*(1), 599-607. doi: 10.1074/jbc.M509644200

Moulder, J. W. (1991). Interaction of *Chlamydiae* and host cells in vitro. *Microbiol Rev, 55*(1), 143-190.

Mueller, K. E., Plano, G. V., & Fields, K. A. (2013). New frontiers in type III secretion biology: The *Chlamydia* perspective. *Infect Immun*. doi: 10.1128/IAI.00917-13

Muschiol, S., Bailey, L., Gylfe, A., Sundin, C., Hultenby, K., Bergstrom, S., . . . Henriques-Normark, B. (2006). A small-molecule inhibitor of type III secretion inhibits different stages of the infectious cycle of *Chlamydia trachomatis*. *Proc Natl Acad Sci U S A, 103*(39), 14566-14571. doi: 10.1073/pnas.0606412103

Muschiol, S., Normark, S., Henriques-Normark, B., & Subtil, A. (2009). Small molecule inhibitors of the Yersinia type III secretion system impair the development of *Chlamydia* after entry into host cells. *BMC Microbiol, 9*, 75. doi: 10.1186/1471-2180-9-75

Nesvizhskii, A. I., Keller, A., Kolker, E., & Aebersold, R. (2003). A statistical model for identifying proteins by tandem mass spectrometry. *Anal Chem, 75*(17), 4646-4658.

Nguyen, B. D., & Valdivia, R. H. (2012). Virulence determinants in the obligate intracellular pathogen *Chlamydia trachomatis* revealed by forward genetic approaches. *Proc Natl Acad Sci U S A, 109*(4), 1263-1268. doi: 10.1073/pnas.1117884109

Nguyen, B. D., & Valdivia, R. H. (2013). Forward genetic approaches in *Chlamydia trachomatis*. *J Vis Exp*(80), e50636. doi: 10.3791/50636

Nimnual, A. S., Yatsula, B. A., & Bar-Sagi, D. (1998). Coupling of Ras and Rac guanosine triphosphatases through the Ras exchanger Sos. *Science, 279*(5350), 560-563.

O'Neill, C. E., Seth-Smith, H. M., Van Der Pol, B., Harris, S. R., Thomson, N. R., Cutcliffe, L. T., & Clarke, I. N. (2013). *Chlamydia trachomatis* clinical isolates identified as tetracycline resistant do not exhibit resistance in vitro: whole-genome sequencing reveals a mutation in porB but no evidence for tetracycline resistance genes. *Microbiology, 159*(Pt 4), 748-756. doi: 10.1099/mic.0.065391-0

Pais, S. V., Milho, C., Almeida, F., & Mota, L. J. (2013). Identification of novel type III secretion chaperone-substrate complexes of *Chlamydia trachomatis*. *PLoS One, 8*(2), e56292. doi: 10.1371/journal.pone.0056292

Parsot, C., Hamiaux, C., & Page, A. L. (2003). The various and varying roles of specific chaperones in type III secretion systems. *Curr Opin Microbiol, 6*(1), 7-14.

Pascolini, D., & Mariotti, S. P. (2012). Global estimates of visual impairment: 2010. *Br J Ophthalmol, 96*(5), 614-618. doi: 10.1136/bjophthalmol-2011-300539

Peters, J., Wilson, D. P., Myers, G., Timms, P., & Bavoil, P. M. (2007). Type III secretion a la *Chlamydia*. *Trends Microbiol, 15*(6), 241-251. doi: 10.1016/j.tim.2007.04.005

Pichlmair, A., Lassnig, C., Eberle, C. A., Gorna, M. W., Baumann, C. L., Burkard, T. R., . . . Superti-Furga, G. (2011). IFIT1 is an antiviral protein that recognizes 5'-triphosphate RNA. *Nat Immunol, 12*(7), 624-630. doi: 10.1038/ni.2048

Rao, X., Deighan, P., Hua, Z., Hu, X., Wang, J., Luo, M., . . . Shen, L. (2009). A regulator from *Chlamydia trachomatis* modulates the activity of RNA polymerase through direct interaction with the beta subunit and the primary sigma subunit. *Genes Dev, 23*(15), 1818-1829. doi: 10.1101/gad.1784009

Reich, N. C. (2013). A death-promoting role for ISG54/IFIT2. *J Interferon Cytokine Res, 33*(4), 199-205. doi: 10.1089/jir.2012.0159

Ribet, D., & Cossart, P. (2010). Post-translational modifications in host cells during bacterial infection. *FEBS Lett, 584*(13), 2748-2758. doi: 10.1016/j.febslet.2010.05.012

Rockey, D. D., Scidmore, M. A., Bannantine, J. P., & Brown, W. J. (2002). Proteins in the chlamydial inclusion membrane. *Microbes Infect, 4*(3), 333-340.

Rzomp, K. A., Moorhead, A. R., & Scidmore, M. A. (2006). The GTPase Rab4 interacts with *Chlamydia trachomatis* inclusion membrane protein CT229. *Infect Immun, 74*(9), 5362-5373. doi: 10.1128/IAI.00539-06

Saka, H. A., Thompson, J. W., Chen, Y. S., Kumar, Y., Dubois, L. G., Moseley, M. A., & Valdivia, R. H. (2011). Quantitative proteomics reveals metabolic and pathogenic properties of *Chlamydia trachomatis* developmental forms. *Mol Microbiol, 82*(5), 1185-1203. doi: 10.1111/j.1365-2958.2011.07877.x

Samudrala, R., Heffron, F., & McDermott, J. E. (2009). Accurate prediction of secreted substrates and identification of a conserved putative secretion signal for type III secretion systems. *PLoS Pathog, 5*(4), e1000375. doi: 10.1371/journal.ppat.1000375

Schachter, J. (1999). Infection and Disease Epidemiology. In R. S. Stephens (Ed.), *Chlamydia: Intracellular Biology, Pathogenesis, and Immunity* (pp. 139-163). Washington, DC: American Society for Microbiology.

Scidmore, M. A., & Hackstadt, T. (2001). Mammalian 14-3-3beta associates with the *Chlamydia trachomatis* inclusion membrane via its interaction with IncG. *Mol Microbiol, 39*(6), 1638-1650.

Siegfried, A., Berchtold, S., Manncke, B., Deuschle, E., Reber, J., Ott, T., . . . Bohn, E. (2013). IFIT2 is an effector protein of type I IFN-mediated amplification of lipopolysaccharide (LPS)-induced TNF-alpha secretion and LPS-induced endotoxin shock. *J Immunol, 191*(7), 3913-3921. doi: 10.4049/jimmunol.1203305

Silva-Herzog, E., Joseph, S. S., Avery, A. K., Coba, J. A., Wolf, K., Fields, K. A., & Plano, G. V. (2011). Scc1 (CP0432) and Scc4 (CP0033) function as a type III secretion chaperone for CopN of *Chlamydia pneumoniae*. *J Bacteriol, 193*(14), 3490-3496. doi: 10.1128/JB.00203-11

Sisko, J. L., Spaeth, K., Kumar, Y., & Valdivia, R. H. (2006). Multifunctional analysis of *Chlamydia*-specific genes in a yeast expression system. *Mol Microbiol, 60*(1), 51-66. doi: 10.1111/j.1365-2958.2006.05074.x

Slepenkin, A., Enquist, P. A., Hagglund, U., de la Maza, L. M., Elofsson, M., & Peterson, E. M. (2007). Reversal of the antichlamydial activity of putative type III secretion inhibitors by iron. *Infect Immun, 75*(7), 3478-3489. doi: 10.1128/IAI.00023-07

Songyang, Z., Shoelson, S. E., Chaudhuri, M., Gish, G., Pawson, T., Haser, W. G., . . . et al. (1993). SH2 domains recognize specific phosphopeptide sequences. *Cell, 72*(5), 767-778.

Sorg, J. A., Blaylock, B., & Schneewind, O. (2006). Secretion signal recognition by YscN, the *Yersinia* type III secretion ATPase. *Proc Natl Acad Sci U S A, 103*(44), 16490-16495. doi: 10.1073/pnas.0605974103

Spaeth, K. E., Chen, Y. S., & Valdivia, R. H. (2009). The *Chlamydia* type III secretion system C-ring engages a chaperone-effector protein complex. *PLoS Pathog, 5*(9), e1000579. doi: 10.1371/journal.ppat.1000579

Stawowczyk, M., Van Scoy, S., Kumar, K. P., & Reich, N. C. (2011). The interferon stimulated gene 54 promotes apoptosis. *J Biol Chem, 286*(9), 7257-7266. doi: 10.1074/jbc.M110.207068

Stenner-Liewen, F., Liewen, H., Zapata, J. M., Pawlowski, K., Godzik, A., & Reed, J. C. (2002). CADD, a *Chlamydia* protein that interacts with death receptors. *J Biol Chem, 277*(12), 9633-9636. doi: 10.1074/jbc.C100693200

Stephens, R. S., Kalman, S., Lammel, C., Fan, J., Marathe, R., Aravind, L., . . . Davis, R. W. (1998). Genome sequence of an obligate intracellular pathogen of humans: Chlamydia trachomatis. *Science, 282*(5389), 754-759.

Stone, C. B., Johnson, D. L., Bulir, D. C., Gilchrist, J. D., & Mahony, J. B. (2008). Characterization of the putative type III secretion ATPase CdsN (Cpn0707) of *Chlamydophila pneumoniae*. *J Bacteriol, 190*(20), 6580-6588. doi: 10.1128/JB.00761-08

Stone, C. B., Sugiman-Marangos, S., Bulir, D. C., Clayden, R. C., Leighton, T. L., Slootstra, J. W., . . . Mahony, J. B. (2012). Structural characterization of a novel *Chlamydia pneumoniae* type III secretion-associated protein, Cpn0803. *PLoS One, 7*(1), e30220. doi: 10.1371/journal.pone.0030220

Subtil, A., Delevoye, C., Balana, M. E., Tastevin, L., Perrinet, S., & Dautry-Varsat, A. (2005). A directed screen for chlamydial proteins secreted by a type III mechanism identifies a translocated protein and numerous other new candidates. *Mol Microbiol, 56*(6), 1636-1647. doi: 10.1111/j.1365-2958.2005.04647.x

Suzuki, M., Mimuro, H., Suzuki, T., Park, M., Yamamoto, T., & Sasakawa, C. (2005). Interaction of CagA with Crk plays an important role in *Helicobacter pylori*-induced loss of gastric epithelial cell adhesion. *J Exp Med, 202*(9), 1235-1247. doi: 10.1084/jem.20051027

Swanson, K. A., Crane, D. D., & Caldwell, H. D. (2007). *Chlamydia trachomatis* species-specific induction of ezrin tyrosine phosphorylation functions in pathogen entry. *Infect Immun, 75*(12), 5669-5677. doi: 10.1128/IAI.01096-07

Terenzi, F., Hui, D. J., Merrick, W. C., & Sen, G. C. (2006). Distinct induction patterns and functions of two closely related interferon-inducible human genes, ISG54 and ISG56. *J Biol Chem, 281*(45), 34064-34071. doi: 10.1074/jbc.M605771200

Thomas, N. A., Deng, W., Baker, N., Puente, J., & Finlay, B. B. (2007). Hierarchical delivery of an essential host colonization factor in enteropathogenic *Escherichia coli*. *J Biol Chem, 282*(40), 29634-29645. doi: 10.1074/jbc.M706019200

Thomas, N. A., Ma, I., Prasad, M. E., & Rafuse, C. (2012). Expanded roles for multicargo and class 1B effector chaperones in type III secretion. *J Bacteriol, 194*(15), 3767-3773. doi: 10.1128/JB.00406-12

Toh, H., Miura, K., Shirai, M., & Hattori, M. (2003). In silico inference of inclusion membrane protein family in obligate intracellular parasites *Chlamydiae*. *DNA Res, 10*(1), 9-17.

Trosky, J. E., Liverman, A. D., & Orth, K. (2008). *Yersinia* outer proteins: Yops. *Cell Microbiol, 10*(3), 557-565. doi: 10.1111/j.1462-5822.2007.01109.x

Tsai, A., & Carstens, R. P. (2006). An optimized protocol for protein purification in cultured mammalian cells using a tandem affinity purification approach. *Nat Protoc, 1*(6), 2820-2827. doi: 10.1038/nprot.2006.371

Une, T., & Brubaker, R. R. (1984). *In vivo* comparison of avirulent Vwa- and Pgm- or Pstr phenotypes of *Yersiniae*. *Infect Immun, 43*(3), 895-900.

Valdivia, R. H. (2008). *Chlamydia* effector proteins and new insights into chlamydial cellular microbiology. *Curr Opin Microbiol, 11*(1), 53-59. doi: 10.1016/j.mib.2008.01.003

Wang, Y., Kahane, S., Cutcliffe, L. T., Skilton, R. J., Lambden, P. R., & Clarke, I. N. (2011). Development of a transformation system for *Chlamydia trachomatis*: restoration of glycogen biosynthesis by acquisition of a plasmid shuttle vector. *PLoS Pathog, 7*(9), e1002258. doi: 10.1371/journal.ppat.1002258

Wilm, M., Shevchenko, A., Houthaeve, T., Breit, S., Schweigerer, L., Fotsis, T., & Mann, M. (1996). Femtomole sequencing of proteins from polyacrylamide gels by nano-electrospray mass spectrometry. *Nature, 379*(6564), 466-469. doi: 10.1038/379466a0

Winnen, B., Schlumberger, M. C., Sturm, A., Schupbach, K., Siebenmann, S., Jenny, P., & Hardt, W. D. (2008). Hierarchical effector protein transport by the *Salmonella Typhimurium* SPI-1 type III secretion system. *PLoS One, 3*(5), e2178. doi: 10.1371/journal.pone.0002178

Wolf, K., Betts, H. J., Chellas-Gery, B., Hower, S., Linton, C. N., & Fields, K. A. (2006). Treatment of *Chlamydia trachomatis* with a small molecule inhibitor of the *Yersinia* type III secretion system disrupts progression of the chlamydial developmental cycle. *Mol Microbiol, 61*(6), 1543-1555. doi: 10.1111/j.1365-2958.2006.05347.x

Wong, A. R., Pearson, J. S., Bright, M. D., Munera, D., Robinson, K. S., Lee, S. F., . . . Hartland, E. L. (2011). Enteropathogenic and enterohaemorrhagic *Escherichia coli*: even more subversive elements. *Mol Microbiol, 80*(6), 1420-1438. doi: 10.1111/j.1365-2958.2011.07661.x

Workowski, K. (2013). In the clinic. *Chlamydia* and *Gonorrhea*. *Annals of Internal Medicine, 158*(3), ITC2-1. doi: 10.7326/0003-4819-158-3-20130205-01002

World Health Organization, W. (2011). Global prevalence and incidence of selected curable sexually transmitted diseases: Overview and estimates.

Zhou, D., & Galan, J. (2001). *Salmonella* entry into host cells: the work in concert of type III secreted effector proteins. *Microbes Infect, 3*(14-15), 1293-1298.

Biography

Yi-Shan Chen was born in Taichung, Taiwan on Sep 13, 1982. She received her degree of Bachelor of Science from National Chiao-Tung University, Department of Biological Science and Technology, Hsinchu, Taiwan, in 2004. She received her degree of Master of Science from National Yang-Ming University, Institute of Biochemistry and Molecular Biology, Taipei, Taiwan, in 2006. She was award a Scholarship for exchange student program in 2003 from National Chiao-Tung University and went to The Australian National University in Canberra, Australia as an exchange student for a year. During her study in college and master degree, she received several academic achievement awards. Her work in master was patented in the US. In August of 2007, she entered the Department of Biochemistry at Duke University where in May of 2008 she joined the lab of Dr. Raphael Valdivia. During her study at Duke, Yi-Shan won the beast oral presentation award in the departmental retreat in 2012 and best poster presentation award in FASEB conference in 2013. She gave oral presentations about her work in CBRS (Chlamydia Basic Research Society) meeting and ASCB (American Society of Cell Biology) in 2013. She was a recipient of a Chairman Travel Award in 2013.

Publications

Chen Y.S., Bastidas R.J., Saka H.A., Carpenter V.K., Richards K.L., Plano G.V., and Valdivia R.H. (2014) The *Chlamydia trachomatis* Type III Secretion Chaperone Slc1 Engages Multiple Early Effectors, Including TepP, a Tyrosine-phosphorylated Protein Required for the Recruitment of CrkI-II to Nascent Inclusions and Innate Immune Signaling. *PLoS Pathog*. In press.

Saka H.A., Thompson J.W., **Chen Y.S.**, Kumar Y., Dubois L.G., Moseley M.A., Valdivia R.H. (2011) Quantitative proteomics reveals metabolic and pathogenic Properties Of Chlamydia trachomatis developmental forms. *Mol Microbiol*. 82(5):1185-203.

Chou H.H., Chang S.W., Lee G.C., **Chen Y.S.**, Yeha T., Akohe C.C., Shaw J.F. (2010) Site-directed mutagenesis improves the thermostability of a recombinant *Picrophilus torridus* trehalose synthase and efficiency for the production of trehalose from sweet potato starch. *Food Chem.* 119(3): 1017–1022.

Spaeth K.E., **Chen Y.S.**, Valdivia R.H. (2009) The Chlamydia type III secretion system C-ring engages a chaperone-effector protein complex. *PLoS Pathog*. 5(9):e1000579.

Chen Y. S., Lee G. C., Shaw J. F. (2006) Gene cloning, expression, and biochemical characterization of a recombinant trehalose synthase from *Picrophilus torridus* in *Escherichia coli. J. Agric. Food Chem.* 54(19) : 7098-104.